Development of Some Novel Nonlinear and Adaptive Digital Image Filters for Efficient Noise Suppression

A thesis submitted to
National Institute of Technology, Rourkela, Orissa (INDIA)
(A Deemed University)

for award of degree

Doctor of Philosophy
in
Electronics Engineering

by

Sukadev Meher
Roll No. 50407003

Department of Electronics & Instrumentation Engineering
National Institute of Technology, Rourkela-769 008, Orissa (INDIA).

December 2004

… in the memory of my father
(Late) Balaram Meher
who left this world
during my doctoral research.

PREFACE

Digital Image Processing, developed during last two and half decades, has become a very important subject in electronics and computer engineering. Image restoration is one of the many areas it encompasses. Image deblurring and image denoising are the two sub-areas of image restoration.

When an image gets corrupted with noise during the processes of acquisition, transmission, storage and retrieval, it becomes necessary to suppress the noise quite effectively without distorting the edges and the fine details in the image so that the filtered image becomes more useful for display and/or further processing.

Many novel digital image filters are proposed in this doctoral thesis. An image is a highly correlated 2-D data (signal). The correlation lies in spatial domain among neighboring pixels. Thus, the neighborhood of a pixel tells much about the pixel. Therefore, spatial domain image filters, if properly designed, perform much better than any transform-domain image filter. Order Statistics (OS) filters are well-known for their simplicity and efficiency in suppressing various types of noise. Efforts are made in this research work to develop some novel nonlinear and adaptive digital image filters to suppress additive and substitutive noise. *Specially, for low noise conditions (considering the practical noise levels), very highly efficient image filters are developed so that they may be used in online and real-time applications such as television, photo-phone, etc.*

Therefore, the present research work may be treated as

(i) **developmental work**; and

(ii) **applied research work**.

All filters developed here are nonlinear. Some of them are fixed and some others are adaptive. Therefore, the title is so. Otherwise, the title of the dissertation could have been “Development of Some Spatial Domain Digital Image Filters” to emphasize the spatial domain processing adopted here.

I would be happy to see other researchers using the results reported in the thesis for developing better image filters. Moreover, I will be contended to find these filters implemented for practical applications in near future.

Sukadev Meher

ACKNOWLEDGEMENT

I express my indebtedness and gratefulness to my teacher and supervisor Prof. Ganapati Panda for his continuous encouragement and guidance. I needed his support, guidance and encouragement throughout the research period. I am obliged to him for his moral support through all the stages during this doctoral research work. I am indebted to him for the valuable time he has spared for me during this work.

I am grateful to my co-supervisor Dr. Banshidhar Majhi for his guidance and support.

I am thankful to Prof. K. K. Mahapatra, Head, Department of Electronics & Instrumentation Engineering who provided all the official facilities to me.

I am grateful to Prof. A. Behera for his valuable suggestions and comments during the thesis compilation.

I would like to thank all my colleagues and friends whose company and encouragement helped me a lot to work hard. Special thanks go to Prof. P. K. Nanda, Dr. G. K. Panda, Dr. A. K. Panda and Dr. S. K. Patra. In addition, I thank my young friends Debi, Manas, Saroj, Sunil, Sabuj, Alekhika and Pankaj for their company and cooperation during this period.

I take this opportunity to express my regards and obligation to my parents whose support and encouragement I can never forget in my life. I remember my father at this moment. He left this world during this research period. He is my teacher. He had introduced me to the world of research during my school days.

Last but not the least, I would like to thank my wife Sobha and daughter Suby for their patience and cooperation. I can't forget their help who have managed themselves during the tenure of my Ph. D. work. I duly acknowledge the constant moral support they provided throughout.

Sukadev Meher

BIO-DATA OF THE CANDIDATE

Name of the candidate	:	Sukadev Meher
Father's Name	:	(Late) Balaram Meher
Present Address	:	C-21, N.I.T. Campus, ROURKELA-769 008, Orissa (INDIA).
Permanent Address	:	Near Post-Office, PATNAGARH-767 025, Orissa (INDIA).
Present Position / Designation	:	*Lecturer (selection grade)*, Electronics & Instrumentation Engineering Department, **N**ational **I**nstitute of **T**echnology, **ROUKELA**-769 008, Orissa (INDIA).

ACADEMIC QUALIFICATION :

(i) **B. Sc. (Engg.)** in Electronics & Tele-communication Engineering,
Sambalur University, BURLA, Orissa (INDIA).

(ii) **M. Sc. (Engg.)** in Electronic Systems & Communication Engineering,
Sambalur University, BURLA, Orissa (INDIA).

PUBLICATION:

(i) Published 07 papers in National and International Conferences;

(ii) Communicated 03 papers to International Journals.

CONTENTS

Abstract

Some nonlinear and adaptive digital image filtering algorithms have been developed in this thesis to suppress additive white Gaussian noise (AWGN), bipolar fixed-valued impulse, also called salt and pepper noise (SPN), random-valued impulse noise (RVIN) and their combinations quite effectively.

The present state-of-art technology offers high quality sensors, cameras, electronic circuitry: application specific integrated circuits (ASIC), system on chip (SOC), etc., and high quality communication channels. Therefore, the noise level in images has been reduced drastically.

In literature, many efficient nonlinear image filters are found that perform well under high noise conditions. But their performance is not so good under low noise conditions as compared to the extremely high computational complexity involved therein. Thus, it is felt that there is sufficient scope to investigate and develop quite efficient but simple algorithms to suppress low-power noise in an image.

When an analog image-signal is transmitted, it gets corrupted with AWGN in the channel. After thresholding at the receiver, the signal gets corrupted with SPN as well. Therefore, the image signal is usually corrupted with a mixed noise (AWGN + SPN).

On the other hand, if a binary-coded digital image signal is transmitted through a linear, noisy and dispersive channel, then some of the bits may not be recognized properly due to the inter-symbol interference (ISI) and additive channel noise. Since the bits get corrupted at some arbitrary locations, it gives an effect of RVIN in an image. In present days, the noise is usually low (<5%) or very low (<1%).

Taking this problem with communication systems, e.g. television, photo phone, etc., it is very important to realize that excellent nonlinear filters are required to suppress low noise power mixed noise (MN) and RVIN quite effectively without distorting the

edges and fine details of the image. The problem is taken up and efforts are made to develop quite efficient image filters for noise cancellation.

The Rank-Ordered Mean (ROM) filter shows better performance than the moving average (MAV) and median (MED) filters under mixed noise conditions. Its performance is further improved by associating a weight vector to it. Thus, various weighted ROM (WROM) filters are proposed for AWGN, SPN and mixed noise conditions.

Three types of decision-directed filters are developed to suppress impulse noise quite effectively. One scheme uses a second-order difference (derivative) based detection scheme; another uses a probability-based detection scheme; and the third implements a deviation based impulse detection scheme.

Adaptive filters adapt themselves to the noise type and noise power level and, thus, they perform better than the fixed filters. Two types of adaptive images filters are proposed in this thesis. One is based on Order statistics and it employs LMS adaptation scheme. It performs much better than the L-filter. It may not need an on-line training always. An off-line training is good enough.

Another adaptive technique proposed here is based on fuzzy logic. Fuzzy WROM (FWROM) image filters are proposed and are seen to be quite efficient in filtering AWGN, SPN, RVIN and mixed noise. Two types of fuzzy membership functions, triangular and Gaussian, are taken and thus two types of filters FWROM-T and FQROM-G are developed. FWROM-G works slightly better than the FWROM-T. But, its computational complexity is much higher than that of FWROM-T. Therefore, the FWROM-T will be more useful in real-time applications like television systems.

Finally, it may be concluded that the proposed algorithms: WROM, PIND, DIND, OS-LMS and FWROM are the winners in their respective categories for suppressing low-power noise of various types in digital images.

List of Abbreviations used

Abbreviations

1.	*AWGN*	Additive White Gaussian Noise
2.	*SPN*	Salt and Pepper Noise
3.	*RVIN*	Random Valued Impulse Noise
4.	*SN*	Speckle Noise
5.	*MN*	Mixed Noise (AWGN + SPN)
6.	*MAV*	Moving Average (filter)
7.	*MED*	Median (filter)
8.	*ROM*	Rank-Ordered Mean (filter)
9.	*OS*	Order Statistics (filter)
10.	*WOS*	Weighted Order Statistics (filter)
11.	*WROM*	Weighted Rank-Ordered Mean (filter)
12.	*FWROM*	Fuzzy WROM (filter)
13.	*FWROM-T*	FWROM with Triangular membership function
14.	*FWROM-G*	FWROM with Gaussian membership function
15.	*DDMF*	Decision-Directed Median Filter
16.	*SOD-DDMF*	Second-Order Difference based DDMF
17.	*PIND*	Probability based Impulse Noise Detection (algorithm)
18.	*DIND*	Deviation based Impulse Noise Detection (algorithm)
19.	*ADC*	Absolute Deviation at the Center (in DIND algorithm); Analog-to-Digital Converter

20. *LMS*	Least Mean Square (algorithm)
21. *MSE*	Mean Squared Error
22. *MAE*	Mean Absolute Error
23. *RMSE*	Root Mean Squared Error
24. *PSNR*	Peak Signal to Noise Ratio
25. *MR-MSE*	Mean Restored Mean Squared Error
26. *NRDB*	Noise Reduction in dB
27. *PSP*	Percentage of Spoiled Pixels
28. *SNR*	Signal-to-Noise Ratio
29. *HVS*	Human Visual System
	SOME IMPORTANT FILTERS AVAILABLE IN LITERATURE
30. *CWM*	Center-Weighted Median
31. *AID-CWM*	Adaptive Impulse Detector using CWM
32. *TSM*	Tri-State Median
33. *MMEM*	Min Max Exclusive Mean
34. *NASM*	Noise Adaptive Soft-switching Median
35. *DRID*	Differential Rank Impulse Detector

List of Symbols used

Symbols	
1. $\mathbf{X}$, $\mathbf{X}(m,n)$	Original (noise-free) Digital Image with discrete spatial coordinates (m,n)
2. $x(m,n)$	Pixel at location (m,n); its gray scale value
3. cp	Center Pixel; its gray-scale value
4. η	Random Variable; Noise
5. $\mathbf{X}_{SPN}$	Image corrupted with Salt and Pepper Noise
6. $\mathbf{X}_{RVIN}$	Image corrupted with Random-Valued Impulse Noise
7. $\mathbf{X}_{AWGN}$	Image corrupted with additive White Gaussian Noise
8. $\mathbf{X}_{MN}$	Image corrupted with Mixed Noise (AWGN+SPN)
9. $\mathbf{Y}$, $\mathbf{Y}(m,n)$	Noisy Digital Image
10. $ROM(p,q)$	A ROM filter taking q number of intermediate order statistics from a total of p^2 number of inputs
11. f (.)	Filtering operation
12. $\tilde{X}$, $\tilde{X}(m,n)$	Restored (filtered) Digital image
13. E (.)	An Expectation Operation; may be MAV, MED, ROM, WROM, etc.
14. γ	A Threshold Value
15. μ	Step Size (in case of LMS adaptation); Fuzzy Membership Function (in case of Fuzzy System)

CHAPTER-1

Introduction

Preview

Digital **I**mage **P**rocessing is a promising area of research in the fields of electronics and communication engineering, consumer and entertainment electronics, control and instrumentation, biomedical instrumentation, remote sensing, robotics and computer vision and computer aided manufacturing (CAM). For a meaningful and useful processing such as image segmentation and object recognition, and to have very good visual display in applications like television, photo-phone, etc., the acquired image signal must be deblurred and made noise free. The deblurring and noise suppression (filtering) come under a common class of image processing tasks known as image restoration.

In this thesis, the various noise conditions are studied and many efficient nonlinear and adaptive digital image filters are designed to suppress additive white Gaussian noise (AWGN), bipolar fixed-valued impulse noise, also called salt and pepper noise (SPN), random-valued impulse noise (RVIN) and mixed noise (MN) quite effectively. The developed filters are meant for online and real-time applications like television, photo-phone, etc.

The following topics are covered in this introductory chapter.

- Fundamentals of Digital Image Processing
- Noise in Digital Images
- Study of Image Filters Reported in the Literature
- Problem Statement
- Image Metrics
- Noise Conditions for Computer Simulation
- Chapter-wise Organization of the Thesis
- Conclusion

1.1 Fundamentals of Digital Image Processing

Digital image processing generally refers to the processing of a 2-dimensional (2-D) picture signal by a digital hardware. In a broader context, it implies processing of any signal using a dedicated hardware, e.g. an application specific integrated circuit (ASIC) or using a general-purpose computer implementing some algorithms developed for the purpose.

An image is a 2-D function (signal), $\mathbf{X}(m,n)$, where m and n are the spatial (plane) coordinates. The magnitude of $\mathbf{X}$ at any pair of coordinates (m,n) is the *intensity* or *gray level* of the image at that point. In a digital image, m,n, and the magnitude of $\mathbf{X}$

are all finite and discrete quantities. Each element of this matrix (2-D array) is called a *picture element* or *pixel*.

It is a hard task to distinguish between the domains of image processing and any other related area such as computer vision. Though, essentially not correct, image processing may be defined as a process where both input and output are images. At the high level of processing and after some preliminary processing, it is very common to perform some analysis, judgment or decision making or perform some mechanical operation (robot motion). These areas are the domains of artificial intelligence (AI), computer vision, robotics, etc.

Digital image processing has a broad spectrum of applications, such as digital television, photo-phone, remote sensing, image transmission, and storage for business applications, medical processing, radar, sonar, and acoustic image processing, robotics, and computer aided manufacturing (CAM) and automated quality control in industries. Fig. 1.1 depicts a typical image processing system [1,2].

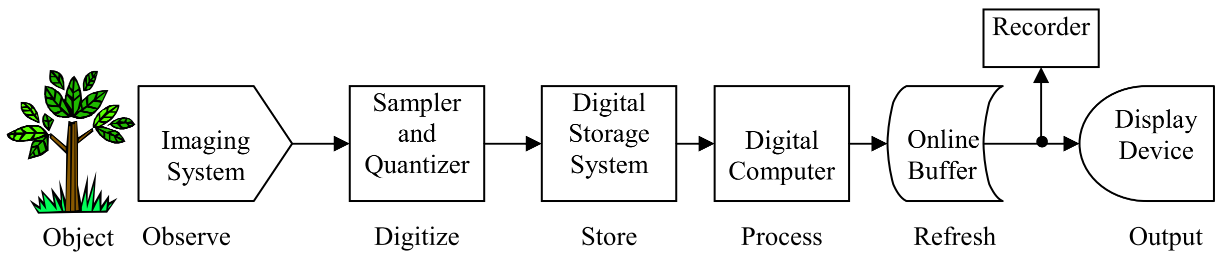

Fig.1.1 A typical digital image processing system

With the exception of image acquisition and display, most of the image processing functions are implemented in software. A significant amount of basic image processing software is obtained commercially. Major areas of image processing are [2]:

(a) Image Representation and Modeling
(b) Image Transform
(c) Image Enhancement
(d) Image Filtering and Restoration
(e) Image Analysis and Recognition
(f) Image Reconstruction
(g) Image Data Compression
(h) Color Image Processing, etc.

Image processing may be performed in the spatial domain or in a transform domain. To perform a meaningful and useful task, a suitable transformer, e.g. discrete Fourier transform (DFT), discrete cosine transform (DCT), discrete wavelet transform (DWT), etc., may be employed. Depending on the application, a suitable transform is used.

Image enhancement techniques are used to highlight certain features of interest in an image. Two important examples of image enhancement are (i) increasing the contrast, and (ii) changing the brightness level of an image so that the image looks better. It is a subjective area of image processing. On the other hand, image restoration is very much objective. The restoration techniques are based on mathematical and statistical models of image degradation. Denoising (filtering) and deblurring tasks come under this category.

Image processing is characterized by specific solutions; hence a technique that works well in one area may totally be inadequate in another. The actual solution to a specific problem still requires a significant research and development.

‘Image restoration and filtering’ is one of the prime areas of image processing and its objective is to recover the images from degraded observations. The techniques involved in image restoration and filtering are oriented towards modeling the degradations and then applying an inverse procedure to obtain an approximation of the original image.

There are various types of imaging systems. X-ray, Gamma ray, ultraviolet, and ultrasonic imaging systems are used in biomedical instrumentation. In astronomy, the ultraviolet, infrared and radio imaging systems are used. Sonic imaging is performed for geological exploration. Microwave imaging is employed for radar applications. But, the most commonly known imaging systems are visible light imaging. Such systems are employed for applications like remote sensing, microscopy, measurements, consumer electronics, entertainment electronics, etc.

An image acquired by optical, electro-optical or electronic means is likely to be degraded by the sensing environment. The degradation may be in the form of sensor noise, blur due to camera misfocus, relative object camera motion, random atmospheric turbulence, and so on [1,2]. The noise in an image may be due to a noisy channel if the image is transmitted through a medium. It may also be due to electronic noise associated with a storage-retrieval system.

Noise in an image is a serious problem. The noise could be AWGN, SPN, RVIN, or a mixed noise. Efficient suppression of noise in an image is a very important issue. Denoising finds extensive applications in many fields of image processing. Conventional techniques of image denoising using linear and nonlinear techniques have already been reported and sufficient literature is available in this area and has been reviewed in the next section. Recently, various nonlinear and adaptive filters have been suggested for the purpose. The objectives of these schemes are to reduce noise as well as to retain the edges and fine details of the original image in the restored image as much as possible. However, both the objectives conflict each other and the reported schemes are not able to perform satisfactorily in both aspects. Hence, still various research workers are actively engaged in developing better filtering schemes using latest signal processing techniques. In the present thesis, efforts have been made in developing some efficient noise removal schemes.

1.2 Noise in Digital Images

In this section, various types of noise corrupting an image signal are studied; the sources of noise are discussed, and mathematical models for the different types of noise are presented.

An image signal gets corrupted with noise during acquisition, transmission, storage and retrieval processes. Acquisition noise is usually additive white Gaussian noise (AWGN) with very low variance. In many engineering applications, the acquisition noise is quite negligible. It is mainly due to very high quality sensors. In some applications like remote sensing, biomedical instrumentation, etc., the acquisition noise may be high enough. But in such a system, it is basically due to the fact that the image acquisition system itself comprises of a transmission channel. So if such noise problems are considered as transmission noise, then it may be concluded that acquisition noise is negligible. The acquisition noise is considered negligible due to another fact that the human visual system (HVS) can't recognize a large dynamic range of image. That is why, an image is usually quantized at 256 levels. Thus, each pixel is represented by 8 bits (1 byte). The present-day technology offers very high quality sensors that don't have noise level greater than half of the resolution of the analog-to-digital converter (ADC), i.e., noise magnitude in time domain, $n(t) < \frac{1}{2} \cdot \frac{V}{2^8}$, where $n(t)$ is the noise amplitude at any arbitrary instant of time t, and V is the maximum output of the sensor and is also equal to the maximum allowed input voltage level for the ADC. That is, for $V = 3.3$ *volts,* the noise amplitude should be less than ~ 6.5 mV. In many practical applications, the acquisition noise level is much below this margin. Thus, the acquisition noise need not be considered.

Therefore, the researchers are mainly concerned with the noise in a transmission system. Usually, the transmission channel is linear, but dispersive due to a limited bandwidth. The image signal may be transmitted either in analog form or in digital form.

If an analog image signal is transmitted through a linear dispersive channel, then the image edges (step-like or pulse like signal) get blurred and the image signal gets contaminated with AWGN since no practical channel is noise free. If the channel is so poor that the noise variance is high enough to make the signal excurse to very high positive or high negative value, then the thresholding operation done at the front end of the receiver will contribute to saturated max and min values. Such noisy pixels will be seen as white and black spots. Therefore, this type of noise is known as salt and pepper noise (SPN). In essence, if analog image signal is transmitted, then the signal gets corrupted with AWGN and SPN as well. Thus, there is an effect of mixed noise.

If the image signal is transmitted in digital form through a linear dispersive channel, then inter symbol interference (ISI) takes place. In addition, the presence of AWGN in a practical channel can't be ignored. This makes the situation worse. Due to ISI and AWGN, it may so happen that a '1' may be recognized as '0' and vice-versa. Under such circumstances, the image pixel values have changed to some random values at random positions in the image frame. Such type of noise is known as *random-valued impulse noise* (RVIN).

The AWGN, SPN, and RVIN are mathematically represented below. The Gaussian noise is given by,

$$n_{AWGN}(t) = \eta_G(t) \tag{1.1}$$

$$\Rightarrow \mathbf{X}_{AWGN}(m,n) = \mathbf{X}(m,n) + \eta_G(m,n) \tag{1.1a}$$

where, $\eta_G(t)$ is a random variable that has a Gaussian probability distribution. It is an additive noise that is characterized by its variance, σ^2, where, σ represents its standard deviation. In (1.1a), the noisy image $\mathbf{X}_{AWGN}$ is represented as a sum of the original uncorrupted image and the Gaussian distributed random noise η_G. When the variance of the random noise η_G is very low, $\eta_G(m,n)$ is zero or very close to zero at many pixel locations. Under such circumstances, the noisy image $\mathbf{X}_{AWGN}(m,n)$ is same or very close to the original image $\mathbf{X}(m,n)$ at many pixel locations (m,n).

Let a digital image $\mathbf{X}(m,n)$, after being corrupted with SPN of density d, be represented by $\mathrm{X}_{SPN}(m,n)$. Then, the noisy image $\mathbf{X}_{SPN}(m,n)$ is mathematically represented as:

$$\mathrm{X}_{\mathrm{SPN}}(m,n) = \begin{cases} \mathbf{X}(m,n) & \text{with probability}, \quad p = 1-d \\ 0 & \quad p = d/2 \\ 1 & \quad p = d/2 \end{cases} \tag{1.2}$$

The impulse noise occurs at random locations (m,n) with a probability of d. The SPN and RVIN are substitutive in nature. A digital image corrupted with RVIN of density d, $\mathbf{X}_{RVIN}(m,n)$, is mathematically represented as:

$$\mathrm{X}_{\mathrm{RVIN}}(m,n) = \begin{cases} \mathrm{X}(m,n) & \text{with probability}, \quad p = 1-d \\ \eta(m,n) & \text{with probability}, \quad p = d \end{cases} \tag{1.3}$$

Here, $\eta(m,n)$ represents a uniformly distributed random variable, ranging from 0 to 1, that replaces the original pixel value $\mathbf{X}(m,n)$. The noise magnitude at any noisy pixel location (m,n) is independent of the original pixel magnitude. Therefore, the RVIN is truly substitutive.

Another type of noise that may corrupt an image signal is the *speckle noise* (SN). In some biomedical applications like ultrasonic imaging and a few engineering applications like synthesis aperture radar (SAR) imaging, such a noise is encountered. The SN is a signal dependent noise, i.e., if the image pixel magnitude is high, then the noise is also high. Therefore, it is also known as multiplicative noise and is given by

$$n_{SN}(t) = \eta(t).S(t) \tag{1.4}$$

or, $$X_{SN}(m,n) = X(m,n) + \eta(m,n).X(m,n) \tag{1.4a}$$

where, $\eta(t)$ is a random variable and $S(t)$ is the magnitude of the signal. The noisy digital image, $\mathbf{X}_{SN}(m,n)$, is represented mathematically in (1.4a). The noise is multiplicative since the imaging system transmits a signal to the object and the reflected signal is recorded. In the forward transmission path, the signal gets contaminated with additive noise in the channel. Due to varying reflectance of the surface of the object, the reflected signal magnitude varies. So also the noise varies since the noise is also reflected by the surface of the object. Noise magnitude is, therefore, more when the signal magnitude is more. Thus, the speckle noise is multiplicative in nature.

The speckle noise is encountered only in a few applications like ultrasonic imaging and SAR, whereas all other types of noise i.e., AWGN, SPN, and RVIN occur in almost all the applications. The AWGN is the most common among all. Under very low noise variance it may look like RVIN. In general, some combinations of AWGN, SPN, and RVIN may represent a practical noise.

In summary, if the image signal is transmitted in analog form, then it is found to be corrupted with AWGN and SPN at the receiver; whereas, the image signal gets contaminated with RVIN if digital image-data is transmitted.

1.3 Study of Image Filters Reported in the Literature

The following three topics are covered in this section.

- An Overview of Digital Image Filters
- A Critical Analysis on the Recent Development
- Conclusion

1.3.1 An Overview of Digital Image Filters

In early days, linear filters were the primary tools in signal and image processing. A linear filter may be described mathematically by using a linear operator $f(.)$ that maps an input signal, $\mathbf{X}$ into an output signal, $\mathbf{Y}$ as:

$$\mathbf{Y} = f(\mathbf{X}) \tag{1.5}$$

The operator $f(.)$ satisfies the superposition principles. Due to the mathematical simplicity of the linear filters, it is easy to design and implement them. However, linear filters have poor performance in the presence of noise that is not additive as well as in systems where system nonlinearities or non-Gaussian statistics are encountered. Linear filters tend to blur edges, do not remove impulsive noise effectively, and do not perform well in the presence of signal dependent noise [1-4]. To overcome these shortcomings, various types of nonlinear filters have been proposed in the literature. For such filters, the operator $f(.)$, described in (1.5), is not a linear function. Different families of nonlinear filters having different characterization have been studied. Most of the currently available image-processing software packages include nonlinear filters. The most popular nonlinear filter is the median (MED) filter. It is computationally efficient, but yields blurred and distorted outputs. Huang *et al.* [5] have proposed a 2-D median filtering that is based on sorting and updating gray level histogram of the picture elements in the window. Subsequently, a fast real-time algorithm has been reported for median filtering of signals and images [6]. In this method, noise filtering based on their local mean and variance for both the additive and multiplicative cases have been suggested. Recently, it has been shown that the use of local statistics works better for removal of additive white and multiplicative noise [7]. However, it is not suitable for the removal of impulse noise as it employs optimal linear approximations.

Another effective algorithm for noise filtering that does not require image modeling for both the additive and multiplicative noise cases has recently been reported [8]. Some statistical properties of a MED filter are analyzed in [9]. It is shown that the MED filter can suppress impulse and low variance Gaussian noise. Kundu *et al*., [10] have proposed a new approach of removing impulse noise from images using a mean filter. This filtering scheme is based on replacing the central pixel value by the general mean of all pixels inside a sliding window. As the probability of noise corruption increases, its performance decreases while that of the median filter remains constant. Besides, if both positive and negative types of impulses are present, the performance of generalized mean filter is unsatisfactory. This filter is also not suitable for simultaneous removal of impulsive and non-impulsive noises. It is reported in the literature [11] that the nonlinear filter based on nonlinear means works well under additive and impulsive noise conditions. Its performance in the presence of signal dependant noise is satisfactory. A novel class of nonlinear filter for image processing known as order statistics (OS) filter has been reported [12]. This filter is used for reduction of white noise, signal-dependent noise, and impulse noise. Another filter known as signal adaptive median filter has been developed [13] that performs better than other nonlinear adaptive filters for different kinds of noise. The adaptive averaging filter proposed in [14] shows poor performance in the presence of impulsive noise and does not remove noise close to the edges. The filtering scheme proposed in [15] cannot suppress the impulsive noise sufficiently, but can preserve the edge better than the mean filter. It is claimed that decision-based order statistics filters can reduce both impulsive and non-impulsive noise and can also enhance blurred edges better than many other OS filters [16]. An adaptive filtering algorithm for the class of stack filters has been proposed [17,18]. Adaptive neural filter [19] removes various kinds of noise such as Gaussian noise and impulsive noise. Adaptive median filters have also been proposed for removing impulse noise and preserving the image sharpness [20]. Two such filters are: the rank-order based adaptive median filter (RAMF), and the size based adaptive median filter (SAMF). A fuzzy operator has been suggested in [21] for enhancement of blurred and noisy images. A new approach to spatial adaptive image restoration, which employs minimum additional computational load compared to the direct techniques, has been proposed [22]. The use of wavelet transform presents a new method for adaptive restoration and yields very good edge preservation in the restored images. A novel algorithm for removing impulse noise from images is presented [23] in which the nature of filtering operation is conditioned on a state variable. The key of the algorithm is a classifier that indicates the probability of impulse corruption by operating on the rank ordered differences within a sliding window. This technique significantly outperforms a number of well-known techniques in the presence of impulsive, Gaussian and mixed type of noise. A reliable and efficient computational algorithm for restoring blurred and noisy images has been proposed by Li and Santosa [24]. By using inverse filtering technique blurred images can be restored. In a recent publication [25], Malladi and Sethian have suggested a unified approach for noise removal, image enhancement, and shape recovery. This approach relies on the level of set formulation of curves and surface motion, which leads to a class of PDE–based algorithm. Enhancement of medical images can be successfully achieved by this technique. Several adaptive Least Mean Square (LMS) filters have also been proposed [26] for noise suppression from images.

A robust approach to image enhancement based on fuzzy logic has been proposed by Choi and Krishnapuram [27]. This approach uses weighted least square error criteria for selecting the filter. A new method for multi-dimensional median filtering is presented [28]. This method employs the reduced vector median filter (RVMF) to a vector data. It has been applied to colored images offering satisfactory performance. A fast algorithm called 1-Norm vector median filtering [29] is presented for filtering of natural images corrupted by spike noise. This algorithm is computationally efficient. An adaptive order statistics filter [30] is proposed for gamma corrupted image sequence. This technique estimates the weights of an adaptive order statistics estimator that adapts to the probability density function of the noise. This approach is quite successful in handling the signal dependent noise. Impulse noise can also be removed using higher order statistics. But this method involves computation of higher order statistical terms, which are computationally expensive [31]. Filtering of impulse noise is also performed using Artificial Neural Network (ANN). It has been reported that a single layer neural network accurately detects the impulse noise of fixed amplitude [32]. However, it doesn't perform well in case of random-valued impulse noise. A plethora of nonlinear and adaptive filtering schemes may be found in literature [32-44]. Many of them are simply some variants of the well-known MED filter. The demerits of these filters are their computational complexities.

For most typical applications, image noise can be modeled with Gaussian, uniform, or impulsive distribution. Gaussian noise can be analytically described and its probability density function has a characteristic of bell shape. In uniform distribution, the gray level values of the noise are evenly distributed across a specific range. Impulsive noise generates pixels with gray level values not consistent with their local neighborhood. In the presence of impulsive noise, linear filters that work with convolution of image with a constant matrix to obtain a linear combination of neighborhood pixel values exhibit poor performance and produce blurred and distorted image output [33]. Popularly used nonlinear MED filter that is implemented across the image even if computationally efficient, suppresses impulse noise, and preserves edges, it removes desirable details in the restored images. To obtain improved performance, various generalized and modified median based filters have been proposed such as multi-stage median (MSM) filter [34], center weighted median (CWM) filter [35], and stack filter [36]. These methods produce good results at low noise conditions, but their performance deteriorates as the noise density increases. One possible solution is to use a filter that is capable of identifying the pixels contaminated by noise prior to filtering and leave noise-free pixels unaltered. Such decision-based median filters realized by threshold operations have been suggested in literature [37-44]. Some of them perform at per with the median filter, whereas, others perform even better. But as the noise density increases, their performance too becomes inferior.

Similarly, removal of Gaussian noise from images is also an important problem in the real world and attempts have been made for developing new efficient methods for this purpose. Discrete Wavelet Transform (DWT) based schemes [45-47] using thresholding is a representative example to restore signals and images from their noisy versions. A novel approach, called ANN-threshold filtering scheme, has been proposed by Zhang [48]. It is an adaptive filter. Since it is based on a neural network, it needs training. Therefore, it is a computational-intensive scheme.

Fuzzy sets and fuzzy logic are proposed by Zadeh [49,50]. The concept of fuzzy logic has revolutionized the research and development in the areas like signal processing, control, instrumentation, etc. [67-70]. Many researchers have used fuzzy logic to develop efficient image filters [81,83,84,93-99,103].

Neural network is another important tool used in signal processing [51,52,63]. Many neural network based noise detectors and noise filters are proposed in the literature [19,32,48,81,84]. A novel impulse detection scheme is proposed by Panda *et al*. [55].

Discrete Wavelet Transform (DWT) [57,58] is a very powerful signal analysis tool. Many researchers have used DWT to design efficient digital image filters [45-47,59, 60]. But they are highly computational intensive algorithms.

The SD-ROM filter of Abreu, *et al*. [43] and the MMEM filter of Han and Lin [71] are some of the landmarks in the field of image filtering. Many novel schemes have been suggested in the recent past. A critical analysis on some of the good filtering algorithms proposed recently is presented.

1.3.2 A Critical Analysis on the Recent Development

The min max exclusive mean (MMEM) [71] developed by W. K. Han and J. C. Lin shows a very good performance in suppressing SPN of high density. It first considers a 3×3 window and rejects the pixels in very high and very low ranges. If nothing more is left, then the window size is increased to 5×5 and the same type of operation is performed. Whatever pixels are left, apart from the very high-valued and low-valued pixels, only these pixels are considered and their average value is calculated. If the average value differs from center pixel value by more than a threshold level, then the filter takes a decision to replace the center pixel with the average value; otherwise the filter keeps the original center pixel value. It may look like a decision-directed ROM filter. But, it is not so. The filtering algorithm is a bit different from the simple ROM. Table1.1 shows the performance of the MMEM filter and other standard filters for comparison purposes.

Table-1.1 PSNR obtained by different filters for SPN corrupted image 'Lena' [71]

SPN Density	MED3×3	MED3×5	Fuzzy [103]	SD-ROM [43]	MMEM [71]
10	34.25	31.23	37.88	**38.98**	38.60
20	29.25	30.60	34.19	36.55	**36.76**
30	23.85	29.72	31.19	33.43	35.41
40	19.18	28.21	28.00	29.88	34.32
50	15.28	24.44	24.97	26.04	32.97
60	12.31	19.09	21.66	21.97	31.76
70	9.95	14.16	18.27	18.12	30.29

This table gives a very serious result. Though the authors claim that the decision-directed filter, MMEM, is very efficient, it shows slightly poorer performance at low SPN density as compared to the SD-ROM filter. This is what is very important to visualize for a designer. Any system that works fine at one extreme end of the input type doesn't work so well at the other extreme end. Thus, there is a scope to investigate and develop very good image filters to suppress the low-density impulse noise.

T. Chan, *et al* [38] have developed a nonlinear filter, called tri-state median (TSM) filter, for preserving image details while effectively suppressing impulse noise. The standard median (MED) filter and the center weighted median (CWM) filter are incorporated into a noise detection framework to determine whether a pixel is corrupted, before applying the filtering operation.

F. Russo has developed an evolutionary neural fuzzy system for noise cancellation in image data [81]. The proposed approach combines the advantages of the fuzzy and neural paradigms. The network structure is designed to exploit the effectiveness of fuzzy reasoning in removing noise without destroying the useful information embedded in input data. The neuro-fuzzy approach is capable of automatic acquisition of knowledge for a given network structure.

F. Farbiz, *et al.*, have proposed a fuzzy logic filter for image enhancement [83]. It is able to remove impulse noise and smooth Gaussian noise. Also, it preserves edges and image details. Though it is claimed that this filter suppresses mixed noise quite effectively, the MSE at the output of this filter reduces to 0.0045 for input mixed noise of AWGN (σ^2=0.0015) and impulse noise 5%. This doesn't show a very high filtering performance.

A data-dependent median filtering method is proposed by Okano, *et al.* to restore images corrupted with SPN [85]. For 20% SPN corrupted Lena image, the filter output has an MSE of 0.0026. Such a filtering performance may be classified in **good** (not very good) category.

H-L Eng and K-K Ma have proposed a noise adaptive soft-switching median (NASM) filter [88]. A soft-switching noise-detection scheme is developed to classify each pixel to be uncorrupted pixel, isolated impulse noise, non-isolated impulse noise or image object's edge pixel. 'No filtering', a standard median (MED) filter or the proposed fuzzy weighted median (FWM) filter is then employed according to respective characteristic type identified. The scheme changes the scrolling window size depending on the impulse noise density. For a 'Lena' image corrupted with 10% impulse noise, the NASM filter shows a PSNR of 42 dB i.e., an MSE of 6.3×10^{-5}. Its performance is **very good** as compared to fixed filters. But it is a highly computational intensive algorithm. For 10% impulse noise density, it takes a computation time of 8.41 seconds when MED3×3 and CWM3×3 take 1.26 seconds and 1.82 seconds, respectively [88]. Since it is a multi-level decision system, it takes much more computation time. Therefore, it is inferred that there is sufficient scope for further research to develop such highly efficient image filters that don't involve much computational complexity.

T. Chen and H-R Wu have developed a scheme for adaptive impulse detection using CWM (AID-CWM) filters [89]. It suppresses SPN as well as RVIN. Its filtering performance is compared with standard filters, and the PSNR values are shown in Table 1.2. The input image is 'Lena' with 20% impulse noise.

Table 1.2 The Filter Performance [89]
(Peak Signal to Noise Ratio (PSNR) in dB)

Filter	**RVIN (20%)**	**SPN (20%)**
MED	31.33	31.42
CWM	32.42	30.39
ROM	**34.71**	**36.15**
TSM	34.13	31.84
AID-CWM	**34.76**	**36.54**

It may be seen that the performance of an ROM filter is comparable to that of the AID-CWM filter. Therefore, such an adaptive decision-directed filtering scheme may not be highly appreciated.

T. Chen and H. R. Wu have designed a space variant median filter [90] for the restoration of impulse noise corrupted images. It is a generalized framework of median based switching scheme, called multi-state median (MSM) filter. By using simple thresholding logic, the output of the MSM filter is adaptively switched among those of a group of CWM filters that have different center weights. Thus, it is equivalent to an adaptive CWM filter with a space varying center weight that is dependent on local signal statistics. At 10% impulse noise density, it shows a PSNR performance of 28 dB as against 22.5 dB for the MED filter. In other words, it gives an output MSE of 0.0016 while the MED filter gives 0.0056.

T. Chen and H. R. Wu have reported a partition based median type filter [86] for suppressing noise in images. The observed sample vector at each pixel location is classified into one of M mutually exclusive partitions, each of which has a particular filtering operation. The observation signal space is partitioned based on differences defined between current pixel value and the output of CWM filters with variable center weights. It works satisfactorily in reducing AWGN as well as mixed noise. For a test image ('Lena face') with AWGN of σ^2=0.12, the filter output has an output MSE of 0.0016, i.e. a PSNR of 27.88 dB. Thus, its performance is shown to be better than that of MED, FM, NLMS-L and PWS filters. This filter also successfully suppresses mixed noise and achieves a PSNR of 28.32 dB and is claimed to be better than MED, FM, NLMS-L and WOS filters.

A recursive LMS L-filter is proposed by Chen and Wu [87] for noise removal in images. The coefficients derived for non-recursive filtering are not optimal for recursive implementation, where the estimate of current pixel depends on the past outputs of the filter. To combat this, analogous to the design of adaptive IIR filters, the optimization scheme referred to as equation error formulation is employed. The recursive filter performs better in suppressing noise than its non-recursive counter part.

M. Ma, *et al,* have developed a fuzzy hybrid filter (FHF) [95] for removal of impulse noise from highly corrupted images. A noise ratio in the filter window is defined and detected. The FHF comprises of a novel detection scheme, a fuzzy decision based on fuzzy rules. The hybrid filter also makes use of MED filter and MMEM filter depending on the noise ratio. The filter works for SPN and mixed noise conditions. This filter achieves a PSNR of 30.87 dB for removing SPN (under mixed noise condition) from the 'Lena' image, while a MED3×3 filter achieves 28.10 dB.

Zhang and Karim have developed a new impulse detector [92] for switching median filter. It is based on the minimum absolute value of four convolutions obtained using one-dimensional Laplacian operators. For a 'bridge' image corrupted with 10 % impulse noise, this scheme achieves an output MSE of 0.0011 as compared to the MED filters performance of 0.0027. This may be classified as a **good** filter; not a very good filter.

F. Russo [93] has developed a novel image enhancement technique combining image sharpening and noise reduction. The method is based on a multiple output system that adopts fuzzy models in order to prevent the noise increase during the sharpening of the image details. It shows good performance in suppressing AWGN. This filter gives an MSE of 0.0005. Thus, its performance is **quite good**.

D.V.D. Ville, *et al.* [97] have developed an image filter for the noise reduction of images corrupted with additive noise. The filter consists of two stages. The first stage computes a fuzzy derivative for 8 directions. The second stage uses these fuzzy derivatives to perform fuzzy smoothing by weighting the contributions of neighboring pixel values. Both the stages are based on fuzzy rules.

F. Russo and A. Lazzari [98] have developed a robust filtering scheme, based on hybrid fuzzy networks, for suppression of impulse noise in images. This method combines rank ordering of the input data and noise correction based on fuzzy reasoning. This hybrid scheme works for SPN as well as RVIN. For SPN of density 0.45, this filter gives an output MSE of 0.0045.

F. Russo has proposed a new approach to the restoration of images corrupted with AWGN [99]. This method combines a nonlinear algorithm for detail preserving smoothing of noisy data and a technique for automatic parameter tuning based on noise estimation. As a key feature, this method doesn't require any *a priori* knowledge about the amount of noise corruption. For AWGN of σ=0.0392, the MSE at the output of the filter is 7.12×10^{-4} in case of 'Boats' image; and 5.97×10^{-4} in case of 'Cameraman' image. It may be classified as a **very good** filter. But it is a highly computational intensive algorithm.

M. Kazubek [101] has developed a wavelet-domain denoising algorithm using thresholding and Weiner filtering. It is shown that the denoising performance increases by pre-processing the images with a thresholding operation. For a 'Lena' image corrupted with AWGN of $\sigma = 0.0196$, it shows a PSNR of 30.1 dB, i.e. the MSE at this filter output is 9.77×10^{-4}. This filter may be classified in **good** category. But it involves very high computational complexity as wavelet transform coefficients are to be calculated in each window. The improvement in the filter performance is not so high though it requires a large volume of computation.

Aizenberg and Butakoff have developed a novel impulse detector based on rank-order criteria [100]. The scheme is called a differential rank impulse detector (DRID). At 1%, 5% and 20 % of SPN, this DRID plus median filtering scheme gives a PSNR of 49.4 dB, 43.84 dB and 36.64 dB respectively. This may be classified as a **very good** filter. Its performance is really very good at low noise density. Further, the computational complexity involved is also not so high.

Another impulse detection scheme, based on pixel-wise MAD (**m**edian of **a**bsolute **d**eviation from median), is proposed by Crnojevic, *et al* [106]. This algorithm is free of varying parameters, requires no previous training or optimization, and successfully removes all types of impulse noise. For 'Lena' image corrupted with 20% SPN, this scheme achieves a PSNR of 33.20 dB (slightly poorer than SD-ROM of Abreu, *et al.*). For the same test image corrupted with 20% RVIN, it achieves a PSNR of 32.82 dB (slightly better than SD-ROM). This shows that this scheme is better than the SD-ROM only if the impulse noise is random-valued. This scheme may be classified as a **good** filter.

1.3.3 Conclusion

It is observed that the researchers have adopted different methodologies: Order statistics, neighborhood relationship, fuzzy logic, neuro-fuzzy system, etc. Some filters are good at suppressing impulse noise whereas some others are good at suppressing additive Gaussian noise. Even, there is a third category of filters that are efficient in suppressing mixed noise.

Many researchers have developed very good image filters to suppress impulse noise medium (10-20%), high (20-30%) and very high (30-40%) noise densities and even some have designed filters for reducing impulse noise of extremely high density (>40%). But these filters don't show very good performance at low (<5%) and at very low (<1%) impulse noise densities. Therefore, there is a scope to develop efficient filters to suppress impulse noise of low and very low density.

When good and very good filters designed to suppress AWGN are analyzed, it is felt that their filtering performance is not so high as compared to the extremely high computational complexity involvement. Therefore, there is sufficient scope to investigate further and develop more efficient digital image filters to suppress AWGN without involving high computational complexity.

Thus, it may be concluded that there is enough scope to develop better filtering schemes, with very low computational complexity that may yield high noise reduction as well as preserve edges and fine details of the image under low and very low noise power conditions.

1.4 The Problem Statement

In the present research work, efforts are made to develop many efficient filtering schemes to suppress AWGN, SPN, RVIN and MN. The speckle noise is not considered in this work. Such a noise doesn't appear in most of electronic applications and communication systems. The present work mainly focuses on efficient suppression of AWGN, SPN, RVIN and MN under low noise conditions. The present-day state-of-art technology offers very high quality photo sensors, high quality electronic circuitry, e.g., system on chip (SOC), and high quality channel as well. Therefore, the noise level has drastically reduced.

In the last two decades, many researchers have attempted to develop filters to suppress high variance AWGN and high density SPN. But the filters that are quite efficient at high noise levels don't perform so well at low noise levels. Therefore, it is very important to design and develop highly efficient image filters that suppress low power noise quite effectively. Further, it is essential to develop efficient filters to suppress mixed noise since the practical systems suffer from such a type of noise.

For real time applications like television, photo-phone, etc. it is essential to reduce the noise power as much as possible and to retain the fine details and the edges in the image as well. Moreover, it is very important to have very low computational complexity so that the filtering operation is performed in a short time for online and real-time applications.

Thus, the problem taken for this doctoral research work is "*Development of Efficient Image Filters to suppress (i) SPN and AWGN and (ii) RVIN for Online and Real-Time Applications"*.

Since linear filters don't perform well, nonlinear filtering schemes are adopted for achieving better performance. In addition, various adaptive filtering techniques are employed that adapt to the noise type, the noise power level and the local statistics of the image. Therefore, the *objective* of this research work is *to develop some novel nonlinear and adaptive digital image filters for efficient noise suppression under low and very low noise power conditions.*

1.5 Image Metrics

The quality of an image is examined by objective evaluation as well as subjective evaluation. For subjective evaluation, the image has to be observed by a human expert. The human visual system (HVS) is so complicated that it is not yet modeled properly. Therefore, in addition to objective evaluation, the image must be observed by a human expert to judge its quality.

There are various metrics used for objective evaluation of an image. Some of them are mean squared error (MSE), root mean squared error (RMSE), mean absolute error (MAE) and peak signal to noise ratio (PSNR).

Let the original noise-free image, noisy image, and the filtered image be represented by $X(m,n)$, $Y(m,n)$, and $\widetilde{X}(m,n)$, respectively. Here, *m* and *n* represent the discrete spatial coordinates of the digital images. Let the images be of size $M \times N$ pixels, i.e. $m=1,2,3,\ldots,M$, and $n=1,2,3,\ldots,N$. Then, MSE and RMSE are defined as:

$$MSE = \frac{\sum_{m=1}^{M}\sum_{n=1}^{N}\left(\widetilde{X}(m,n)-X(m,n)\right)^{2}}{M \times N} \tag{1.6}$$

$$RMSE = \sqrt{MSE} \tag{1.7}$$

The MAE is defined as:

$$MAE = \frac{\sum_{m=1}^{M}\sum_{n=1}^{N}\left|\left(\widetilde{X}(m,n)-X(m,n)\right)\right|}{M \times N} \tag{1.8}$$

The PSNR is defined in logarithmic scale, in dB. It is a ratio of peak signal power to noise power. Since the MSE represents the noise power and the peak signal power is unity in case of normalized image signal, the image metric PSNR is defined as:

$$PSNR = 10 \cdot \log_{10}\left(\frac{1}{MSE}\right) \tag{1.9}$$

Another image metric, a noise reduction factor, usually expressed in dB, is the **noise reduction in dB** (NRDB). It is given by:

$$NRDB = 10.\log_{10}\left(\frac{\text{noise power at the input of the filter}}{\text{noise power at the output of the filter}}\right) \tag{1.10}$$

$$\Rightarrow NRDB = 10 \cdot \log_{10}\left(\frac{MSE_{in}}{MSE_{out}}\right) \tag{1.11}$$

$$\Rightarrow NRDB = 10.\log_{10}\left(\frac{MSE(Y, X)}{MSE(\tilde{X}, X)}\right) \tag{1.11a}$$

where, MSE_{in} and MSE_{out} are the mean squared error at the input and output of the filter. Equivalently, they are the noise power at the input and the output of the filter. Thus, the image metric, NRDB, is a very important parameter for objective evaluation of a filter's performance. It is not important to find the MSE at the output. Rather, it is very important to see how much the noise power has been attenuated by the filter. This is what the parameter NRDB talks about.

Though these image metrics are extensively used for evaluating the quality of a restored (filtered) image and thereby the capability and efficiency of a filtering process, none of them gives a true indication of noise in an image. It is very important to note that RMSE, MAE and PSNR are all related to MSE. Thus, an objective evaluation with only the MSE metric is sufficient enough. Many researchers have used PSNR as the image metric. But, for low noise conditions, the performance of many filters will almost be the same in dB range if PSNR is evaluated. Therefore, only MSE is used to examine the performance of an image filter in this thesis. Further, a slight modification to MSE is proposed to comply with HVS. If there is a small dc offset in the restored image, then MSE metric gives a reasonably large error. In fact, the restored image may not have any noise. As far as HVS is concerned, a small dc offset does not contribute to any noise; rather it may be a better image, for instance, a dark image might have been enhanced by providing a positive dc offset. To nullify the effect of dc offset in a restored image, a new image metric, called mean restored mean squared error (MR-MSE), is suggested here.

Let $avg1$ and $avg2$ represent the average pixel values in the original and the restored image. Then, the mean restored filtered signal, $\widetilde{X}'$, is given by:

$$\widetilde{X}' = (avg1/avg2).\widetilde{X} \tag{1.12}$$

The image metric MR-MSE is, then, given by:

$$\text{MR-MSE}(X, \widetilde{X}) = \text{MSE}(X, \widetilde{X}') \tag{1.13}$$

This proposed image metric alongwith MSE is used to evaluate the performance of various filters in this thesis.

Another parameter that is usually employed in evaluating the performance of a digital image filter meant for impulse noise suppression is the **p**ercentage of **s**poiled **p**ixels (PSP). It is defined as:

$$PSP = \frac{\text{Number of uncorrupted pixels being distorted due to the filtering operation}}{\text{Total number of uncorrupted pixels in the image}} \tag{1.14}$$

The image metrics: MSE, PSNR, PSP and the proposed metric MR-MSE are used in this thesis to evaluate the performance of a digital image filter. However, only the MSE and MR-MSE are used in most occasions in the present research work. Of course, the significance of PSP in evaluating an impulse noise filter is high enough and, thus, it can’t be ignored. But, when a filter is designed for AWGN, this parameter can’t be used.

1.6 Noise Conditions for Computer Simulation

The following topics are covered in this section.

- Choosing a Standard Test Image
- Noise Level Classification
- Conclusion

1.6.1 Choosing a Standard Text Image

It is very important to test the performance of a filter. Usually, a digital image filter is tested by computer simulation before a prototype is developed. There are various standard test images, used extensively in literature, for this purpose. They are ‘Lena’, ‘Lisa’, ‘Boats’, ‘Cameraman’, ‘Clown’, ‘House’, etc. ‘Lena’ is the most widely used image among all. There are three types of images, derived from the original Lena, used in literature. They are:

(i) Lena (512×512 pixels)
(ii) Lena (256 ×256 pixels)
(iii)Lena face (200×200 pixels)

The first one is the original image with high resolution; whereas, the second one is a low resolution version of the original image. The third image, Lena face, is a 200×200 slice taken from the original high resolution image showing the face portion. In the recent past, many researchers have used the ‘Lena face’ image as the test image. Its image complexity is moderate; neither as low as that of ‘House’ nor as high as that of ‘Cameraman’. The ‘Lena face’ has high image complexity as compared to the original ‘Lena’. Therefore, in the recent past, this image has gained much popularity. This may be taken as a very good standard test image since there are many features and the feature sizes are not very small or very large. These properties of the ‘Lena face’ are well appreciated and mainly this image is used as the test image in this thesis. The original ‘Lena’ image and the selected test image ‘Lena face’ are shown in Fig.1.2.

In literature, many researchers report the filter performance using various test images. It may be well understood that if a filter’s performance is very good for ‘House’ test image, then it is good for ‘Lena’ image and fair for ‘Cameraman’ image. It is due to low, moderate and high image complexity of the ‘House’, ‘Lena’, and ‘Cameraman’ images, respectively. So, there is no need to evaluate the performance of a filter taking different test images. Rather, the simulation may be carried out using only the ‘Lena face’ image that has higher image complexity than the original ‘Lena’ image.

a	b

Fig. 1.2 (a) The original Lena image
(b) The ‘Lena face’ Test Image

1.6.2 Noise Level Classifications

If the 'Lena face' is taken as the standard test image, then the next question arises: *How much noise should be added to this image to simulate a practical noise condition*? It is inferred in Section-1.2 that the most serious noise among all is the channel noise. Normally, the signal-to-noise ratio (SNR) is better than 20dB in a communication channel. Quite seldom, it becomes poorer than 10dB. That is why, an SNR poorer than 10dB represents a high noise condition whereas an SNR better than 20dB represents a low noise condition. Table1.3 gives a comprehensive list of noise level classifications.

Table-1.3 Noise Level Classifications

Noise Level	**Signal-to-Noise Ratio (SNR)**
Very Low	≥ 30 dB
Low	≥ 20 dB
Medium	≥ 15 dB
High	≥ 10 dB
Very High	≥ 5 dB
Extremely High	< 5 dB

This table gives a rough and fuzzy classification. Yet, it represents practical noise conditions. Therefore, this classification may be used for simulation purposes.

The standard test image 'Lena face' is taken for the simulation purpose. Various types of noise are added to it. In case of SPN and RVIN, the noise density is varied whereas; the noise variance is varied in case of AWGN. The noise power and the SNR are calculated in each case. The noise simulation results for salt and pepper noise are presented in Table-1.4.

Table-1.4 The Noise Levels at various SPN Densities

SPN Density (%)	Signal Power	Noise Power	SNR (dB)	Noise Level Classification
0.1	0.2400	0.0002638	29.5891	Low (Very Low)
0.5		0.0013	22.5527	Low
1		0.0029	19.1781	Medium (Low)
2		0.0060	16.0206	Medium
3		0.0085	14.5079	Medium (High)
4		0.0115	13.1951	High
5		0.0151	12.0123	High
6		0.0180	11.2494	High
7		0.0210	10.5799	High
8		0.0240	10.0000	High (Very High)
9		0.0263	9.6026	Very High
10		0.0300	9.0309	Very High
15		0.0438	7.3874	Very High
20		0.0586	6.1231	Very High
25		0.0740	5.1098	Very High (Extremely High)
30		0.0883	4.3425	Extremely High
35		0.1020	3.7161	Extremely High
40		0.1163	3.1463	Extremely High

These noise conditions are plotted in Fig.1.3. In most practical situations, the SNR is better than 20dB and seldom falls below 10 dB. That is why, SPN density of 1%-8% should usually be considered. To simulate low noise conditions SPN density below 1% should be taken. In essence, it may be stated, in general, that

(a) SPN of density below **0.1%** may be regarded as **very low** noise condition
(b) SPN of density **0.1-1%** may be regarded as **low noise** condition
(c) SPN of density **1-3%** may be regarded as **medium noise** condition
(d) SPN of density **3-10%** may be regarded as **high noise** condition

Therefore, the proposed filters are more often tested in subsequent chapters using SPN density below 10%. A plot of SNR versus the SPN density is given in Fig.1.3. This plot clearly indicates the fact that 10% SPN is a high noise condition.

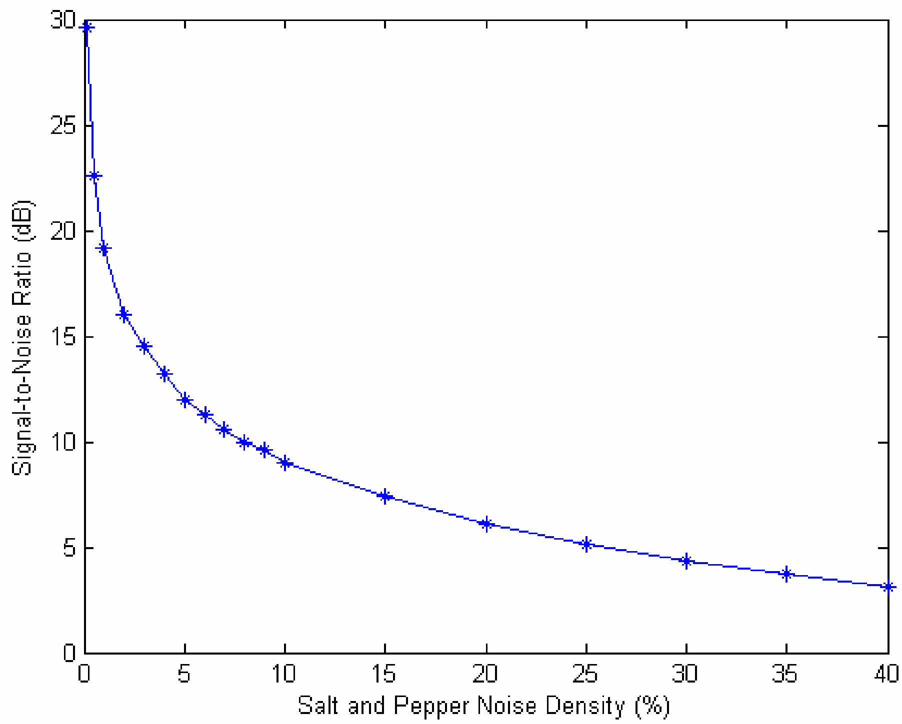

Fig.1.3 SNR versus Noise Density for Salt and Pepper Noise

The RVIN of varying density is simulated on the 'Lena face' test image. The results are presented in Table1.5. A plot of SNR versus the RVIN density is given in Fig.1.4.

Table 1.5 The Noise Levels at Various RVIN Densities

RVIN Density (%)	Signal Power	Noise Power	SNR (dB)	Noise Level Classification
0.1	0.2400	0.000123	32.9031	Very Low
0.5		0.00073	25.1689	Low
1		0.0013	22.6627	Low
2		0.0026	19.6524	Medium (Low)
3		0.0036	18.2391	Medium
4		0.0049	16.9002	Medium
5		0.0063	15.8087	Medium
6		0.0071	15.2895	Medium (High)
7		0.0087	14.4069	High
8		0.0102	13.7161	High
9		0.0111	13.3489	High
10		0.0129	12.6962	High
15		0.0189	11.0375	High
20		0.0240	10.0000	High
25		0.0306	8.9449	Very High
30		0.0375	8.0618	Very High
35		0.0446	7.3088	Very High
40		0.0505	6.7692	Very High

It may be observed that the noise power reduces to approximately 40%-45% of that for SPN with the same noise density. Therefore, a higher random-valued impulse noise density is required to have the same SNR as in the case of fixed valued impulse noise. In general, it may be stated that

(a) RVIN of density below **0.1%** may be regarded as **very low** noise condition
(b) RVIN of density **0.1-1%** may be regarded as **low noise** condition
(c) RVIN of density **1-5%** may be regarded as **medium noise** condition
(d) RVIN of density **5-20%** may be regarded as **high noise** condition

Therefore, the developed filters are tested in subsequent chapters using RVIN density below 20%.

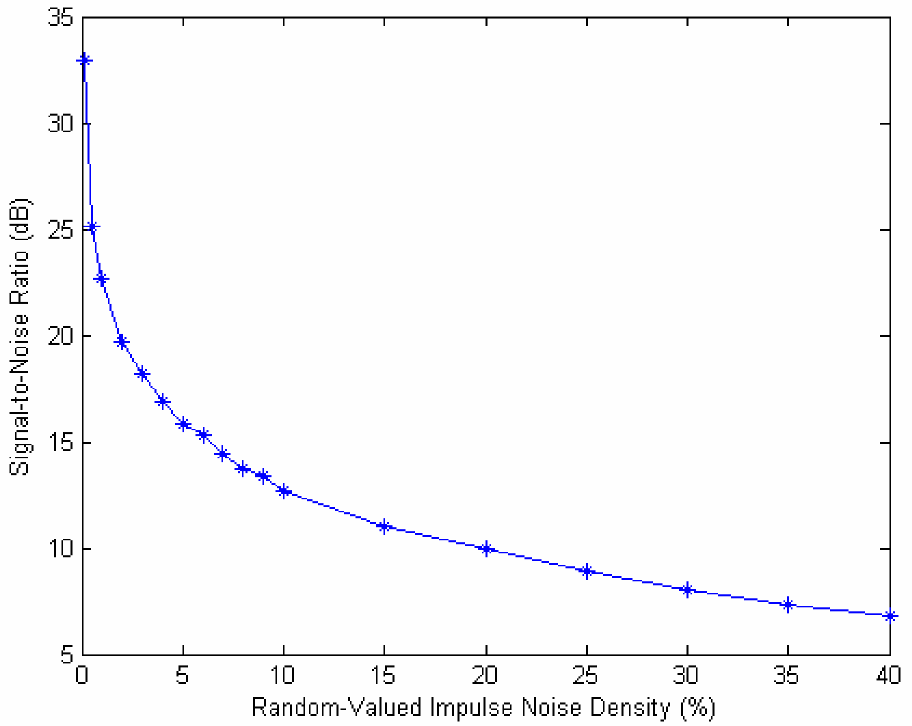

Fig.1.4 SNR versus Noise Density for Random-Valued Impulse Noise

Next, the test image is corrupted with additive white Gaussian noise. The variance of AWGN is varied from 0.001 to 0.50 and the noise level in each case is found out. The results are presented in Table1.6. A plot of SNR versus noise variance is given in Fig.1.5. The test image with simulated additive white Gaussian noise of variance 0.001, 0.01, 0.1 and 0.3 are shown in Fig.1.6.

Table 1.6 The Noise Levels at Various AWGN Noise-Variance Values

AWGN Variance	Signal Power	Noise Power	SNR (dB)	Noise Level Classification	Comment
0.001	0.2400	0.0098	13.8899	Medium-High	Similar to RVIN
0.002		0.0098	13.8899	Medium-High	
0.003		0.0098	13.8899	Medium-High	True AWGN
0.004		0.0098	13.8899	Medium-High	
0.005		0.0098	13.8899	Medium-High	
0.006		0.0099	13.8458	Medium-High	
0.007		0.0099	13.8458	Medium-High	
0.008		0.0099	13.8458	Medium-High	
0.009		0.0099	13.8458	Medium-High	
0.01		0.0100	13.8021	Medium-High	
0.02		0.0103	13.6737	Medium-High	
0.03		0.0107	13.5083	High	
0.04		0.0115	13.1951	High	
0.05		0.0124	12.8679	High	
0.06		0.0133	12.5636	High	
0.07		0.0146	12.1586	High	
0.08		0.0160	11.7609	High	
0.09		0.0177	11.3224	High	
0.10		0.0193	10.9465	High	
0.15		0.0314	8.8328	Very High	
0.20		0.0472	7.0627	Very High	
0.25		0.0672	5.5284	Very High	
0.30		0.0897	4.2742	Extremely High	
0.35		0.1145	3.2141	Extremely High	Saturated Noise (SPN)
0.40		0.1405	2.3253	Extremely High	
0.45		0.1659	1.6036	Extremely High	
0.50		0.1904	1.0054	Extremely High	

The above table reveals many facts on the range of variance for AWGN to be used for simulation purposes. First of all, variance more than 0.3 gives saturated noise and, hence, it contributes to SPN. Even the image gets blurred. Such noise conditions don't arise in any practical situation. In the other extreme end, the AWGN of variance less than 0.003 gives an effect similar to that of a random-valued impulse noise. Thus, to simulate a true AWGN, the noise variance should be between **0.003** and **0.3**. It may be noted that there is no appreciable change in the net noise power when the variance of the added Gaussian noise is varied from 0.001 to 0.1. This happens so because of low precision (8-bit) image data. As far as the human visual system (HVS) is concerned, this much precision is enough. Thus, it is concluded that

(a) AWGN of variance below **0.003** may be regarded as **RVIN**
(b) AWGN of variance **0.003-0.03** may be regarded as **medium-high noise** condition
(c) AWGN of variance **0.03-0.1** may be regarded as **high noise** condition
(d) AWGN of variance **0.1-0.3** may be regarded as **very high noise** condition
(e) AWGN of variance above **0.3** may be regarded as **SPN**

Therefore, the noise variance should be varied from **0.003** to **0.3** to simulate the effect of a true AWGN. But a variance larger than 0.1 gives a very high noise condition (SNR less than 10dB). Such a situation seldom occurs in practice. Thus, the variance is restricted to a range, from **0.003** to **0.1**, to simulate AWGN in the subsequent chapters.

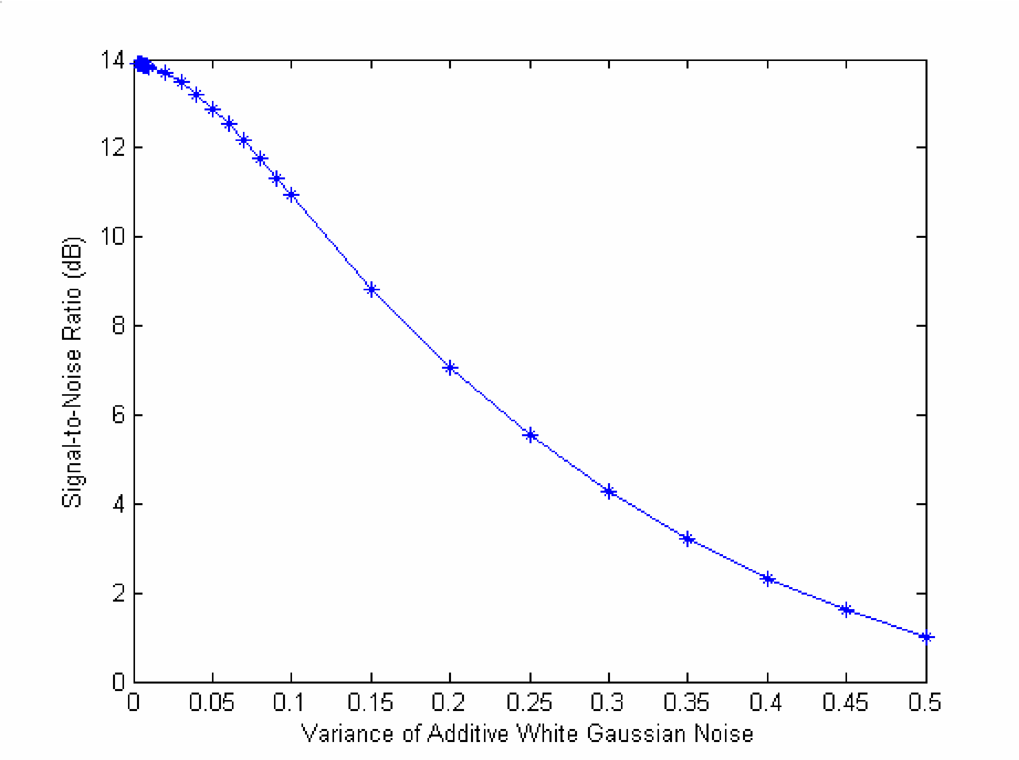

Fig.1.5 SNR versus Noise Variance for Additive White Gaussian Noise

The noisy images in Fig.1.6 give a lot of information. Fig1.6 (a) shows the image being corrupted with AWGN of variance, 0.001. Only a few pixels have been corrupted in this image. In addition, the noise level is so less that the overall effect seems to be that of a low density RVIN. Fig.1.6 (b) shows the image being corrupted with AWGN of variance, 0.01 and Fig.1.6 (c), the image being corrupted with AWGN of variance, 0.1. These two images show a good simulated result of additive noise corruption. The noisy image shown in Fig.1.6 (d) is the test image with AWGN of variance, 0.3. The noise level is high enough. The noise saturation effect has just started at this value of variance. Some of the pixels in this image have been corrupted with SPN. A little blurring effect is also seen in this image. So, this value of variance should be taken as a cutoff point. For all simulation purposes, AWGN of variance less than 0.3 should be taken. It is better if a variance less than or equal to 0.1 is taken to simulate AWGN so that a pure additive noise without any blurring is simulated.

Continued in the next page.

Continued from the previous page

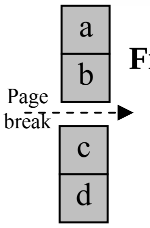

Fig.1.6 Effect of Simulated AWGN on the Test Image, 'Lena face'

(a) with variance=0.001 (b) with variance=0.01
(c) with variance=0.1 (d) with variance=0.3

1.6.3 Conclusion

The following conclusions are drawn.

(i) 'Lena face' should be taken as a standard test image that has moderate image complexity.

(ii) Considering practical channel noise levels, a rough and fuzzy noise level classification (low, medium, high, etc.) is presented.

(iii) (a) SPN of density less than 10% should be used to simulate a practical situation.

(b) SPN of density of less than 1% should be used to simulate a low noise system.

(iv) (a) RVIN of density less than 20% should be used to simulate a practical situation.

(b) RVIN of density less than 2% should be used to simulate a low noise system.

(v) (a) Additive Gaussian noise of variance, from 0.003 to 0.30, should be used to simulate a true AWGN effect in an image.

(b) AWGN of variance below 0.1 should be used to simulate a practical noisy system.

(c) AWGN of variance, from 0.003 to 0.03, should be used to simulate a low noise system.

1.7 Chapter-wise Organization of the Thesis

The chapter-wise organization of the rest part of the thesis is outlined.

Chapter-2: Order Statistics Filters

- *Preview*
- *Fundamentals of OS Filters*
- *Mean and Median Filters*
- *ROM Filters*
- *L-filters*
- *WROM Filters*

  Various WROM filters are developed for efficient noise suppression. They show high filtering performance as compared to MAV, MED and ROM filters without much computational complexity.
- *Conclusion*

Chapter-3: Development of Decision-Directed Filters for Impulse Noise Suppression

- *Preview*
- *Introduction to Decision-Directed Filters*
- *Second Order Difference based Decision Directed Median Filter (SOD-DDMF)*

The second order difference (derivative) based decision directed filter proposed by Panda *et al.*, [53] is modified to give better performance. The threshold value, required for the decision making, is made adaptive depending on the noise level. An empirical formula is also derived for the threshold value [P1].

- *Probability based Impulse Noise Detection (PIND) Algorithm*

  A simple probability based impulse detection scheme is proposed. This algorithm shows excellent performance at low SPN density.
- *Deviation based Impulse Noise Detection (DIND) Algorithm*

  In the DIND algorithm, an absolute deviation from the expected value, computed with a WROM filter, is found. If the **a**bsolute **d**eviation at the **c**enter (ADC) is found to be more than a threshold value, then an impulse is supposed to be present. This algorithm is robust enough to detect SPN in the presence of AWGN [P2].
- *Conclusion*

Chapter-4: Development of Adaptive Image Filters

In order to overcome the shortcomings of fixed filters, adaptive filters [61-65] are designed that adapt themselves to the changing conditions of signal and noise. The following two types of adaptive filters are developed for efficient noise suppression.

- *Preview*
- *Fundamentals of LMS Adaptive Filters*
  - *Adaptive LMS L-Filter*

    LMS adaptive L-filter is proposed by Kotropoulos and Pitas [26] to update the filter weight for online image processing. This filter needs a reference noise-free image frame. The reference image should be very similar to the image that has to be filtered, i.e. a very high degree of correlation must be there between the reference frame and the image frame that has to be filtered

- *Development of an Efficient OS-LMS Adaptive Image Filter*

  In the present research work, a novel LMS adaptive image filter is proposed that gets trained with totally a different type of image. Various order statistics are given as the input to the adaptive filter. The training may not be required always. Even an off-line training may give a very good filter performance.

- *Fundamentals of Fuzzy Logic*
- *Designing Fuzzy Adaptive Image Filters*

  In the recent past, fuzzy filters have gained high popularity [81,83,84,94,95,97,98]. Many fuzzy adaptive image filters have been developed during the last five years. But they involve high computational complexity and their performance is slightly better than the simple OS filters. Instead of having a fuzzy inference system, Kwan and Cai [94] designed fuzzy MAV and fuzzy MED filters by associating fuzzy weights with the order statistics.

  The WROM filters [P4], discussed in Chapter-2, show much better performance than any standard OS filters. Their performance can still be improved by associating fuzzy weights to the order statistics. Two different types of membership functions are chosen and thus the following two types of fuzzy adaptive filters are developed:

  - *FWROM with triangular membership function (FWROM-T)*
  - *FWROM with Gaussian membership function (FWROM-G)*

  The FWROM-G shows slightly better performance than the FWROM-T. Since the computational complexity for calculating Gaussian membership function is much more than that needed for a triangular membership function, it is suggested to use FWROM-T for real time applications [P5].

- *Conclusion*

Chapter-5: Conclusion

- *Preview*
- A Comparative Study
- Conclusion

  The different filters developed are comparatively analyzed. Finally, it is concluded that many novel nonlinear and adaptive digital image filters are designed to suppress various types of noise under very low and low noise power conditions.
- Scope for Future Work

1.8 Conclusion

In this introductory chapter, the fundamentals of digital image processing, sources of noise and types of noise in an image, the existing filtering schemes and their merits and demerits and the various image metrics are studied. In communication applications like television and photo-phone, the noise power may be very low. Digital image filters performing quite well under such low noise conditions are not available in the literature. Therefore, it is decided to make efforts to develop efficient filters to suppress low-density impulse noise and low variance additive noise.

A new image metric, the mean restored mean squared error (MR-MSE), is defined and the advantage of using such a metric for objective evaluation is discussed. The 'Lena face' is taken as the standard test image since it possesses moderate image complexity.

Extensive computer simulation is carried out to find what amount of impulse noise density and what variance of additive white Gaussian noise should be used to simulate very low, low, medium and high noise conditions. This idea enables a designer to simulate a practical noise condition and thus to test a filter for a practical application.

CHAPTER-2

Order Statistics Filters

Preview

Order statistics (OS) filters are an important class of nonlinear filters used in 1-D and 2-D signal processing. The MED filter is the most well-known member of this class. Various OS filters are studied in this chapter. Then, weighted rank-ordered mean (WROM) filters [P3] are developed for efficient suppression of RVIN, AWGN, SPN and mixed noise.

The following topics are presented in this chapter.

- *Fundamentals of OS Filters*
- *Mean and Median Filters*
- *ROM Filters*
- *L-filters*
- *Development of WROM Filters*
- *Conclusion*

2.1 Fundamentals of OS Filters

Order Statistics (OS) filters are a class of nonlinear digital filters which have been proved useful in applications where robust signal smoothing is required. OS filters may be viewed either as a modification to linear FIR (finite-impulse response) filters (the samples are algebraically ordered prior to linear filtering), or as a generalization of the median (MED) filter (all of the ordered samples are utilized instead of a single one) [73]. While there exist many signal processing domains where OS filters offer advantages over linear filters, there are some other situations where the converse holds, or where the filters produce similar results.

The MED filter [74] was proposed by Tukey in 1971 as a smoothing device for discrete signals. In particular, he noted this filtering process to be quite effective in suppressing impulse noise as well as preserving the locally monotonic signal structures often containing significant information. The MED filter has been extensively used in image processing, particularly for suppressing impulse noise in an image. Many variants of the MED filter have also been proposed. One modified version of it is the center weighted median (CWM) filter [35]. The ranked-ordered mean (ROM) is another variant.

Gallagher and Wise [75], and Tyan [76] have demonstrated certain deterministic properties of MED filter. They showed that certain signals, called *root signals*, are invariant to median filtering if they possess a minimum degree of smoothness (local monotonicity), and that repeated application of the filter to any finite-length signal converges to a root in a finite number of passes.

These results gave the median filter a theoretical ground work, and spurred the development of a number of extensions and generalizations, including *rank-order filters* (RO filters), where a single order statistics (generally other than the median) from the windowed data set is reproduced at each signal coordinate [77], and the more general order statistics (OS) filters (also called L-filter) [78,80,26], where a linear combination of the order statistics is taken as the filter output at each coordinate.

OS filters are interesting because:

a) they offer a compromise in performance between linear filters and MED filters;
b) it is possible to design an optimal (among OS filters) MSE filter for estimating a signal immersed in noise, whose performance is superior to linear filtering.

There exists a vast body of literature on use of order statistics for parameter estimation [80]. This provides a strong justification for using moving function of OS to recover smooth varying signals immersed in noise.

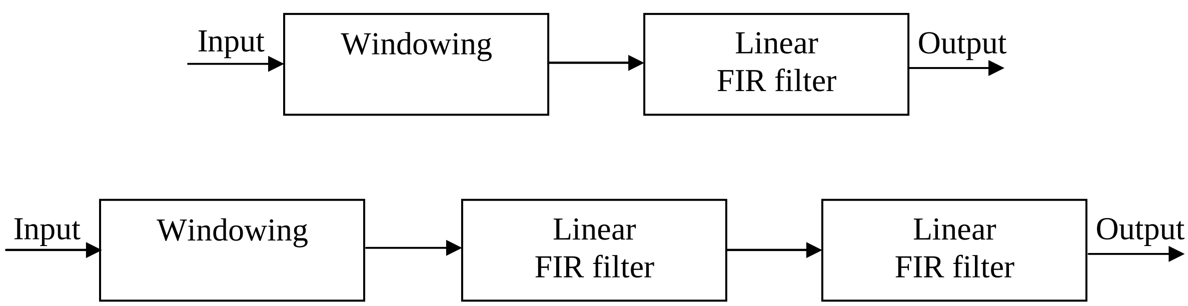

a
b

Fig. 2.1 Two Processes:
(a) Linear FIR filtering
(b) Order Statistics filtering

The similarity and differences between the linear FIR filtering and OS filtering can be understood from the block diagrams of the processes shown in Fig. 2.1. When both of them are compared, it is easily realized that the OS filtering process is similar to FIR filtering except the inclusion of an extra intermediate stage, the algebraic ordering. Thus, the OS and the linear filters are equivalent operations over sufficiently smooth regions of signal. On the other hand, these two processes must result in different outputs for the signals that are not sufficiently smooth.

2.1.1 Some properties of OS filters

Although an OS filter differs from a linear FIR filter only via the inclusion of an ordering element, it provides a very nonlinear characteristic that greatly affects the response of the filter. However, an OS filter does enjoy a limited number of linear properties, e.g., it is translation-invariant and it preserves linear trends.

An erroneous property often attributed to a general OS filter is its tendency to *preserve edges* and *suppress impulses*. This idea has largely come about as a byproduct of the interpretation of OS filters as *generalized median filters*. The only OS filters that preserve ideal edges (step signals) up to a shift are RO filters. And the only OS filter which exactly preserves edges is the median filter. However, OS filters do a better job of simultaneously preserving edges and smoothing noise, at least for additive white noise of arbitrary distribution [79,80].

2.1.2 OS Filters:

Sliding windowing technique [2] is used to perform pixel-by-pixel operation in a filtering algorithm. The local statistics obtained from the neighborhood of the center pixel give a lot of information about its expected value. If the neighborhood data are ordered (sorted), then ordered statistical information is obtained. If this order statistics vector is applied to a finite impulse response (FIR) filter, then the overall scheme becomes an OS filter.

For example, if a 3×3 window is used for spatial sampling, then 9 pixel data are available at a time. First of all, the 2-D data is converted to a 1-D data, i.e. a vector. Let this vector of 9 data be sorted. Then, if the mid value (5^{th} position pixel value in the sorted vector of length 9) is taken, it becomes median filtering with the filter weight vector [0 0 0 0 1 0 0 0 0]. If all the order statistics are given equal weightage, then it becomes a mean or moving average (MAV) filter. Strictly speaking, the MAV filter is a simple linear filter and it has nothing to do with the ordered statistics. Since the MAV operation gives equal emphasis to each input data, it is immaterial whether the input vector is sorted or not. Thus, simply to have a generalization of OS filters, the MAV is considered a member of this class. Otherwise, it is quite different from all other members of this family of filters. The min, max, ROM are some members of this interesting family. The ROM could be of various types. For example, only 3, 5, or 7 mid-ordered statistics may be taken and their mean value may be computed; giving rise to ROM(3,3), ROM(3,5), or ROM(3,7) filter structure, respectively. Here, a filter nomenclature taken is ROM(p,q); p representing a p×p window and q representing the actual number of mid-ordered statistics taken for computation. If all ordered statistics are taken for computation and different weights (not necessarily equal weightage) are given to each input, then it is the general OS filter. It is also known as L-filter [26] since the output is a ***l****inear combination* of all ordered statistics.

The MAV filter removes Gaussian noise quite effectively but its performance is very poor in case of impulsive noise. On the other hand, the MED is a very good candidate for removal of impulsive noise. But it does not perform well if the image is corrupted with Gaussian noise. The ROM is another OS filter that is used for removing both AWGN and SPN impulsive noise. But it neither excels in suppressing AWGN nor in, SPN.

Therefore, it needs further investigations to modify the ROM and the OS filters, in general, so that they perform very well in the presence of SPN, AWGN and mixed noise. In this chapter, this problem is dealt with and some novel filters are suggested for this purpose. Associating different weights with various ordered statistics, the weighted OS

(WOS) and the weighted ROM (WROM) filters are developed. These filters show superior performance over the standard filters for efficient suppression of various types of noise.

In the next section, the performance of the MAV and the MED filters is studied.

2.2 Mean and Median Filters

2.2.1 Fundamentals of Mean and Median Filters

The mean or moving average (MAV) filter is a simple linear filter [2]. All the input data are summed together and then the sum is divided with the number of data. It is very simple to implement in hardware and in software. The computational complexity is very little. It works fine for very low variance AWGN. As the noise power increases, its filtering performance degrades. If the noise power is high, then a larger window should be employed for spatial sampling to have better local statistical information. As the window size increases, the MAV filter produces a reasonably high blurring effect and thus the edges and the fine details in the image are lost.

The MED [73-76], on the other hand, is a nonlinear filter. It is a very simple operation. Once, the sorting (ordering) operation is performed on the input vector, the job is done as the mid-value is taken as the output. Of course, if the length of the input vector is even, then the average of two mid-ordered statistical data is taken as the output. Usually, such a computation is not required in most of image processing applications as the window length is normally an odd number. Thus, the MED operation can be completed in a very short time. That is, a MED filter may be used for online and real time applications to suppress noise.

What types of noise does a MED filter suppress?

In literature, the MED filter is described as a very good filter for suppressing SPN. It can even suppress RVIN of low density. If an image signal is corrupted with a very low variance AWGN, then also this filter can perform a good filtering operation. One very important merit of this MED filter is its edge-preserving characteristic. If an image is contaminated with low or medium density SPN, then a MED filter can do justice by rejecting the outliers very easily. But at some locations, the density of impulses could be very high. At those points, the simple MED filter fails. Even if the impulse noise density in an image is very low, the MED can never guarantee the true pixel replacement.

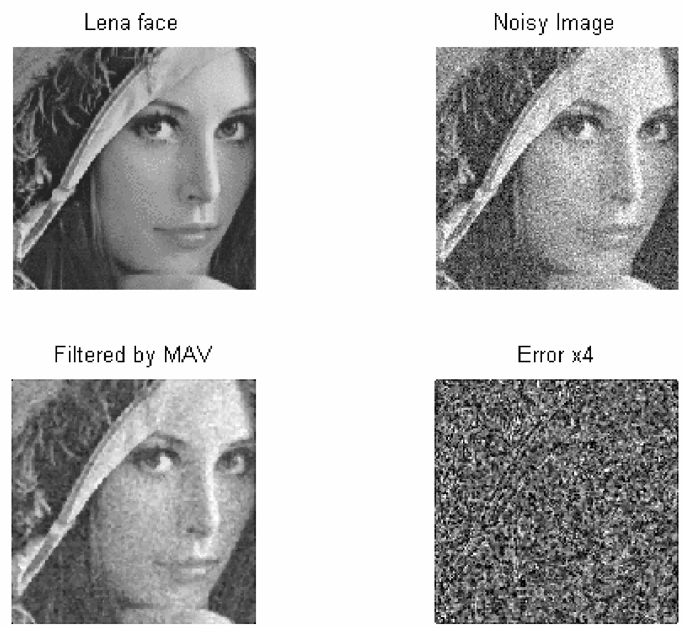

a	b
c	d

Fig.2.2 Performance of Mean filter in the presence of AWGN
(a) Original Test Image, 'Lena face'
(b) Noisy Image (corrupted with AWGN of variance=0.1)
(c) Output of Mean Filter
(d) Error in the output (magnified 4 times)

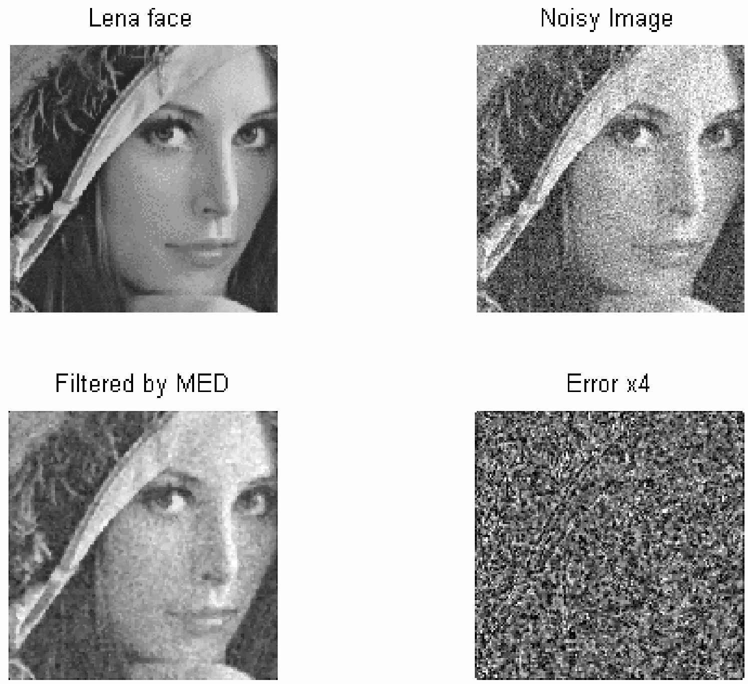

a	b
c	d

Fig.2.3 Performance of Median filter in the presence of AWGN
(a) Original Test Image, ‘Lena face’
(b) Noisy Image (corrupted with AWGN of variance=0.1)
(c) Output of Median Filter
(d) Error in the output (magnified 4 times)

The MED operation changes the pixel value to the median of the neighborhood unnecessarily even if the center pixel is noise-free. Thus, there is some unwanted error in the output. To overcome this problem, decision-directed median filters [37,43] are proposed in the literature. Such filters are described in the next chapter.

2.2.2 Performance Evaluation

To illustrate the performance of MAV and MED filters in the presence of AWGN, SPN and RVIN the following simulation is carried out. The test image ‘Lena face’ is corrupted with:

(a) AWGN of variance, σ^2 varying from 0.003 to 0.1

(b) SPN of density, d varying from 0.01 to 0.1

(c) RVIN of density, d varying from 0.01 to 0.2

(d) Mixed noise (MN) with

  (i) AWGN (σ^2 = 0.003) + SPN (d = 0.003)

  (ii) AWGN (σ^2 = 0.01) + SPN (d = 0.01)

  (iii) AWGN (σ^2= 0.1) + SPN (d = 0.1)

In online applications like television and photo-phones, for which novel efficient filters are to be designed, it is already observed that the noise level is very low. This is mentioned in Chapter-1. Therefore the noise levels, in this simulation work, are very low and low. It is interesting to observe the combinations of AWGN and SPN noise levels in part (d) mentioned above. The SPN density increases as the AWGN variance increases in a practical communication application. Such an effect is simulated in part (d).

The performance of MAV and MED filters incase of AWGN, SPN, RVIN and MN is evaluated by finding the MSE, MR-MSE (defined in Section-1.5). The NRDB1 is the NRDB computed with output noise level MSE_{out}, where as the NRDB2 is the NRDB computed with the output noise level MR-MSE. All the image metrics are tabulated in Table-2.1, Table-2.2, Table-2.3 and Table-2.4 for AWGN, SPN, RVIN and MN. To have a subjective evaluation of these filters, the original, noisy and filtered images are shown in Fig. 2.3, Fig. 2.4, Fig. 2.5, Fig. 2.6 and Fig. 2.7. The performance measure plots (NRDB or MSE) in Fig. 2.8, Fig. 2.9, Fig. 2.10 and Fig. 2.11 demonstrate the filtering performance of MAV and MED filters for suppressing AWGN, SPN and RVIN respectively.

2.2.3 Conclusion

It is observed from the figures that the MAV is better than the MED in suppressing AWGN, whereas the MED performs better than the MAV in case of impulse noise (SPN and RVIN). These results are, in fact, in conformity with the established facts in literature. But, an interesting point that has to be noted here is that the MED is not a poor performer in case of low variance AWGN. Under such a condition, its performance is close to that of a MAV filter. On the other hand, the MAV severely fails in suppressing SPN. The MAV yields a considerable amount of blurring effect on the image. In addition, it shows poor performance, in terms of performance measure MSE, as compared to the MED. Moreover, the MED outperforms the MAV in suppressing RVIN.

Therefore, it may be concluded that MED is a better filter than the MAV in image restoration.

Table-2.1: Performance Evaluation for AWGN

σ^2	MSEin	MAV				MED			
		MSEout	MR-MSE	NRDB1	NRDB2	MSEout	MR-MSE	NRDB1	NRDB2
0.003	0.0097	0.0026	0.0026	5.75	5.75	0.0029	0.0029	5.26	5.26
0.01	0.0100	0.0026	0.0026	5.80	5.80	0.0030	0.0029	5.27	5.36
0.02	0.0101	0.0028	0.0026	5.57	5.87	0.0031	0.0028	5.14	5.50
0.03	0.0106	0.0032	0.0027	5.15	5.99	0.0036	0.0029	4.72	5.67
0.06	0.0134	0.0057	0.0030	3.73	6.49	0.0063	0.0031	3.28	6.31
0.1	0.0194	0.0115	0.0037	2.66	7.19	0.0124	0.0037	1.93	7.19

Table-2.2: Performance Evaluation for SPN

d	MSEin	MAV				MED			
		MSEout	MR-MSE	NRDB1	NRDB2	MSEout	MR-MSE	NRDB1	NRDB2
0.01	0.0029	0.0018	0.0018	2.05	2.05	0.0010	0.0010	4.62	4.62
0.03	0.0086	0.0025	0.0025	5.34	5.34	0.0011	0.0011	8.90	8.90
0.05	0.0144	0.0032	0.0032	6.53	6.53	0.0011	0.0011	11.19	11.19
0.1	0.0290	0.0052	0.0052	7.44	7.44	0.0015	0.0015	12.90	12.90

Table-2.3: Performance Evaluation for RVIN

d	MSEin	MAV				MED			
		MSEout	MR-MSE	NRDB1	NRDB2	MSEout	MR-MSE	NRDB1	NRDB2
0.01	0.0012	0.0017	0.0016	-1.41	-1.35	0.0010	0.0010	0.73	0.73
0.03	0.0040	0.0020	0.0020	2.92	2.92	0.0010	0.0010	5.77	5.77
0.05	0.0057	0.0023	0.0023	3.99	3.99	0.0011	0.0011	7.19	7.19
0.10	0.0125	0.0033	0.0034	5.70	5.70	0.0012	0.0012	10.07	10.07
0.20	0.0254	0.0060	0.0061	6.24	6.19	0.0017	0.0017	11.79	11.79

Table-2.4: Performance Evaluation for Mixed Noise (MN)

	AWGN, $\sigma^2 = 0.003$ + SPN, d = 0.003			AWGN, $\sigma^2 = 0.01$ + SPN, d = 0.01			AWGN, $\sigma^2 = 0.1$ + SPN, d = 0.1		
	MSEin	MSEout	NRDB	MSEin	MSEout	NRDB	MSEin	MSEout	NRDB
MAV	0.0109	0.0027	6.03	0.0126	0.0030	6.26	0.0464	0.0142	5.15
MED		0.0029	5.72		0.0030	6.19		0.0127	5.61
ROM33		0.0024	6.56		0.0025	6.97		0.0122	5.80
ROM35		0.0023	6.75		0.0024	7.24		0.0122	5.80
ROM37		**0.0022**	**6.98**		**0.0023**	**7.32**		0.0129	5.57
ROM511		0.0023	6.75		**0.0023**	**7.32**		**0.0114**	**6.08**
ROM513		0.0023	6.75		0.0024	7.28		**0.0114**	**6.08**
ROM721		0.0029	5.72		0.0030	6.30		0.0116	6.00

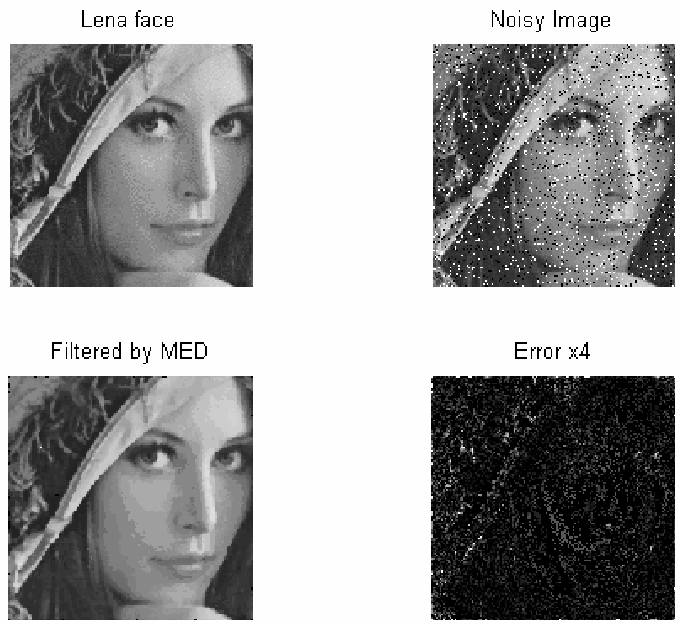

a	b
c	d

Fig.2.4 Performance of Median Filter in the presence of SPN

(a) Original Test Image, ‘Lena face’
(b) Noisy Image (Image Corrupted with 10% SPN)
(c) Output of Median Filter
(d) Error in the Output Image (magnified 4times)

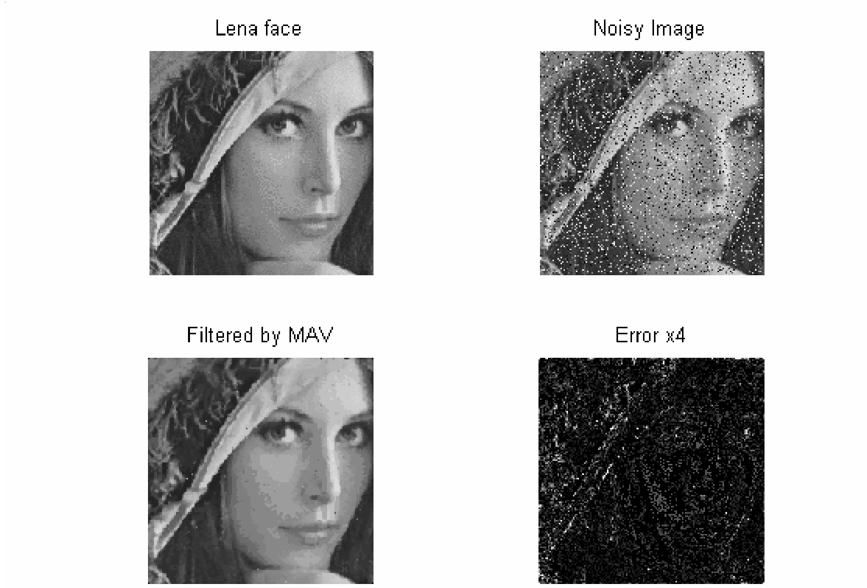

a	b
c	d

Fig.2.5 Performance of Mean filter in the presence of RVIN

(a) Original Test Image, ‘Lena face’
(b) Noisy Image (corrupted with RVIN of density=0.2)
(c) Output of Mean Filter
(d) Error in the Output Image (magnified 4times)

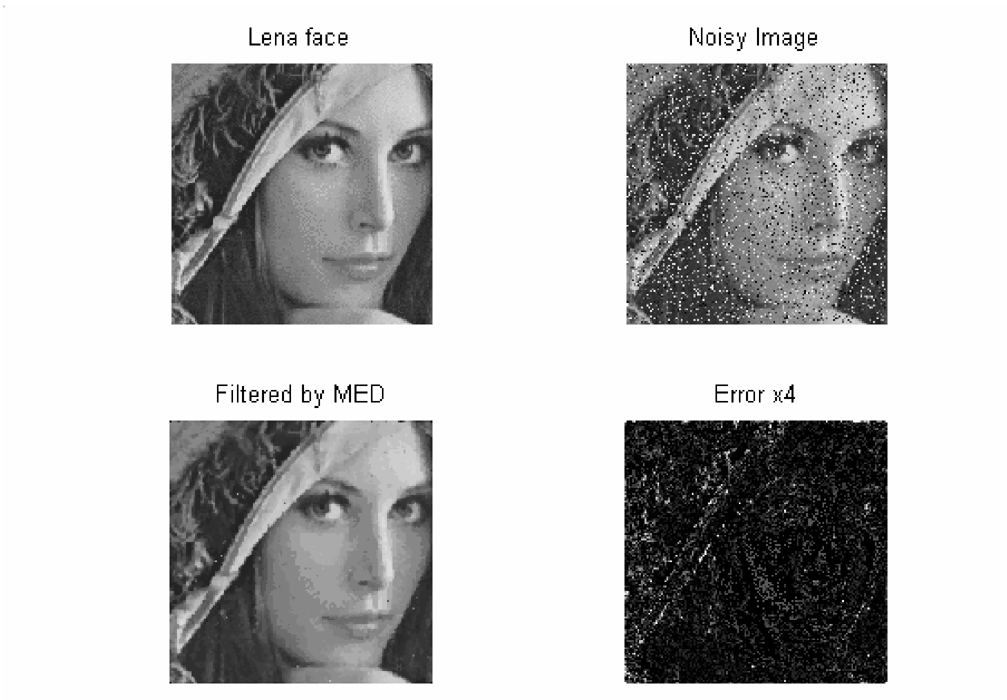

a	b
c	d

Fig.2.6 Performance of Median filter in the presence of RVIN

(a) Original Test Image, ‘Lena face’
(b) Noisy Image (corrupted with RVIN of density=0.2)
(c) Output of Median Filter
(d) Error in the output (magnified 4 times)

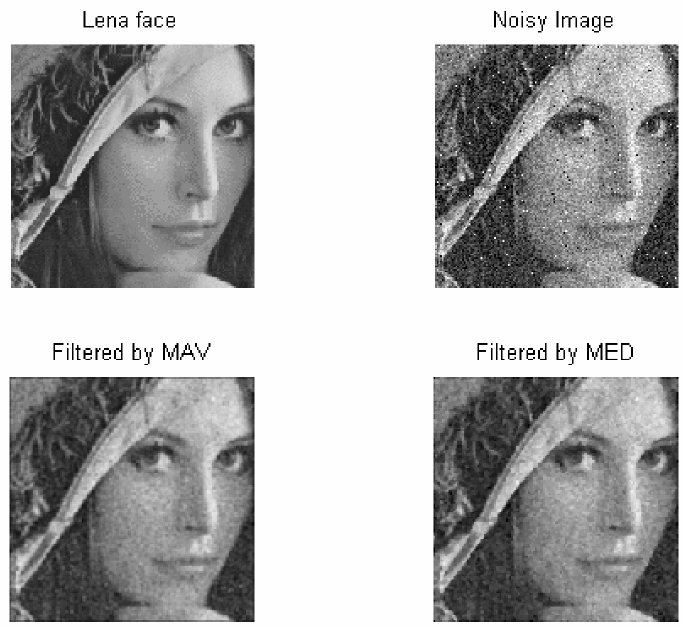

a	b
c	d

Fig.2.7 Performance of Various Filters under mixed noise condition

(a) Original Test Image, ‘Lena Face’
(b) Noisy Image (corrupted with AWGN of variance=0.01 and SPN of density=0.01)
(c) Output of Mean Filter
(d) Output of Median Filter

Cont….

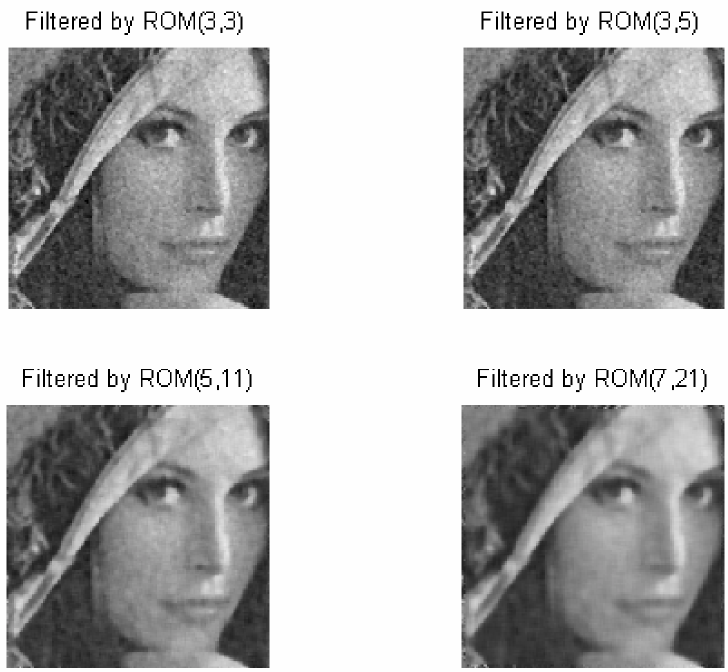

e	f
g	h

Fig.2.7 Performance of Various Filters under mixed noise condition (cont…)
(e) Output of ROM(3,3) Filter
(f) Output of ROM(3,5) Filter
(g) Output of ROM(5,11) Filter
(h) Output of ROM(7,21) Filter

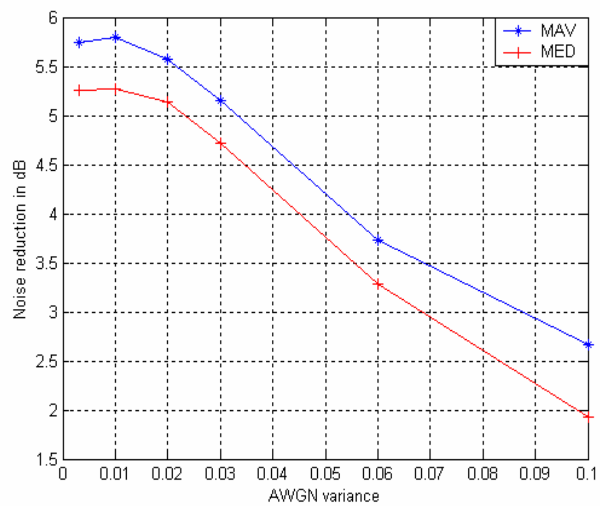

Fig.2.8 Performance of MAV filter in case of AWGN

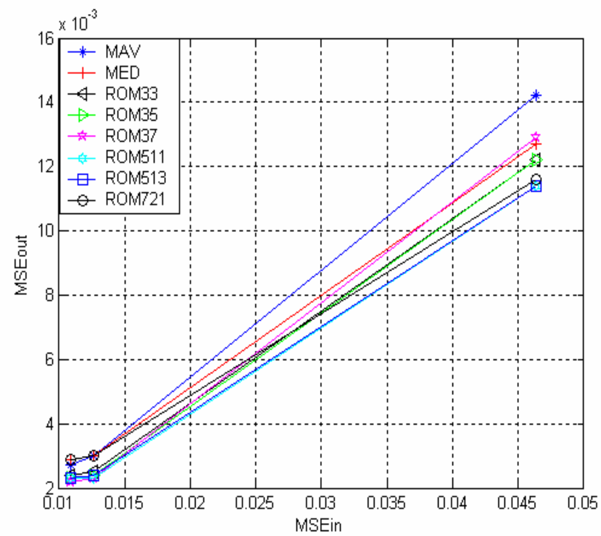

Fig.2.9 Performance of MED filter in case of AWGN

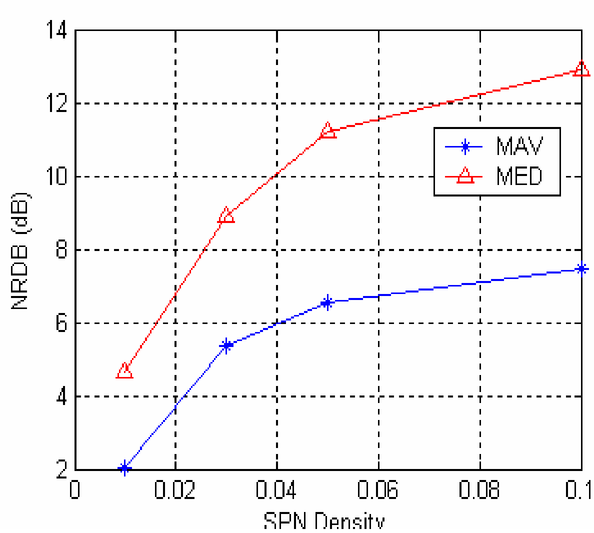

Fig.2.10 Performance of MAV and MED filters in case of SPN

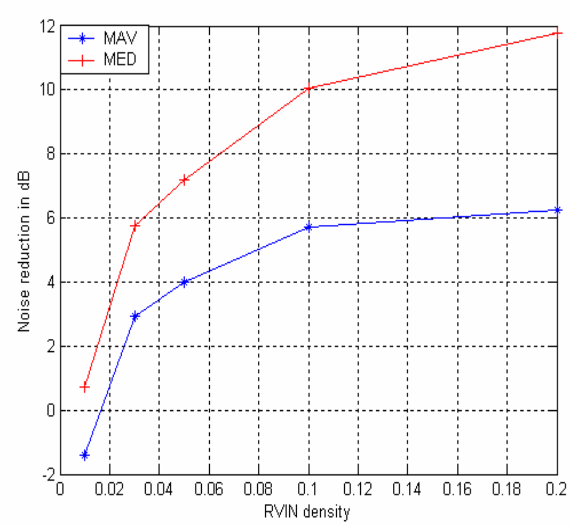

Fig.2.11 Performance of MAV and MED filters in case of RVIN

2.3 ROM Filters

The ROM filters are a good compromise between the two extreme candidates: the MAV and the MED. Thus, an ROM filter, if properly designed, can show very good performance in suppressing various types of noise.

As mentioned in Section 2.1, there are many types of ROM filters. The ROM(3,3), ROM(3,5), ROM(3,7),ROM(5,13), ROM(5,11) are some important members of this family. It is very important to understand the fact that the performance of ROM(3,7) is very close to that of the MAV. Similarly, the performance of ROM(3,3) is very close to that of MED. Therefore, all ROM filters can suppress mixed noise quite effectively and their performance is much better than the MAV and the MED in this respect. If the additive noise is high and the impulse density is low, then ROM(3,7) performs better than ROM(3,3) and ROM(3,5). On the other hand, if the impulse noise density is high, then the ROM(3,5) and ROM(3,3) may show better performance.

2.4 L-Filters

The general OS filter is known as L-filter [26]. All the sorted neighborhood pixel values are used for computing the filter output. Usually, an L-filter is used with an LMS adaptive algorithm so that the FIR filter weights vary depending on the noise type and noise power level. This is a highly computational intensive operation since the adaptive filter needs training always to update itself. One more problem with this filter is that it needs a noise-free reference image for training. Such a reference image is not available in many situations.

To avoid high computational complexity as well as to achieve high level of filtering performance, various types of weighted ROM (WROM) filters are developed [P3] and presented in the next section.

2.5 Development of WROM Filters

A simple ROM(p,q) filter gives equal emphasis to all the q number of order statistics taken out of a total p^2 number of inputs. If the noise behavior is clearly understood, then some intuitive decisions may be taken to find a suitable weight vector that may give a very good filtering performance.

In fact, a WROM filter is a modification to the simple ROM that performs better than the latter. Its output $\tilde{X}(m,n)$ is given by,

$$\tilde{X}(m,n) = f\left[\mathbf{X}_{MN}(m,n)\right] = \{\varphi(\mathbf{x})\} \tag{2.1}$$

where, $\mathbf{X}_{MN}(m,n)$, the input noisy digital image (corrupted with mixed noise, a combination of AWGN and SPN), is a 2-D array of gray scale values of pixels ranging from 0 to 2^B-1 for a B-bit system or, equivalently, from 0 to 1 in the normalized scale;
(It may be noted that the noise type could be RVIN, AWGN, SPN or MN. Therefore, the input digital image could be X_{RVIN}, X_{AWGN}, X_{AWGN} or X_{MN} in (2.1). The general noise condition in many practical applications is a mixed noise. Thus, for simplicity, the input image is expressed as X_{MN} in this equation.)

f(.) is the filter function operated on $\boldsymbol{X}_{\mathrm{MN}}$**;**
$\varphi(\cdot)$ is the sub-function, the true WROM, that is applied to a small region of image (called a window),
x, centered at a pixel $x(m,n)$ to get an estimate of the original pixel $\hat{x}_0(m,n)$. This function is defined as:

$$\varphi(\mathrm{x}_{MN}) = \frac{\sum_{k=1}^{N} w_k x_{(k)}}{\sum w_k} \tag{2.2}$$

where,

$x_{(k)}$ is the k^{th} order statistics of $\mathbf{x}_{MN}$ such that $x_{(k-1)} \le x_{(k)} \le x_{(k+1)}$ for $2 \le k \le N-1$;

w_k is the weight associated with $x_{(k)}$;

N is the size of order statistics taken ($N=p\times p$).

The order statistics is a 1-D array. Let it be a column vector represented by $\mathbf{x}_{(\ )}$. Let the weight be represented by another column vector **w.** Then, (2.2) is modified as:

$$\varphi(\mathrm{x}_{MN}) = \frac{\mathrm{w}^T \cdot \mathrm{x}_{(\ )}}{\sum \mathrm{w}} = \tilde{x}(m,n) \tag{2.3}$$

If the weight vector is normalized, i.e. $\sum \mathbf{w} = 1$, then the WROM formula, in matrix representation, is given by:

$$\tilde{x}(m,n) = \mathbf{w}^{\mathbf{T}} \times \mathbf{x}_{(\ )} \tag{2.4}$$

where, $\times$ is a matrix multiplication operation.

In an ROM filter, some of the extreme-ended order statistics are not considered. But in case of a general OS filter all the order statistics are taken into consideration. Thus, the weight vector, **w**, associated with a weighted ROM (WROM) filter will have necessarily some zeros at extreme ends, whereas it is not so for a general weighted OS (WOS) filter. Now the main issue is to choose a suitable weight vector **w** that operates on the ordered input vector $\mathbf{x}_{(\,)}$ so that a good quality image output is achieved.

If different weights are taken, i.e. w_i not necessarily equal to w_j for $i \neq j$, then the filter becomes a WROM filter. This type of filter is different from *L-filters* [26] that consider all the ordered statistics of the neighborhood though the weights are different. Such filters may be made adaptive. Otherwise, some fixed weights may be taken.

A simple intuitive decision works out to be fruitful to some extent to suppress RVIN, and AWGN, SPN and mixed noise.

Proposed WOS and WROM Filters

Four WOS filters and eight WROM filters for suppression of AWGN, SPN, and mixed noise in digital images are proposed. The choice of the weights is intuitive. The weight vector should be symmetric. To eliminate the outliers in the image, for SPN and mixed noise conditions, the extreme-end weights must be zero and the central weight (weight associated with the median) must be the maximum. Thus, the weights are tapered from maximum (central) to zero (extreme-end) for WROM filters, whereas they are tapered from maximum to a minimum non-zero value for WOS filters. This is so for the WOS filter, which is designed to suppress AWGN, since there are no outliers if an image is corrupted with AWGN only. This is how the weights are selected in (2.5)-(2.16).

The proposed four WOS filters have weight vectors $W1$, $W2$, $W3$, $W4$, respectively, to suppress Gaussian noise effectively. The weight vectors are given by:

$$W1 = \frac{W1'}{\sum W_1'}, \quad \text{where,} \quad W1' = [5\ 7\ 8\ 9\ 10\ 9\ 8\ 7\ 5]^T \tag{2.5}$$

$$W2 = \frac{W2'}{\sum W2'}, \quad \text{where,} \quad W2' = [4\ 4\ 4\ 4\ 5\ 4\ 4\ 4\ 4]^T \tag{2.6}$$

$$W3 = \frac{W3'}{\sum W3'}, \quad \text{where,} \quad W3' = [2\ 3\ 3\ 4\ 4\ 4\ 3\ 3\ 2]^T \tag{2.7}$$

$$W4 = \frac{W4'}{\sum W4'}, \quad \text{where,} \quad W4' = [3\ 3\ 4\ 4\ 5\ 4\ 4\ 3\ 3]^T \tag{2.8}$$

These filters perform better than the MAV and the ROM filters for Gaussian noise removal.

Similarly, four WROM filters with weight vectors *W*5, *W*6, *W*7, *W*8 respectively, have been proposed to eliminate SPN from digital images. The weight vectors are given by:

$$W5 = \frac{W5'}{\sum W5'}, \quad \text{where,} \quad W5' = [0\ 0\ 0\ 1\ 2\ 1\ 0\ 0\ 0]^T \tag{2.9}$$

$$W6 = \frac{W6'}{\sum W6'}, \quad \text{where,} \quad W6' = [0\ 0\ 0\ 1\ 3\ 1\ 0\ 0\ 0]^T \tag{2.10}$$

$$W7 = \frac{W7'}{\sum W7'}, \quad \text{where,} \quad W7' = [0\ 0\ 0\ 1\ 4\ 1\ 0\ 0\ 0]^T \tag{2.11}$$

$$W8 = \frac{W8'}{\sum W8'}, \quad \text{where,} \quad W8' = [0\ 0\ 0\ 1\ 5\ 1\ 0\ 0\ 0]^T \tag{2.12}$$

These filters work effectively as compared to MED and ROM filters for removing SPN noise. Though MED is quite effective in removing SPN, it spoils the pixel values unnecessarily and doesn't consider any other pixel(s) except the median value in the neighborhood. The ROM filter also removes SPN effectively. But its performance is not very good as it gives equal emphasis to all the q number of order statistics taken out of a total p^2 number of data in the neighborhood.

Though the performance of the MED filter is very good, it doesn't excel in removing SPN because any other quite likely order statistics are not considered. Therefore, a compromise between the MED and the ROM filters is needed. In a 3×3 window, if more than 3 order statistics are taken, then the ROM filter gives a lot of blurring effect. Thus, 3 numbers of order-statistics may be taken at best.

Now, the question arises: ‘Should equal emphasis be given to all of them?’ If equal emphasis is given, then it becomes a simple ROM filter and its performance is poorer than the MED in removing SPN. Therefore, the central order statistics must be given more weightage than the other two order statistics. This is the reasoning behind choosing the various weight vectors W5, W6, W7 and W8.

Also, four different types of WROM filters: WROM-V, WROM-VI, WROM-VII and WROM-VIII are proposed for efficient suppression of mixed noise in digital images. These filters have weights $W9$, $W10$, $W11$ and $W12$ respectively, given by:

$$W9 = \frac{W9'}{\sum W9'}, \quad \text{where,} \quad W9' = [0\ 1\ 2\ 4\ 5\ 4\ 2\ 1\ 0]^T \tag{2.13}$$

$$W10 = \frac{W10'}{\sum W10'}, \quad \text{where,} \quad W10' = [0\ 0\ 1\ 2\ 3\ 2\ 1\ 0\ 0]^T \tag{2.14}$$

$$W11 = \frac{W11'}{\sum W11'}, \quad \text{where,} \quad W11' = [0\ 0\ 0\ 2\ 3\ 2\ 0\ 0\ 0]^T \tag{2.15}$$

$$W12 = \frac{W12'}{\sum W12'}, \quad \text{where,} \quad W12' = [0\ 0\ 0\ 1\ 2\ 1\ 0\ 0\ 0]^T \tag{2.16}$$

To suppress the mixed noise, an efficient filter structure must be a compromise between the WOS and the WROM. Further, it signifies the fact that the number of order statistics to be considered has to be more than or equal to 3 and less than 9. So it has to be either 7 or 5 or 3. Thus, various WROM filter structures: WROM-V, WROM-VI, WROM-VII and WROM-VIII taking different number of order statistics are proposed.

Simulation and Results

Extensive computer simulations are carried out to assess the performance of the proposed filters and to compare the same with the standard MAV, MED and ROM filters. A selected slice of size 200×200 pixels (face portion) from the standard Lena image is taken as the reference image. The image is corrupted with noise, for three different types of noise conditions, as described below:

i.) AWGN : Gaussian noise of variance varying from 0.006 to 0.012 is added.
ii.) SPN : Impulse noise of density 1% to 15% is added.
iii.) Mixed noise: Gaussian noise of variance, as in (i), with 1% SPN noise.

The performance of the standard MAV, MED, ROM filters and the proposed filters is summarized in Table-1, Table-2, and Table-3 for AWGN, SPN and mixed noise condition respectively. The **MSE** is taken as the *performance measure*. The MSE values for the various filters obtained from simulation are listed in Table-2.5, Table-2.6 and Table-2.7. Since the **MSE** values are very small, they are multiplied with 10^4 and the product values are shown in the tables. The **MSE** values are plotted in Fig. 2.12, Fig. 2.13 for MN and AWGN respectively. The various filter-output images are shown in Fig. 2.14 for subjective evaluation.

Table-2.5: Performance Comparison of WOS Filters with other standard filters for AWGN

Gaussian Noise Variance σ^2	MSEin ($\times 10^{-4}$)	MSE out($\times 10^{-4}$)							
		MAV	MED	ROM33	ROM35	WOS-I	WOS-II	WOS-III	WOS-IV
0.006	59.2925	53.075	56.065	54.1275	53.2075	52.7875	53.02	52.78	52.8475
0.007	69.8975	54.2575	57.5725	55.3975	54.4375	53.955	54.1975	53.9425	54.0125
0.008	77.815	55.0225	59.245	56.7875	55.64	54.815	54.975	54.8075	54.85
0.009	89.2225	56.385	61.485	57.64	57.24	56.2125	56.345	56.21	56.2375
0.01	96.8875	57.2025	62.62	59.685	58.2225	57.0525	57.1675	57.05	57.0675
0.011	105.79	58.205	64.5225	61.345	59.6325	58.1275	58.175	58.13	58.12
0.012	117.1075	59.3775	66.375	62.9175	61.025	59.3175	59.35	59.325	59.305

Table-2.6: Performance Comparison of WROM Filters with other standard filters for SPN

SPN Density	MSEin ($\times10^{-4}$)	MSE out($\times10^{-4}$)							
		MAV	MED	ROM33	ROM35	WROM-I	WROM-II	WROM-III	WROM-IV
1%	26.025	49.615	45.33	44.6975	44.8575	**44.68**	44.7275	44.78	44.83
5%	146.33	64.135	46.39	45.645	46.0975	**45.625**	45.68	45.7325	45.8025
10%	286.775	83.175	47.8	47.25	49.6	**45.1**	**45.1**	45.15	45.2
15%	434.8	103.75	49.6	49.975	56.025	49.375	49.175	**49.1**	**49.1**

Table-2.7: Performance Comparison of WROM Filters with other standard filters for MN
(1% SPN along with AWGN of variance, σ^2)

Gaussian Noise Variance, σ^2	MSE in ($\times10^{-4}$)	MSE out($\times10^{-4}$)							
		MAV	MED	ROM33	ROM35	WROM-V	WROM-VI	WROM-VII	WROM-VIII
0.006	88.0775	56.6425	56.4775	54.5275	53.64	**53.5825**	53.9225	54.6375	54.755
0.007	95.6725	57.325	58.02	55.8025	54.78	**54.6925**	55.1175	55.9325	56.07
0.008	107.5875	58.7675	60.2075	57.775	56.5825	**56.4675**	56.99	57.9175	58.07
0.009	121.5175	59.9575	61.6	58.8625	57.52	**57.405**	57.9875	59.03	59.205
0.01	126.9575	60.52	63.0525	60.23	58.8075	**58.63**	59.295	60.3925	60.565
0.011	136.2225	62.0125	65.365	62.1725	60.535	**60.345**	61.11	62.36	62.5625
0.012	146.5475	63.0675	66.3725	63.05	61.45	**61.245**	62.0075	63.25	63.4575

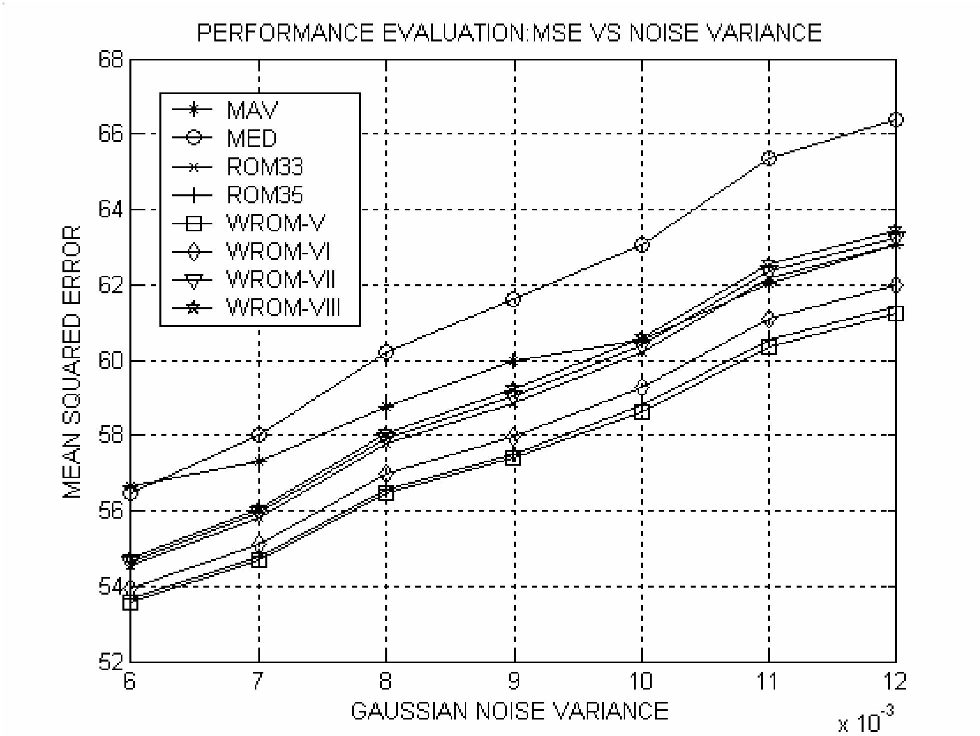

Fig. 2.12 Performance of various filters under mixed noise conditions.

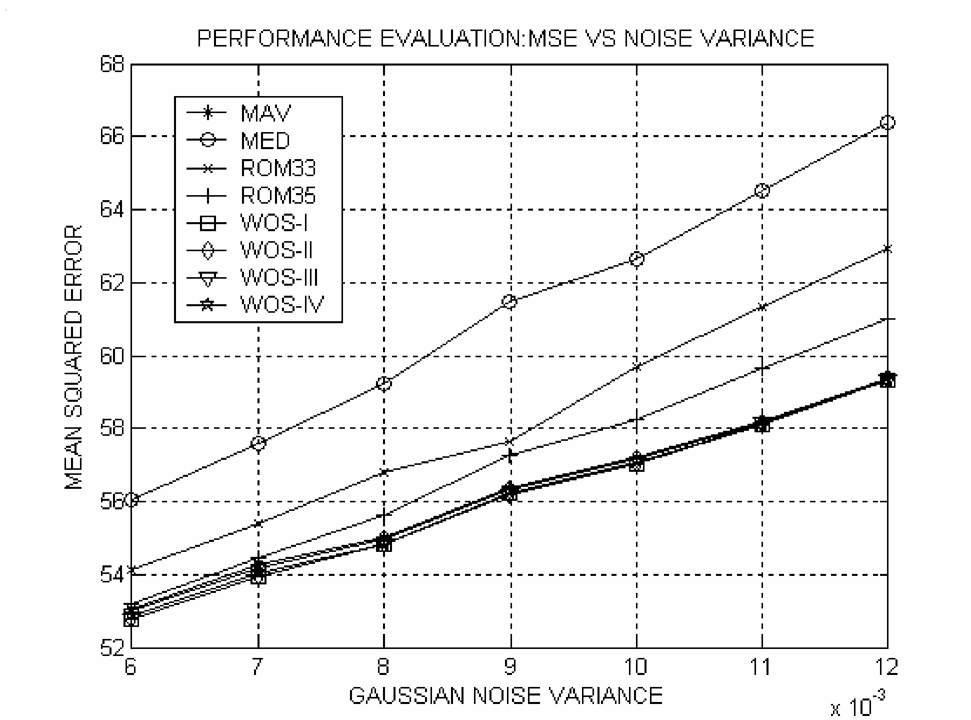

Fig. 2.13 Performance of various filters for additive Gaussian noise.

The Original Lena face

Noisy Lena Face

MED

MAV

ROM33

ROM35

Continued in the next page.

Continued from the previous page.

WROM-V

WROM-VI

WROM-VII

WROM-VIII

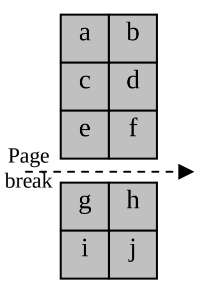

Fig. 2.14 Images for visual performance comparison

(a) The original Lena face image

(b) Noisy Lena face with Gaussian noise (σ^2=.01) and SPN (d=1%)

(c), (d), (e), (f),(g), (h), (i) and (j): The various filter-output images.

2.6. Conclusion

It is observed that the proposed WOS and WROM filters excel in removing various noises from an image. The proposed WOS-III and WOS-IV excel in removing AWGN under low and high noise variances respectively. Different WROM filters show good performance under various impulse noise densities. The WROM-I, WROM-II, and WROM-III & WROM-IV perform much better than the MAV, MED and ROM filters under very low (<5%), low (5-10%) and medium (15%) impulse noise density, respectively. To remove mixed noise, the proposed filter WROM-V shows much superior performance over all standard MAV, MED and ROM filters.

Thus, the proposed filters: WOS-III, WROM-I and WROM-V are excellent in removing Gaussian, impulse and mixed noise respectively. These weighted filters show very high performance without requiring high computation.

The proposed WOS and WROM filters show better performance than the standard OS filters under various noise conditions. But their performance is not as good as adaptive filters. However, such filters may be employed in time-invariant systems.

CHAPTER-3

Development of Decision-Directed Filters for Impulse Noise Suppression

Preview

Median (MED) and Center-Weighted Median (CWM) [35] filters suppress impulse noise in an image quite effectively. But, applying a filtering operation to each pixel of the image gives distortion and edge-blurring unnecessarily. Therefore, it is always better to detect an impulse first. If an impulse noise is found at a pixel, then only some filtering operation may be applied. This way, unwanted distortion and blurring can be reduced. Such schemes are called decision-directed filters as a filtering operation is directed by a decision of an impulse detector [37-44,86-92]. Since the filtering operation that follows the detector is usually a median operation, many decision-directed median filters (DDMF) are proposed by researchers. The NASM filter proposed by Eng and Ma [88], the AID-CWM filter proposed by Chen and Wu [89] and the DRID algorithm proposed by Aizenberg and Butakoff [100] show very good filtering performance. But, they are quite computational intensive algorithms. In this chapter, many novel impulse detection schemes are proposed.

The second-order difference (SOD) based decision-directed filter [P1] developed here is a very good scheme to suppress impulse noise up to 40% noise density. The probability-based impulse noise detection (PIND) algorithm is a very simple algorithm that can be applied in any real-time application. The deviation-based impulse noise detection (DIND) algorithm, proposed here, is a robust impulse noise detector. It can detect an impulse under mixed noise (MN) conditions. In addition, it can suppress low-density RVIN. That is why, it is more useful in real-time applications like television systems where the noise could be low-power MN or RVIN.

The following topics are covered in this chapter.

- Introduction to Decision-Directed Filters
- Second-Order Difference (SOD) based Decision-Directed Median Filter (SOD-DDMF)
- Probability-based Impulse Noise Detection (PIND) Algorithm
- Deviation-based Impulse Noise Detection (DIND) Algorithm
- Conclusion

3.1 Introduction to Decision-Directed Filters

In a practical situation, since the probability of having an impulse noise is less than 1, all the pixels of a digital image are not corrupted with the impulse noise. Therefore, it is expected that a noisy pixel is surrounded by at least some non-noisy pixels. However, this assumption is not always true when the noise density is very high. In any case, the total number of corrupted pixels is less than the total number of pixels in the image. Hence, it is not required to perform filtering operation on every pixel for eliminating the impulse noise. Rather, it is computationally economical to filter only the corrupted pixels leaving the non-noisy pixels unchanged. This approach reduces the blurring effect in the restored image, as the magnitude of a non-noisy pixel is not affected by filtering.

Basically, the noise removal method proposed here constitutes two tasks: *identification* of corrupted pixels and *filtering* operation only on those corrupted pixels. Thus, the effectiveness of this scheme lies on the accuracy and robustness of detection of noisy pixels and efficiency of the filtering methodology employed. Many researchers [12-15] have suggested various methods for locating the distorted pixels as well as filtering techniques. Each of these methods has different shortcomings and hence fails to reproduce images very close to original ones. It is over-filtering distortion, blurring effect or high computational involvement. In addition, as the density of the impulse noise is gradually increased, the quality of the image recovered by the existing methods correspondingly degrades. A decision directed filter is represented by a block schematic as shown in Fig. 3.1.

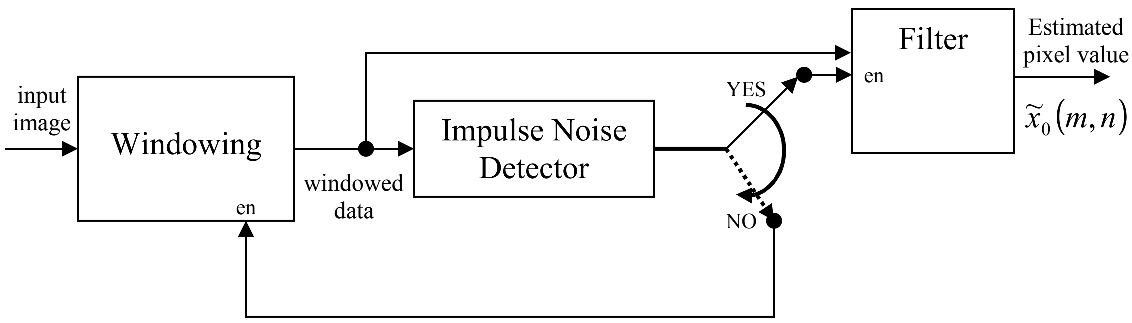

Fig. 3.1 Block Schematic of a Decision-Directed Filter

The input image is a 2-D matrix. It is spatially sampled and a windowed data, usually 3×3 or 5×5, comes to the processing system at an instant. To take a decision on a pixel its neighborhood pixels are considered. That is why, the spatial windowing is employed to sample the image data. The impulse noise detector must precede the filter (may be MED or some variant of MED or any special filter) as shown in Fig.3.1. If the impulse detector has detected an impulse (output state of detector = 'YES') at a particular instant, then only control signal is passed to the filter unit to perform filtering operation on the windowed data set. On the other hand, if the impulse detector doesn't find any noise, then no control signal is given to the filter unit; rather, the window sampler is enabled to take the next data sample.

3.2 Second-Order Difference (SOD) based Decision-Directed Median Filter (SOD-DDMF)

A novel scheme is developed here to detect an impulse noise in a digital image [P1]. The proposed scheme employs a second order difference based impulse detection mechanism at the location of a test pixel. The mathematical formulation of the proposed method is presented in (3.1).

$$\tilde{\mathrm{X}}(n) = \begin{cases} \tilde{\mathrm{Y}}(n), & \text{if } \; d(n)=0 \\ \mathrm{X}(n), & \text{if } \; d(n)=1 \end{cases} \tag{3.1}$$

where, *d(n)* is the decision index that controls the filtering operation and estimates the filtered output $\tilde{\mathrm{X}}(n)$ from the observed image $\mathrm{X}(n)$, and $\tilde{\mathrm{Y}}(n)$ is the filtered pixel value. If the impulse detector determines that the center pixel of test window is noisy, then *d(n)= 0,* otherwise *d(n)=1*. If *d(n)=0,* then the corrupted pixel undergoes median filtering. On the other hand (*d(n)=1*), the window is skipped and the process is repeated . Unlike in other conventional methods, the filtering operation is performed selectively based on the decision of the impulse detector. Hence the proposed method is named as Decision Directed Median Filter (DDMF).

The schematic diagram of the proposed filtering scheme is shown in Fig. 3.2. The impulse detector takes an input of size 3×5 pixels and makes one decision on the corrupted pixel at each step.

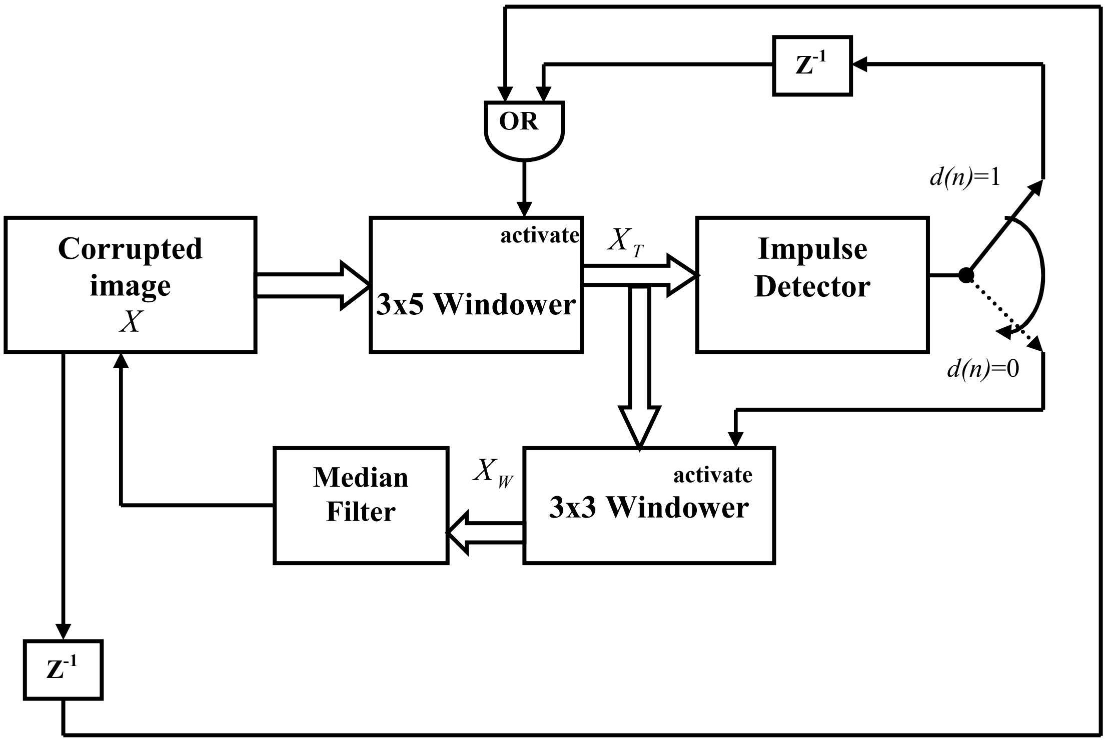

Fig. 3.2 Schematic Representation of Second-Order Difference based Decision-Directed Median Filter (SOD-DDMF)

The proposed algorithm works in two phases: the detection of impulsive noise at the center pixel of a window followed by selective median filtering. The detailed algorithm for impulse detection and filtering is described here.

3.2.1 Algorithm for Impulse Noise Detection

Step 1: Choose a test window $\mathbf{X}_T$ of size 3×5 located at the topmost left corner of the observed image $\mathbf{X}$.

$$\mathbf{X}_T = \begin{pmatrix} x(m-1,n-2) & x(m-1,n-1) & x(m-1,n) & x(m-1,n+1) & x(m-1,n+2) \\ x(m,n-2) & x(m,n-1) & x(m,n) & x(m,n+1) & x(m,n+2) \\ x(m+1,n-2) & x(m+1,n-1) & x(m+1,n) & x(m+1,n+1) & x(m+1,n+2) \end{pmatrix} \quad (3.2)$$

Consider a 3×3 sub-window $\mathbf{X}_W$ from $\mathbf{X}_T$ defined as:

$$\mathbf{X}_W = \begin{pmatrix} x(m-1,n-1) & x(m-1,n) & x(m-1,n+1) \\ x(m,n-1) & x(m,n) & x(m,n+1) \\ x(m+1,n-1) & x(m+1,n) & x(m+1,n+1) \end{pmatrix} \quad (3.3)$$

Step 2: Compute the first order 3×4 difference matrix *fd* from $\mathbf{X}_T$:

$$fd = \begin{pmatrix} fd(m-1,n-1) & fd(m-1,n) & fd(m-1,n+1) & fd(m-1,n+2) \\ fd(m,n-1) & fd(m,n) & fd(m,n+1) & fd(m,n+2) \\ fd(m+1,n-1) & fd(m+1,n) & fd(m+1,n+1) & fd(m+1,n+2) \end{pmatrix} \quad (3.4)$$

where an element of window, *fd* is obtained as:

$$fd(m+k,n+l) = \mathbf{X}(m+k,n+l) - \mathbf{X}(m+k,n+l-1), \quad k=-1,0,1, \quad l=-1,0,1,2$$

Step 3: Compute the second order 3×3 difference matrix *sd* from *fd*:

$$sd = \begin{pmatrix} sd(m-1,n-1) & sd(m-1,n) & sd(m-1,n+1) \\ sd(m,n-1) & sd(m,n) & sd(m,n+1) \\ sd(m+1,n-1) & sd(m+1,n) & sd(m+1,n+1) \end{pmatrix} \quad (3.5)$$

where an element of window, *sd* is given by:

$$sd(m+r,n+s) = fd(m+r,n+s+1) - fd(m+r,n+s), \quad r=-1,0,1, \quad s=-1,0,1$$

Step 4: Apply the following rule for impulse detection at pixel X*(m,n)* as:

- If $sd(m,n)$ is a high magnitude negative quantity then **X***(m,n)* is corrupted by a positive impulse noise.

- If $sd(m,n)$ is a high magnitude positive quantity then **X***(m,n)* is corrupted by a negative impulse noise.

Since the objective is to detect the presence of an impulse noise rather than its type, compute the absolute value of the second order difference *sd* i.e. $|sd|$.

Step 5: Obtain a matrix d by passing the magnitude of each element of *sd* through a hard limiter (H) that saturates at a threshold value γ_1, chosen from (3.7) (see Section-3.2.2). The output of the hard limiter is given by:

$$d(m+r,n+s) = H(|\,sd(m+r,n+s)\,|) = \begin{cases} 0, & \text{if } |sd(m+r,n+s)| > T \\ 1, & \text{otherwise} \end{cases} \tag{3.6}$$

Step 6: Apply the binary decision rule for impulse detection at **X***(m,n)* as:

- If $d(m,n)$ is zero, then the test pixel **X***(m,n)* is corrupted by impulse noise and invoke the filtering operation to substitute the gray level of the test pixel with a filtered gray value. Then go to Step 7.
- If $d(m,n)$ equals to one, then the test pixel is healthy. Skip the test window and go to Step 7.

Step 7: Shift the moving window $\mathbf{X}_T$ by one column from left to right and top to bottom as shown in Fig. 3.2.

Step 8: Repeat Steps 2 through 6 for all the windows in the row.

Step 9: Obtain the next moving window by shifting it by one row.

Step 10: Repeat Steps 2 through 7 till the complete image is covered.

Step 11: Repeat steps 1 through 10 in the vertical direction with a different threshold value, γ_2, chosen from (3.8) (see Section-3.2.2).

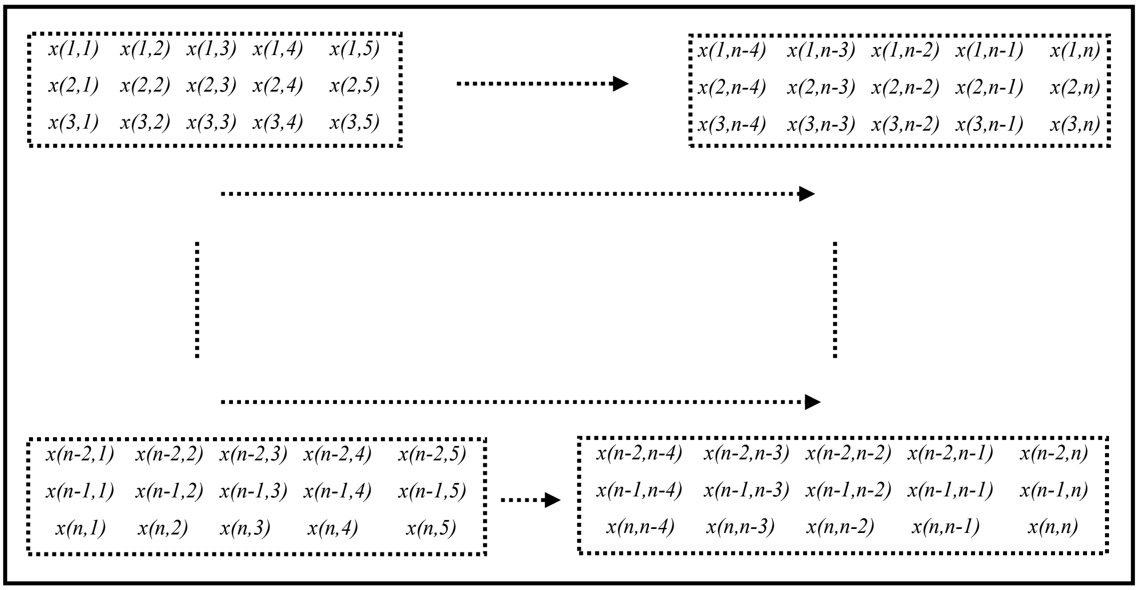

Fig. 3.3 Typical window selection for an N×N image in horizontal direction

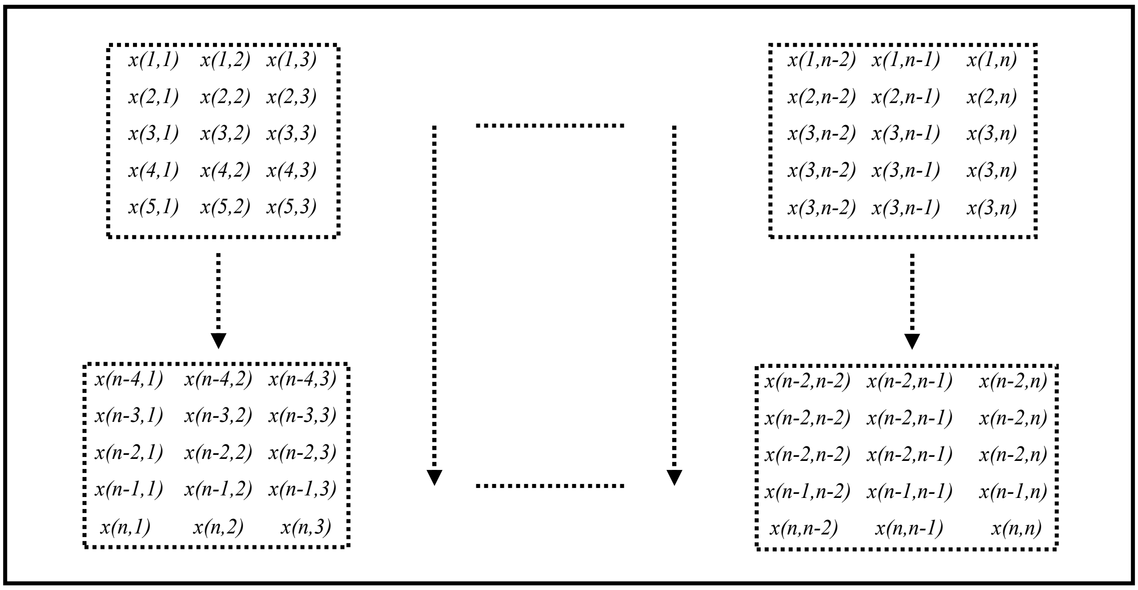

Fig. 3.4 Typical window selection for an N×N image in vertical direction

3.2.2 Threshold Selection

Zhang and Karim [92] have demonstrated a method to choose an optimal threshold value for an impulse detector. Adopting the same procedure, the filter performance is simulated varying the threshold values from 0.01 to 0.50 for various test images. It is observed that the threshold value depends on the mean and variance of the noisy image. Empirical formulae for the optimal threshold values are developed to fit to the data obtained from the simulation. Two thresholds γ_1 and γ_2, required for the first-pass and second-pass of the proposed impulse detection scheme, respectively are given by:

$$\gamma_1 = -\frac{1}{170} e^{-25\sigma_x^2} + \frac{\bar{x}}{2.25} \tag{3.7}$$

where σ_x^2 is the variance and $\bar{x}$ is the mean of the noisy image,

and

$$\gamma_2 = \frac{\gamma_1}{0.7}. \tag{3.8}$$

Using these empirical formulae, optimal threshold values are calculated for each noisy image. Such optimal threshold values enhance the filtering performance to a great extent.

3.2.3 Filtering Algorithms

Based on the algorithm depicted in Section-3.2.1, the corrupted pixels are identified throughout the image. In the first pass γ_1 and in the second pass γ_2 is used to identify the corrupted pixels. The filtering operation is carried out only on those distorted pixels once in each pass. The proposed filtering algorithm proceeds as follows:

The filtering operation computes the median value of a 3×3 window $\mathbf{X}_W$ surrounding the corrupted center pixel and substitutes this value at the location of the faulty pixel like the conventional median filter. In the next adjacent window, the healthiness of its center pixel is tested considering the gray level of the already filtered pixel rather than that of the original one.

Mathematically,

$$\mathbf{X}(m,n) = \widetilde{\mathbf{X}}(m,n) = median(\mathbf{X}_W) \qquad (3.9)$$

3.2.4. Simulation Results

The performance of the proposed filtering scheme is evaluated by conducting three simulation experiments. Various standard gray level images are used for the purpose. The noisy images are generated by corrupting them with SPN with equal probability. Various standard methods, such as median with 3×3 and 5×5 window size, Center Weighted Median (CWM) with center weight k = 1 and 3, Rank-Ordered Mean (ROM), Peak and Valley (pkvly), Rank-Ordered Mean-Switching Median (ROM-SM) are also simulated along with DDMF to compare their performance with the proposed one.

Experiment 1:

Experiment 1 is conducted to show the image quality which are retained after filtering at different noise conditions. In this experiment Boat image is selected and its noisy version are generated by adding SPN noise of densities 5 to 30. The noisy images are filtered by the proposed SOD-DDMF as well as other standard methods. In each case PSNR (dB) and PSP (%) are obtained from the simulation and plotted in Fig. 3.5(a) and (b). These two plots show that the SOD-DDMF scheme is superior to all other standard methods as it offers highest PSNR (dB) and lowest PSP (%) for all noise conditions.

Experiment 2:

In this experiment, seven different standard images are selected and each one is corrupted with 15% SPN. Many standard techniques are simulated to filter the noise component from this noisy image. From the filtered images the PSNR (dB) and PSP (%) are computed and have been listed in Table-3.1. The tabular data clearly indicates that the filtering performance of the SOD-DDMF is the best with respect to the parameters in all cases.

Experiment 3:

The performance of the proposed SOD-DDMF is further checked for RVIN. The ‘Lena’ image is corrupted with RVIN of varying noise density and then the proposed filtering scheme is applied. The simulation results are given in Table-3.2. The results are quite satisfactory for RVIN of density upto 20%.

3.2.5 Conclusion

The proposed filter is a novel scheme for filtering impulse noise from corrupted images under varying noise densities. Unlike the standard reported methods of filtering, the proposed SOD-DDMF method detects the presence of an impulse noise at every pixel location. However, the filtering operation (median filtering) is performed selectively on the detected noisy pixels. Hence, the filtering time is reduced and undue distortion is eliminated in restored images. On exhaustive computer simulation on different images under various noise conditions, it is observed that the proposed SOD-DDMF scheme exhibits superior performance over other standard methods. This scheme also shows better performance, in terms of PSNR, than the Rank-Ordered Mean (ROM) based Switching Median scheme proposed by Zhang and Karim [92] as seen in Fig. 3.4(a). It also shows a moderate performance suppressing RVIN as illustrated in Table-3.2.

At 15% noise density, this filter yields a PSNR of 34.5 dB and 30.82 dB in case of SPN and RVIN respectively for the same 'Lena' image. Thus, it is observed that this filter is a very good scheme for suppressing SPN and its performance is good in filtering RVIN. It performs well for low density RVIN. In real-time applications like digital television systems, where RVIN density is usually below 20%, such a filter may be employed.

Table 3.1: Comparison of PSNR (dB) and PSP (%) computed from different filtered images at 15% noise

Filters	PSNR(dB)					PSP(%)				
	Lena	Lisa	Girl	Clown	Gatlin	Lena	Lisa	Girl	Clown	Gatlin
Median(3x3)	32.2	35.6	34.0	31.8	39.2	68.4	41.6	69.2	52.6	36.4
Median(5x5)	30.5	33.5	33.8	31.0	41.8	80.3	53.3	80.1	58.5	48.2
CWM (k=1)	29.8	30.3	30.0	32.9	33.7	38.1	19.4	38.5	33.0	17.6
CWM(k=3)	22.7	23.1	22.7	28.2	24.9	18.5	8.1	18.1	19.6	7.7
Pkvly	28.2	32.1	30.4	30.9	39.2	51.9	29.5	51.0	46.7	26.6
ROM	30.6	35.0	33.6	30.9	41.5	85.2	70.2	85.2	73.2	58.4
DDMF	**34.5**	41.5	38.2	34.23	41.4	13.1	6.1	11.15	12.0	3.8

Table 3.2: PSNR (dB) at different Random-Valued Impulse Noise for Lena Image

RVIN d (%)	PSNR (dB)
01	38.87
05	35.24
10	32.60
15	**30.82**
20	29.59

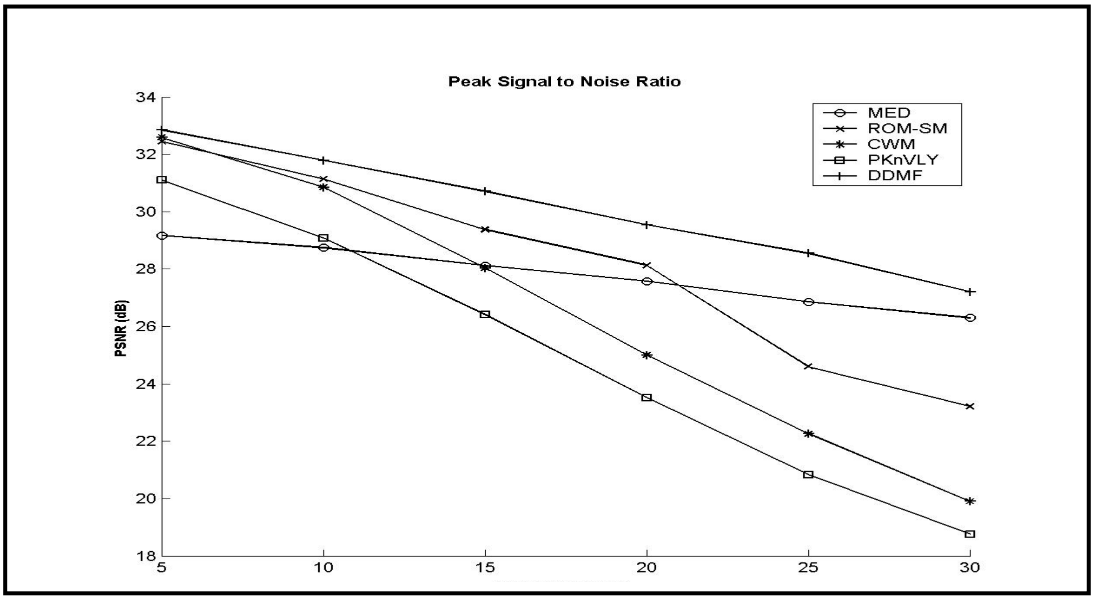

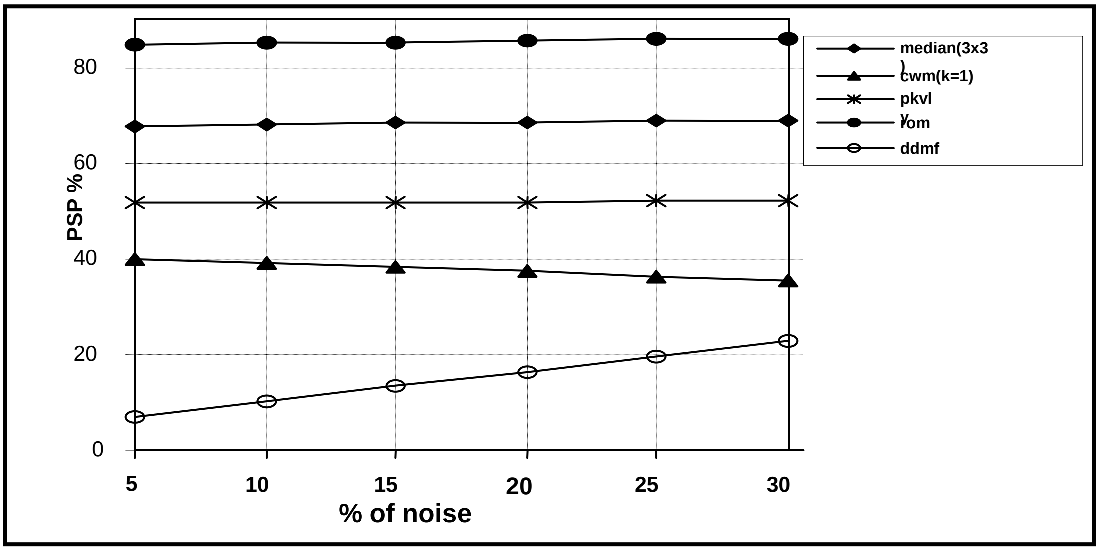

a
b

Fig. 3.5 Performance comparison of different methods for filtering on Corrupted Boat image

(a) Variation of PSNR (dB) with Impulse Noise Density

(b) Variation of PSP with Impulse Noise Density

3.3 Probability based Impulse Noise Detection (PIND) Algorithm

This algorithm is based on the theory of probability. It believes that under low density SPN it is very less probable to find all pixels black or all pixels white in a sampled window if the original image pixels are not so.

It is already mentioned in Section-3.1 that filtering operation on every pixel is not required for eliminating the impulse noise. Rather, it is computationally economical to filter only the corrupted pixels leaving the non-noisy pixels unchanged. This approach reduces the blurring effect in the restored image since the magnitude of a non-noisy pixel is not affected by filtering. The most common OS filter MED is employed after detecting an impulse.

The organization of this section is outlined below.

- The PIND Algorithm
- An Analysis on the PIND Algorithm
- Simulation Results
- Conclusion

3.3.1 The PIND Algorithm

Let a 3×3 window be taken for sampling the image data. The detection algorithm and the filtering operation are applied on this data set $\{x_i\}$ to detect an impulse and to filter the pixel at the center of the window, i.e. the center-pixel.

Let cp = gray-scale magnitude of the center pixel.

$= x_i$ for i = (m_0, n_0) where m_0 and n_0 are two integers representing the coordinates of the center-pixel.

Let s = sum of gray-scale magnitudes of all the pixels in the 3×3 neighborhood.

$= \sum_i x_i$ for $i = (m, n) = (m_0 - 1: m_0+1, n_0 - 1: n_0+1)$.

Then, the proposed detection algorithm is:

PIND Algorithm

IF (***cp*=0 OR *cp*=1**) **AND** (s**≠9**×pc)
THEN *impulse_detected*=**YES**
ELSE *impulse_detected*==**NO**
END (3.10)

3.3.2 An Analysis on the PIND Algorithm

At low density d (10%) of salt (cp = 0) and pepper (cp = 1), i.e. $d \leq 0.1$, if all x_i's are of same value, either 0 or 1, in a 3×3 windowed sample, then most probably, it doesn't represent an impulse. It is so because the probability of all x_i's being 0 or 1 in a 3×3 neighborhood, $p = 2\times(0.1/2)^9 \ll 1$. This is an optimistic estimation. In fact, the situations are quite different in case of a practical image signal. This may be very well visualized if a typical example, as shown in Fig.3.6, is taken.

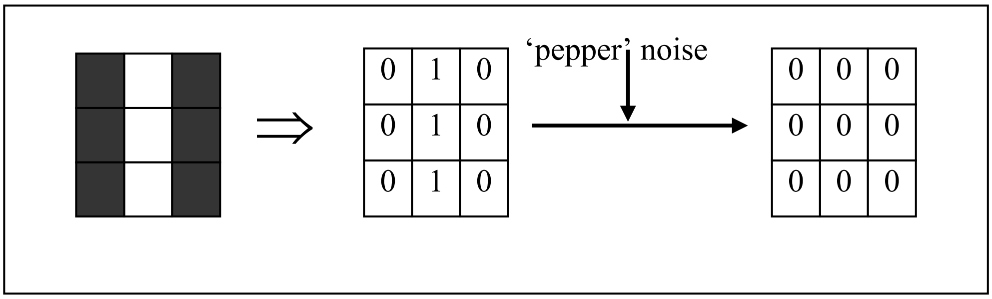

Fig. 3.6 A Typical Windowed Data and the Effect of Impulse Noise

This represents an edge in an image. If all the three pixels (each having value '1') are corrupted with 'pepper' noise so that their values become '0', then all the pixels in the window have the same gray-scale value. Thus, the proposed PIND algorithm fails to detect an impulse noise here. This is a pessimistic estimation. Such conditions occur in edge points only. Even under such circumstances, the probability of such an occurrence is,

$$p = 2\times(0.1/2)^3=0.00025=0.025\% \qquad (3.11)$$

There is a multiplying factor '2' in (3.11) to represent the effect of both 'salt' and 'pepper'.

Thus, even the pessimistic estimation of detection failure rate is very less under low density (≤ 0.1) SPN. Therefore, the proposed PIND algorithm is an excellent impulse noise detector under low density SPN. It is a very simple algorithm. Its computational complexity is extremely low. So such an algorithm may be employed for any real-time application where the impulse noise density seldom exceeds 10%.

3.3.3 Simulation Results

Extensive simulation is carried out to study the filtering performance of the proposed PIND algorithm and to have a comparative study of this scheme vis-à-vis some standard schemes available in literature. The standard test image, 'Lena face' is corrupted with SPN of density 0%, 5%, 10%, 15% and 20%. The performance measures: MAE, MSE, PSNR and PNEP are obtained for this filter. The percentage of no-error pixels (PNEP) indicates what percentage of pixels in a filtered image has been perfectly recovered. These values are listed in Table-3.3. This table clearly indicates a superb performance of the proposed scheme under low noise density. A plot MSE versus SPN density is given Fig. 3.7. To have a subjective evaluation, the noisy and the recovered images for low and high noise densities are shown in Fig. 3.8 and Fig. 3.9 respectively. These figures clearly show the high quality of the recovered images. The restored image quality is excellent upto 10% impulse density.

Most important point here is the PNEP. The PIND algorithm yields extremely high PNEP at low SPN density. When there is no noise, this scheme doesn't distort the image at all and it yields 100% PNEP, whereas the MED and CWM filters yield 49.4% and 68% PNEP, respectively. Thus the proposed PIND algorithm is an excellent scheme for removal of low density SPN.

3.3.4 Conclusion

The proposed PIND algorithm followed by MED filtering is an excellent scheme to suppress low density SPN. Its performance is extremely high compared to standard filters like MED, CWM, etc.

Recently, three very nice schemes have been proposed by researchers. The MAD algorithm developed by Crnojevic *et al*. [106], the SWM algorithm proposed by Zhang and Karim [92] and the DRID algorithm developed by Aizenberg and Butakoff [100] are very good impulse noise detectors. The SWM algorithm yields a PSNR of 29.59 dB when the PIND algorithm yields 37.58 dB at 10% SPN. The MAD and the proposed PIND algorithms show almost the same quality in restoration. Both of them yield approximately 32 dB PSNR at 20% SPN. The PIND and DRID algorithms yield PSNR of 41.2 dB and 43.8 dB respectively at 5% SPN.

Thus, it is observed that the proposed PIND algorithm shows slightly poor performance as compared only to DRID algorithm. However, it is its simplicity and very low computational complexity that can't be challenged by any of these three recently reported filters. Therefore, the PIND is highly suited for real-time applications where the low computational complexity is an advantage.

The whole scheme of PIND followed by MED may be made recursive, similar to the algorithm presented in Section-3.2, to yield better performance at higher noise density. It is observed that the recursive scheme performs well up to 30% SPN density.

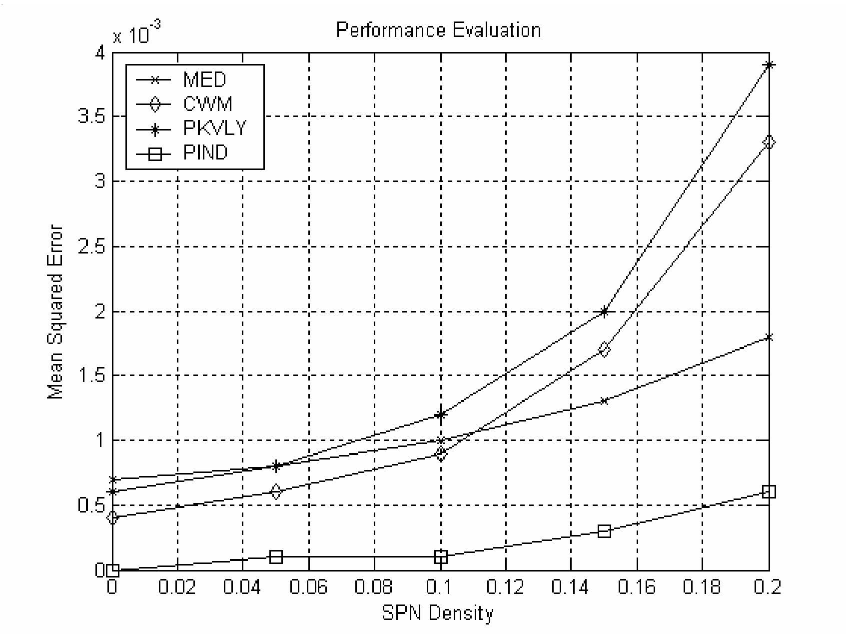

Fig. 3.7 Mean Squared Error (MSE) Performance of Various Filters

Table-3.3 Performance Parameters calculated under various noise conditions

(a) At 0% noise density

Parameters	**MED**	**CWM**	**pkvly**	**PIND+Filter**
MAE	0.0150	0.0087	0.0123	**0**
MSE	0.0007	0.0004	0.0006	**0**
PSNR(dB)	31.3975	34.1599	32.1930	**∞**
PNEP	49.4350	68.0737	58.5632	**100**

(b) At 5% noise density

Parameters	**MED**	**CWM**	**pkvly**	**PIND+Filter**
MAE	0.0158	0.0098	0.0134	**0.0011**
MSE	0.0008	0.0006	0.0008	**0.0001**
PSNR(dB)	30.7203	32.1137	31.2266	**42.1502**
PNEP	48.4474	66.8602	57.2994	**96.8006**

(c) At 10% noise density

Parameters	**MED**	**CWM**	**pkvly**	**PIND+Filter**
MAE	0.0167	0.0110	0.0151	**0.0023**
MSE	0.0010	0.0009	0.0012	**0.0001**
PSNR(dB)	29.9342	30.2891	29.2832	**38.2587**
PNEP	47.4869	65.5613	55.8064	**93.4528**

(d) At 15% noise density

Parameters	**MED**	**CWM**	**pkvly**	**PIND+Filter**
MAE	0.0178	0.0132	0.0173	**0.0037**
MSE	0.0013	0.0017	0.0020	**0.0003**
PSNR(dB)	28.8542	27.5849	27.0567	**34.7619**
PNEP	46.5649	24.8817	54.1882	**90.0739**

(e) At 20% noise density

Parameters	MED	CWM	pkvly	PIND+Filter
MAE	0.0194	0.0167	0.0219	**0.0053**
MSE	0.0018	0.0033	0.0039	**0.0006**
PSNR(dB)	27.3322	24.8117	24.0656	**32.2341**
PNEP	45.6337	62.5679	52.4151	**86.7039**

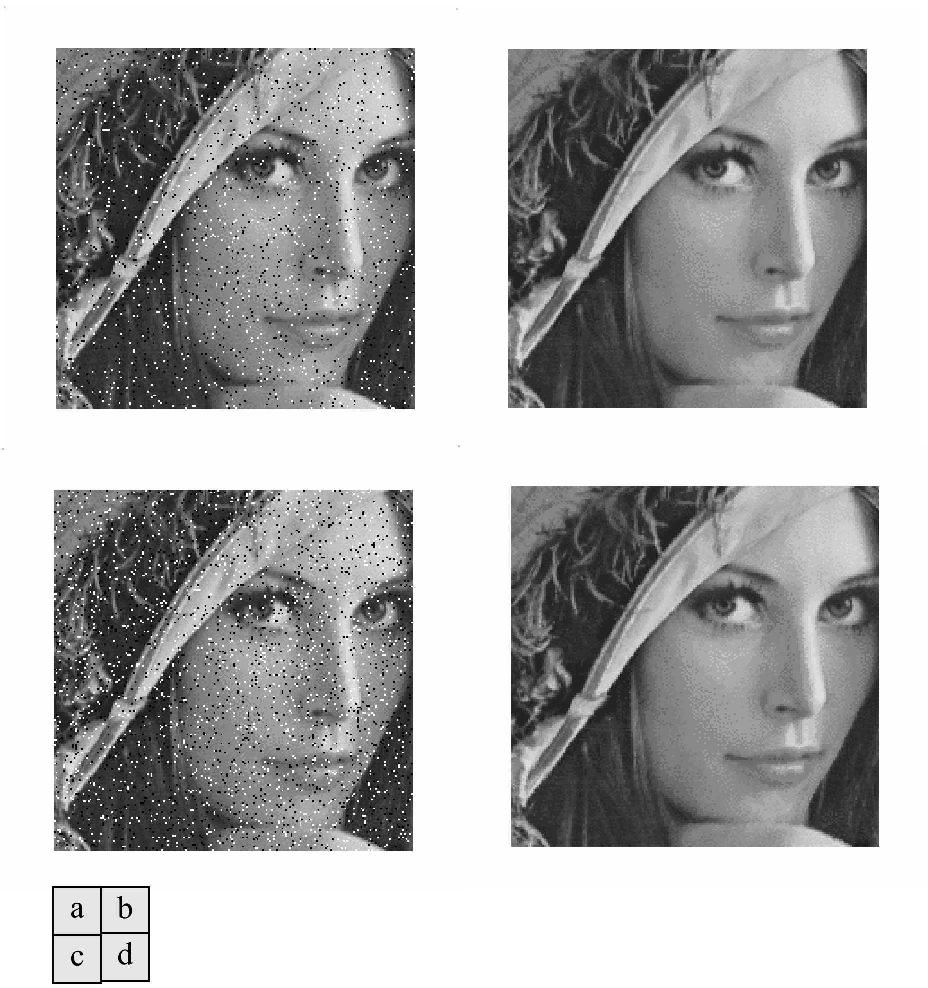

Fig. 3.8 Performance of PIND Algorithm under low density SPN

(a) Noisy ‘Lena face’ with 5% SPN
(b) Recovered Image for input Image (a)
(c) Noisy ‘Lena face’ with 8% SPN
(d) Recovered Image for input Image (c)

a	c
b	d

Fig.3.9 Performance of PIND Algorithm under SPN

(a) The Test Image, ‘Lena face’ corrupted with 10% SPN
(b) The Restored Image for Input Image in (a)
(c) The Test Image, ‘Lena face’ corrupted with 15% SPN
(d) The Restored Image for Input Image in (c)

3.4 Deviation based Impulse Noise Detection (DIND) Algorithm

A novel impulse detection scheme, **d**eviation based **i**mpulse **n**oise **d**etection (DIND) algorithm, is proposed for detecting impulses quite effectively. The algorithm, presented here, shows very good performance in case of SPN and RVIN. A slightly modified version performs well even under **mixed noise** conditions.

The DIND algorithm may look similar to the MAD algorithm proposed by Crnojevic *et al.*[106]. However, they are quite different. The DIND algorithm is based on a robust OS estimation operation, the ROM(5,11), whereas the MAD is based on the most common OS operation, the median (MED). That is why, the DIND performs well under mixed noise conditions.

The organization of this section is outlined below.

- The DIND Algorithm
- Simulation Results
- Conclusion

3.4.1 The DIND Algorithm

It is seen that ROM(5,11) is a very good estimator of the expected value under mixed noise condition. The filter: ROM(5,11) takes a 5×5 window, centered at the pixel to be filtered, and considers only 11 intermediate order statistics rejecting 7 very low and 7 very high values. Let this order statistics (OS) estimation operation be represented by $E_1(.)$.Similarly, two more OS estimators are defined: $E_2(.)$ = ROM(5,3) and $E_3(.)$=ROM(3,3). The ROM(5,3) considers only 3 intermediate order statistics rejecting 11 low and 11 high values. On the other hand, the ROM(3,3) estimation operation takes a 3×3 window and considers only 3 intermediate order statistics rejecting 3 low and 3 high values.

Let $\{x_i\}$ represent the gray scale values of the center pixel, the pixel to be filtered, and the pixels in its 5×5 neighborhood. Then, the ROM(5,11) applied on $\{x_i\}$ gives a robust estimate of the expected value, $E_1(\{x_i\})$. Corresponding to each pixel in the window, a pixel-deviation, Δ_i, is computed:

$$\Delta_i = x_i - E_1(\{x_i\}) \tag{3.12}$$

The gray-scale value, x_{13}, represents the center pixel. Now, a parameter called the **a**bsolute value of the **d**eviation at the **c**enter pixel, **ADC** is defined by:

$$\mathbf{ADC} = |\Delta_{13}| = |x_{13} - E_1(\{x_i\})| \tag{3.13}$$

The detection algorithm is given by (3.14) and the filtering algorithm, by (3.15).

Detection Algorithm:
IF ADC ≥ γ,
THEN
impulse_detected = **YES**,
ELSE
impulse_detected = **NO**
END.

(3.14)

Filtering Algorithm:
IF im*pulse_detected* = **YES**
filter-output, $x_o = E_1(\{x_i\}) + E_2(\{\Delta_i\})$
ELSE
filter-output, $x_o = x_{13}$
END.

(3.15)

where, γ is a threshold parameter. A threshold value of 0.15 is taken. This value works fine for detecting impulses of density 0 to 30%. Of course, this value can be made adaptive as it is done in Section-3.2. The filtering algorithm, presented in (3.15), is applied after the detection. Under mixed noise conditions, the impulse detection algorithm is slightly modified.

Modified Algorithm

Let a new expectation operation, E(.) ,a linear combination of $E_1(.)$ and $E_2(.)$, be defined as:

$$E(\{x_i\}) = [\ E_1(\{x_i\})+2\cdot E_2(\{x_i\})]\ /\ 3 \tag{3.16}$$

Then, the ADC is computed with the help of (3.12) and (3.13) where the expectation operation is E(.) in place of $E_1(.)$. The detection methodology now uses the same DIND algorithm of (3.14). But, the associated filtering algorithm, for use under mixed noise condition, is given by (3.17).

Filtering Algorithm (under MN condition):
IF im*pulse_detected* = **YES**
filter_output, $x_o = E(\{x_i\}) + E_2(\{\Delta_i\})$
ELSE
filter_output, $x_o = E(\{x_i\})$
END

(3.17)

3.4.2 Simulation and Results

Taking the standard 'Lena face' image and adding SPN of varying density, the performance of MED, ROM and the proposed filter is found. The MSE is taken as the performance measure. The MSE values are given in Table-3.4. The last column in the table shows the performance parameter, NRDB for the proposed filter. The MSE values for RVIN and SPN are given in Table-3.5 and Table-3.6. Plots of MSE versus SPN density, MSE versus RVIN density and MSE versus input noise power (under MN) are shown in Fig.3.10, Fig.3.11 and Fig. 3.12. The original, noisy, and recovered images are shown in Fig.3.13, Fig.3.14 and Fig.3.15 for subjective evaluation of the filters.

Table-3.4 Performance of Various Filters under SPN of Varying Density

SPN d(%)	MSE_{in}	MSE_{out}				NRDB (dB) (proposed scheme)
		MED3×3	MED5×5	ROM(5,11)	DIND+Filter	
0	0	.00089	.0016	.0016	.00033	-- --
1	.0029	.00091	.0017	.0016	.00036	9.09
2	.0056	.00093	.0017	.0016	.00037	11.78
3	.0086	.00097	.0017	.0016	.00040	13.27
4	.0117	.00098	.0017	.0016	.00042	14.43
5	.0140	.0010	.0017	.0017	.00046	14.84
10	.0292	.0011	.0018	.0017	.00054	17.36
15	.0441	.0015	.0019	.0019	.00074	17.76
20	.0579	.0023	.0020	.0020	.00089	18.13
25	.0732	.0030	.0020	.0021	.00094	18.91
30	.0899	.0051	.0022	.0025	.0012	18.62

Table: 3.5 Performance (MSE) of various filters under RVIN

RVIN, d %	MSEin	MSEout			
		MED3×3	MED5×5	ROM(5,11)	DIND+Filter
5	0.0063	9.98×10^{-4}	0.0017	0.0017	5.47×10^{-4}
10	0.0130	0.0011	0.0018	0.0017	7.52×10^{-4}
15	0.0187	0.0013	0.0019	0.0019	9.789×10^{-4}
20	0.0247	0.0015	0.0020	0.0020	0.0013
25	0.0314	0.0019	0.0022	0.0020	0.0016
30	0.0384	0.0027	0.0024	0.0025	0.0019

Table: 3.6 Performance (MSE) of various filters under MN (AWGN, σ^2=0.001 with SPN of density, d)

SPN, d %	MSEin	MSEout					
		MED3	MED5×5	ROM(5,11)	MAV3×3	MAV5×5	DIND+Filter
1	0.0063	0.0127	0.0027	0.0023	0.0024	0.0027	0.0020
2	0.0130	0.0154	0.0027	0.0023	0.0027	0.0027	0.0020
3	0.0187	0.0179	0.0028	0.0024	0.0030	0.0029	0.0021
5	0.0247	0.0246	0.0030	0.0024	0.0039	0.0033	0.0022
10	0.0314	0.0378	0.0033	0.0025	0.0056	0.0042	0.0023

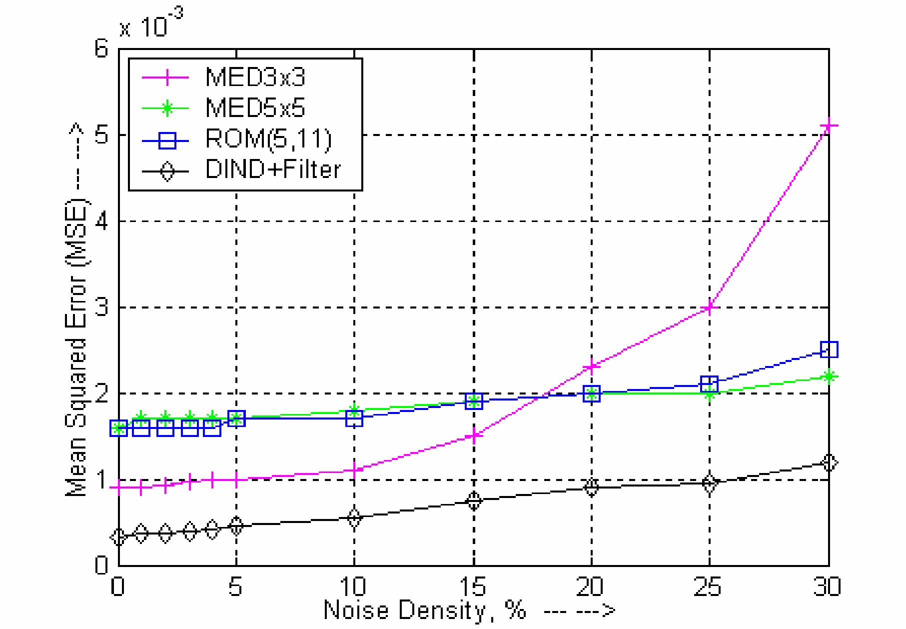

Fig. 3.10 Performance (MSE) of Various Filters under SPN of varying noise density.

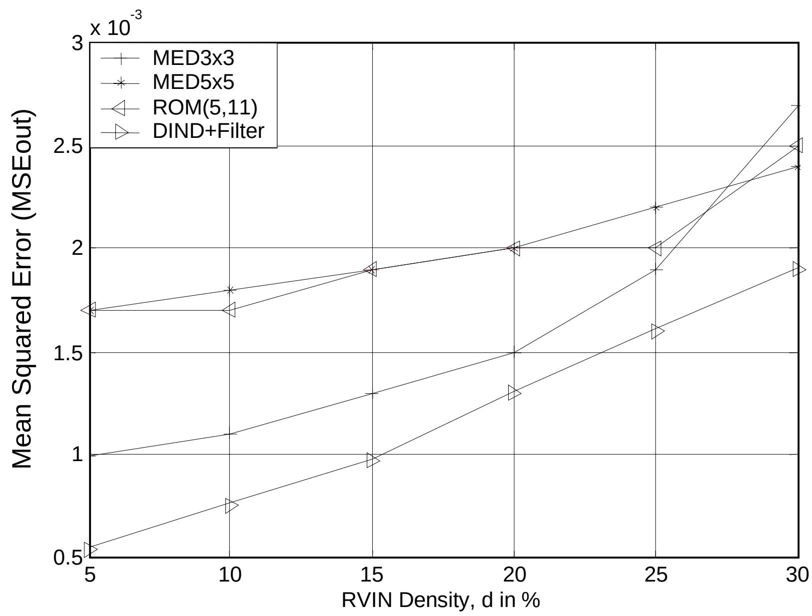

Fig. 3.11 Performance (MSE) of Various Filters under RVIN of Varying Noise Density.

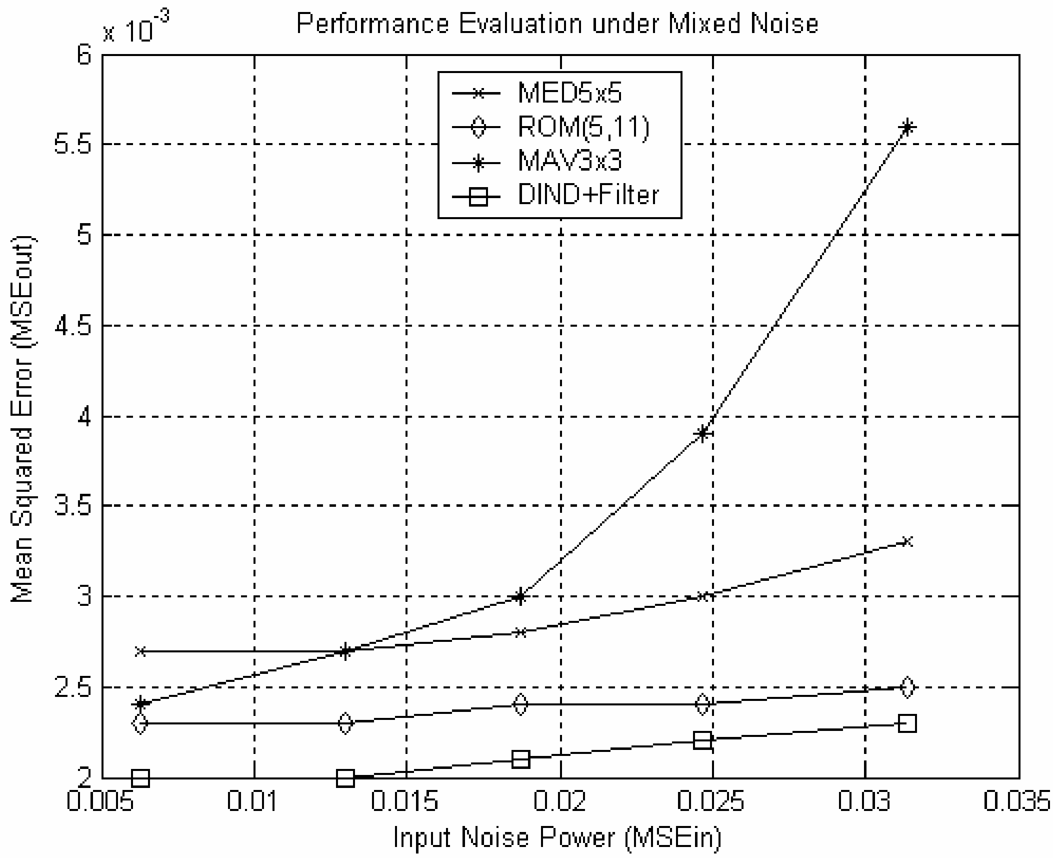

Fig.3.12 A Plot of MSEout versus MSEin for Performance Evaluation of Various Filters under Mixed Noise Conditions.

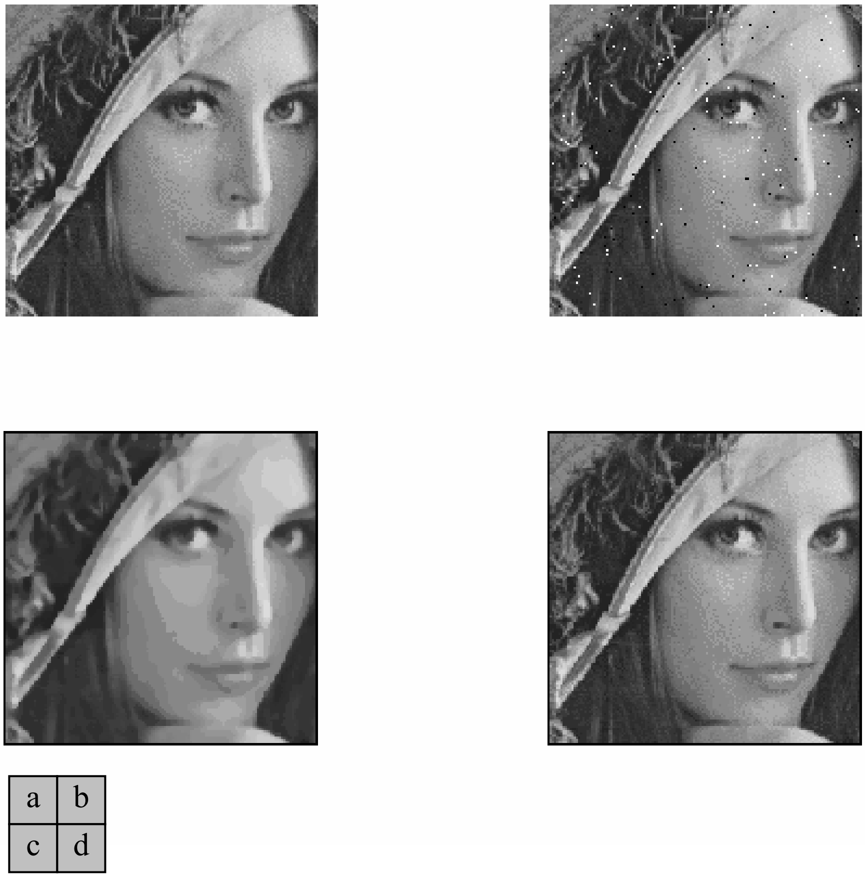

Fig. 3.13 Performance of Various Filters for SPN (d = 5%)

(a) Original 'Lena face' Image
(b) Noisy 'Lena face' Image
(c) ROM(5, 11) Filter Output Image
(d) DIND + Filter

a	b
c	d

Fig. 3.14 Performance of Various Filters for RVIN (d = 10%)

(a) Original ‘Lena face’ Image
(b) Noisy ‘Lena face’ Image
(c) ROM (5, 11) Filter Output Image
(d) DIND + Filter

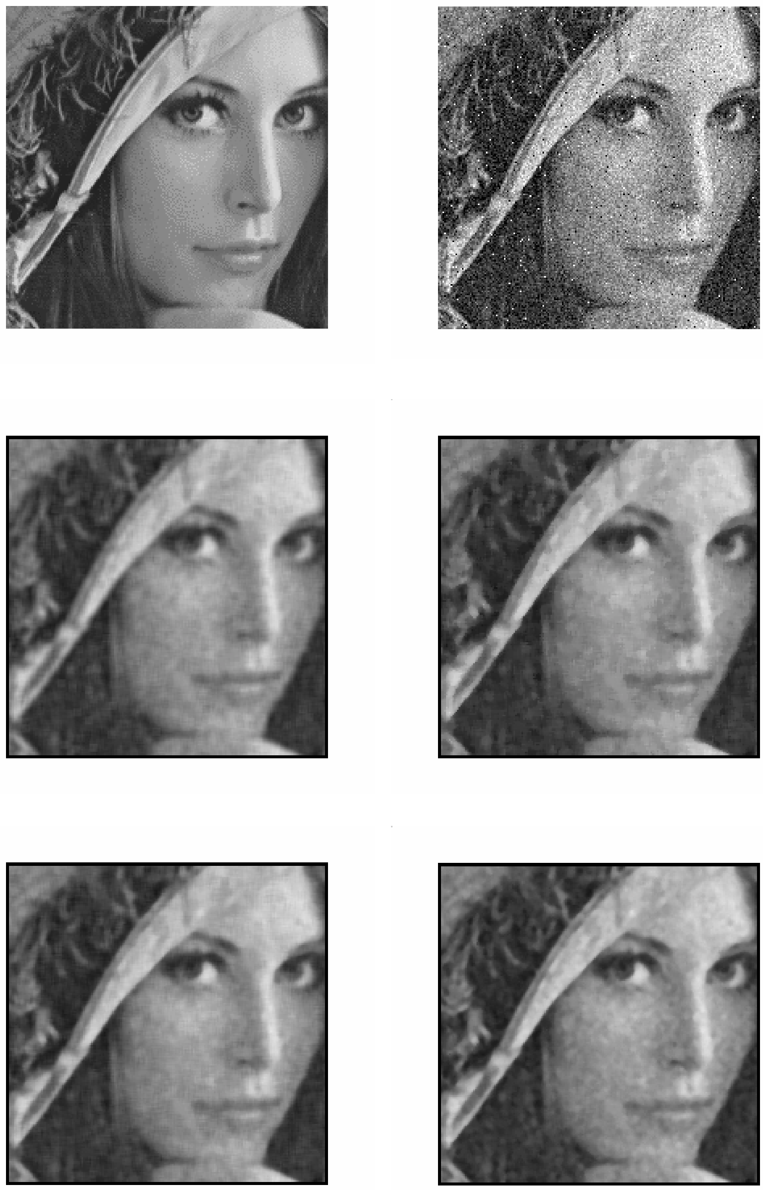

a	b
c	d
e	f

Fig. 3.15 Performance of Various Filters under Mixed Noise Condition (AWGN, σ^2 =0.005 with SPN, d = 1%).

(a) Original 'Lena face' Image
(b) Noisy 'Lena face' Image
(c) MAV5×5 Filter Output Image
(d) MED5×5 Filter Output Image
(e) ROM(5, 11) Filter Output Image
(f) DIND + Filter

3.4.3 Conclusion

It is observed from Fig.3.10 and Fig. 3.11 that the proposed scheme shows excellent performance and is much superior to the standard filters for removing impulse noise (both SPN and RVIN) from an image. Fig.3.12 shows its superior performance in suppressing SPN under mixed noise condition when all other standard OS filters fail. The images, shown in Fig.3.13, Fig.3.14 and Fig.3.15 clearly indicate a superb noise rejection and image edge-retention capability of the DIND algorithm-based filter. Therefore, the proposed filter will be highly useful in real-time applications like television, photo-phone, etc.

3.5 Conclusion

In this chapter, many novel impulse detectors are proposed. The SOD-DDMF [P1] is a very good filter to suppress SPN. It works fine for low density RVIN (upto 20%) as well. The probability based algorithm PIND is an excellent SPN detector at low density and its performance is seen to be excellent. Though it is a very simple algorithm, its performance is next only to the recently reported DRID algorithm [100]. Since the PIND is a very simple algorithm, it may be used for real-time applications.

The third scheme proposed here is the DIND algorithm. A simple DIND algorithm is presented for removal of SPN and RVIN. Further, a slight modification to this algorithm is proposed to detect SPN under mixed noise condition (AWGN+SPN). Such a scheme very well detects an impulse under MN condition. Therefore, this algorithm is highly suited for real-time applications where the image gets contaminated with MN.

In Chapter-1, the various practical noise conditions have been studied for communication applications like television systems. For analog transmission the received image signal gets contaminated with AWGN and SPN, i.e., a mixed noise (MN). On the other hand, the image signal gets corrupted with RVIN for a digital transmission system. Therefore, the proposed DIND with the filtering scheme will be very much useful in television systems where the effective noise could be MN or RVIN. Depending on the transmission system, a user may switch between the two different filtering schemes designed for RVIN and MN.

CHAPTER-4

Development of Adaptive Image Filters

Preview

To overcome the shortcomings of fixed filters, adaptive filters are designed that adapt themselves to the changing conditions of signal and noise. The filter characteristics change as the signal statistics, noise type, and noise power level vary from time to time. The two broad categories of adaptive image filters proposed, for efficient noise suppression, and presented in this chapter are: (i) Order Statistics LMS Adaptive Filter, and (ii) Fuzzy Adaptive Filters. They show high filtering performance as compared to the fixed filters. But, they are computational intensive algorithms.

It is a well known fact that to achieve something, one has to sacrifice something else. Thus, to achieve high noise filtering capability as well as to preserve the image integrity, an image filter has to perform some extra computation as compared to simple filters like MAV, MED, CWM, ROM, WROM etc. Such simple filters are good for offline applications where an image may be filtered by an expert using a computer and some software algorithm. Since the human expert understands the type of noise and the noise power level looking at the noisy image frame, he (she) can apply the specific filtering operation depending on the requirement. Even the expert may change the filtering operation from one type to another, if he (she) is not satisfied with the filtered image output. But, such human decision can't be taken for an online and real-time application. For example, if a digital television system is considered, the channel noise produces the effect of RVIN. The amount of noise varies from time to time. A frame comes after another just after a few milliseconds. A human expert can't take a decision to choose a filter at that high speed. After all, it becomes an open-loop control that needs a human expert to make a judgment always. If the whole process has to be fully automated, then an adaptive image filter must be used. In such an application, the image filter must adapt to the image local statistics, the noise type, and the noise power level and, thereby, it must adjust itself to change its characteristics so that the overall filtering performance has been enhanced to a high level.

The adaptation could be based on a simple LMS algorithm, a neural network, or fuzzy logic. In the last decade, many researchers have developed various adaptive image filters using LMS adaptive filtering [26], neural network structures [48,55], and fuzzy logic [81,83,84,94,95,97,98].

In real life situations, an image gets corrupted with RVIN or a mixed version of AWGN and SPN depending on whether the image signal has been transmitted in digital or analog form, respectively. The reported adaptive filters don't show good filtering capability in case of RVIN even though they may be quite efficient in filtering SPN. Similarly, there are many good filters designed for AWGN and for SPN separately. But, a few have been developed for a mixed noise condition. It is very important in engineering to analyze a real life problem. Then only, a researcher can find a solution to it.

Since the noise in a practical system could be RVIN or a mixed version of AWGN and SPN, efforts are made in the present research work to develop efficient adaptive image filters under such noise conditions.

This organization of this chapter is outlined below.

- Fundamentals of LMS Adaptive Filters
- Development of an Efficient OS LMS Adaptive Image Filter
- Fundamentals of Fuzzy Logic
- Designing Fuzzy Weighted ROM (FWROM) Image Filters
- Conclusion

4.1 Fundamentals of LMS Adaptive Filters

There are various types of adaptive filters used in signal processing. In 1960, Widrow and Hoff developed a *least mean square* (LMS) *algorithm* [62]. The LMS algorithm is an important member of the family of *stochastic gradient algorithms.* A stochastic gradient method differs from a deterministic gradient approach such as steepest descent method [61]. There is a plethora of LMS adaptive filters in literature [61-66].

An LMS algorithm doesn't need the computation of a convolution matrix, nor does it require a matrix inversion. It is a very simple algorithm. In fact, it is the simplicity of the LMS algorithm that has made it the standard against which other linear adaptive filtering algorithms are benchmarked.

The LMS algorithm is a linear filtering algorithm. It comprises of two basic processes:

(a) a *filtering process* that involves (i) computing the output of a linear filter in response to an input signal, and (ii) generating an estimation error by comparing the output with a desired response;

and

(b) an *adaptive process* that performs an automatic adjustment of the parameters of the filter in accordance with the estimation error.

These two processes work together. Their combination constitutes a feedback loop. The whole process is shown, in block diagrammatic form, in Fig. 4.1. The adaptive control mechanism changes the filter weights, in each iteration, depending on the sign and magnitude of the error, *e*(n), and the input vector, **u**(n). The error at the n^{th} iteration is the difference between the desired output, d(n) and the estimated filter output, $\tilde{d}(n)$. Since the filter tap weight vector w(n) changes at each iteration depending on the error, the weight vector will converge to the desired value w_0 when the error is zero or extremely low.

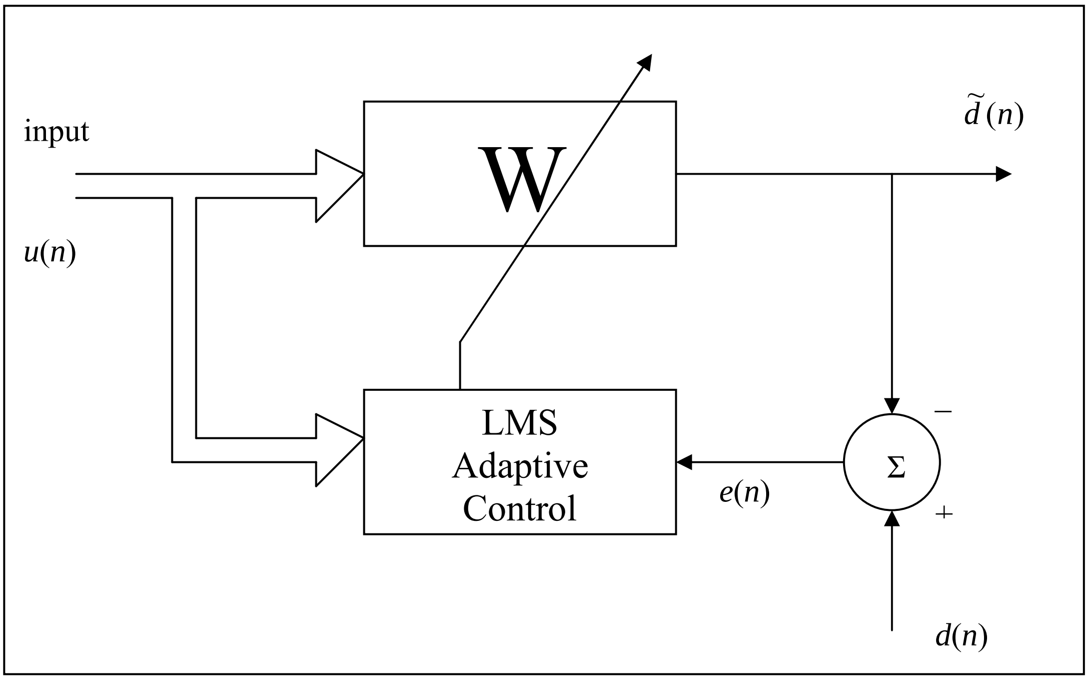

Fig. 4.1 The Block Schematic of an LMS Adaptive Filter

The filter weight vector updating formula, i.e. the LMS algorithm [61], is given by:

$$\mathbf{w}(n+1) = \mathbf{w}(n) + \mu \cdot e(n).\mathbf{u}(n) \tag{4.1}$$

where, μ is learning rate, also known as the step size, for the LMS algorithm. The step size is greater than 0 and less than 1. If the step size is more, then the learning speed is high and the algorithm may converge fast. But, such convergence may not provide good precision $\mathbf{w}$. On the other hand, a small value of μ usually guarantees a high precision convergence, though it takes a longer adaptation (training) time. Therefore, it is always very important to take a particular step size that provides a compromise between a short adaptation time and a high precision convergence in a specific application for a particular type of input. Of course, many new modifications have been proposed to this basic adaptive filter structure using variable and adaptive step size schemes. Such filters achieve much faster and high precision convergence.

Adaptive LMS L-Filter

Based on the simple LMS updation scheme, an adaptive image filter has been proposed by Kotropoulos and Pitas [26]. This is known as Adaptive LMS L-Filter. The windowed data set is applied to the input of this adaptive system. The filter trains itself using the LMS updation rule. Thus, it is basically an adaptive WOS filter. This filter does not possess a good training capability. It needs a reference image that is very similar to the image to be filtered. Thus, such a filter is not very useful.

4.2 Development of an Efficient OS-LMS Adaptive Image Filter

In the present research work, a novel OS-LMS adaptive filter is proposed that gets trained with totally a different type of image. Various order statistics are given as the input to the adaptive filter. The training may not be required always. Even an off-line training may give a very good filter performance.

4.2.1 The Proposed OS-LMS Adaptive Image Filter Structure

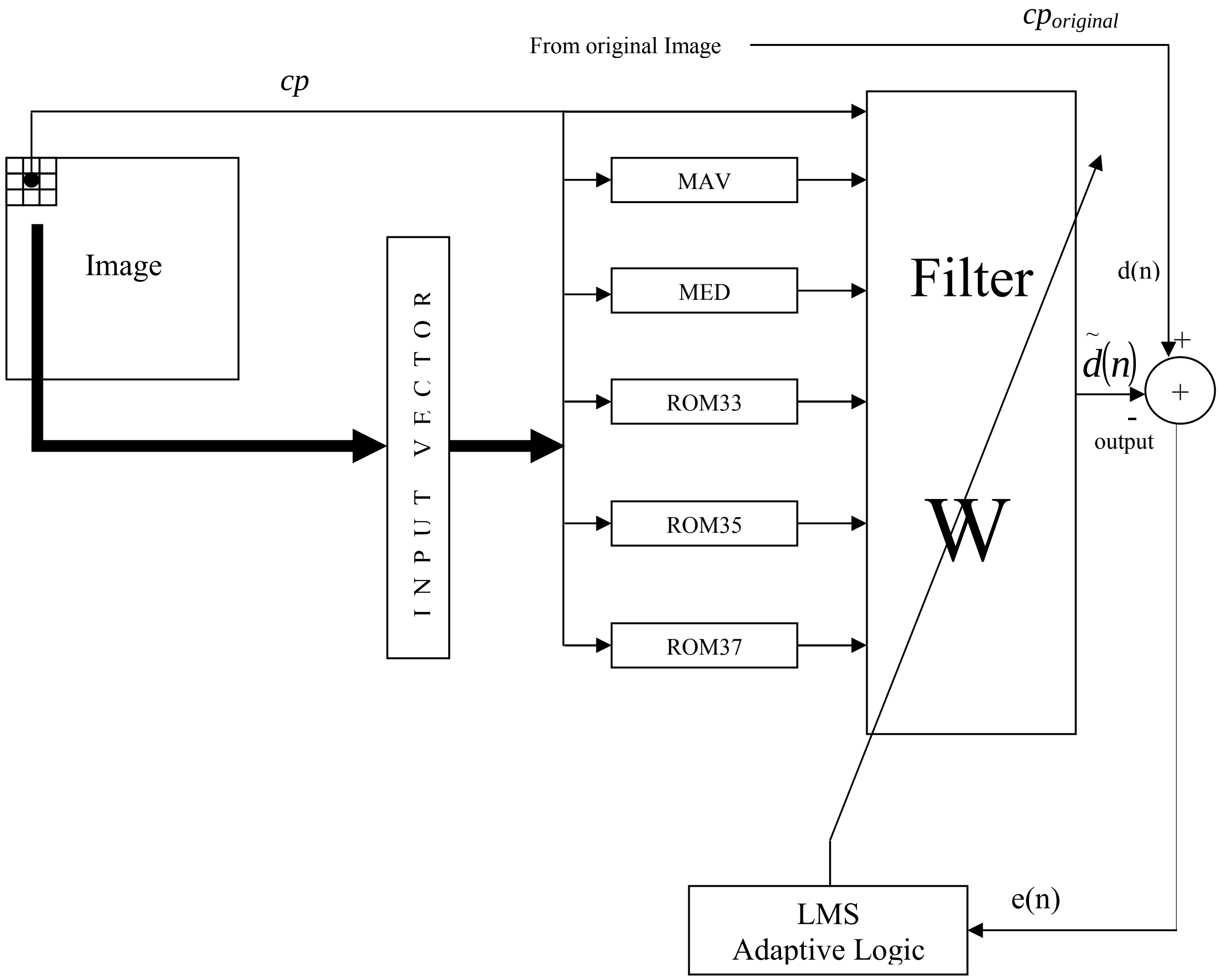

Fig. 4.2. OS-LMS Adaptive Image Filter

Fig. 4.2 shows the schematic of the proposed OS-LMS adaptive image filter. From the sliding windowed data, various OS expectations: mean, median, ROM(3,3), ROM(3,5) and ROM(3,7) are calculated. These five OS expectations along with the center pixel, *cp*, are taken as the input to the adaptive filter. The rest is common to any LMS adaptive filter. The rest is common to any LMS adaptive filter. The desired output, during the training, is the *cp* itself. Once the filter is trained, there is no need of the desired output, d(n). Now the trained filter **w** can compute the filter output $\tilde{d}(n)$.

The windowed data may be represented as a vector,

$$\boldsymbol{x} = [x_1 \quad x_2 \quad x_3 \quad x_4 \quad x_5 \quad x_6 \quad x_7 \quad x_8 \quad x_9]^T \tag{4.2}$$

Let the input vector be represented by $\boldsymbol{z}$.

Then $$\boldsymbol{z} = [z_1 \quad z_2 \quad z_3 \quad z_4 \quad z_5 \quad z_6]^T \tag{4.3}$$

where $z_1 = cp$

$$\left.\begin{aligned} z_2 &= f_1(\boldsymbol{x}) \\ z_3 &= f_2(\boldsymbol{x}) \\ z_4 &= f_3(\boldsymbol{x}) \\ z_5 &= f_4(\boldsymbol{x}) \\ z_6 &= f_5(\boldsymbol{x}) \end{aligned}\right\} \tag{4.4}$$

where $f_1(\boldsymbol{x})$, $f_2(\boldsymbol{x})$, $f_3(\boldsymbol{x})$, $f_4(\boldsymbol{x})$, $f_5(\boldsymbol{x})$ are the various OS expectation functions: mean, median, ROM(3,3), ROM(3,5), and ROM(3,7) respectively.

4.2.2 Simulation Results

The OS-LMS adaptive filter is trained with a reference image, 'Lena face' with the following noise added to it.

(i) RVIN of density, d=10%

(ii) AWGN of variance, σ^2=0.01

(iii) MN: AWGN, σ^2=0.1 + SPN, d=0.05

The corresponding weight vectors obtained after the training are given by:

(i) $\boldsymbol{w} = [0.603 \quad -0.159 \quad 0.3562 \quad 0.0000 \quad 0.3380 \quad 0.2613]$ for RVIN

(ii) $\boldsymbol{w} = [0.1345 \quad 0.3614 \quad 0.0685 \quad 0.1004 \quad 0.1840 \quad 0.1512]$ for AWGN

(iii) $\boldsymbol{w} = [0.0568 \quad -0.2411 \quad 0.1518 \quad 0.1562 \quad 0.3482 \quad 0.5280]$ for MN

Then the corresponding trained filters are used to filter another noisy image. For this purpose, the 'tree' image shown in Fig. 4.3, is used. It is very important to note that the tree image doesn't have any correlation with the reference image 'Lena face'.

Fig. 4.3 The Reference Image, 'trees' Required for Training

Table-4.1 Performance (MSE and NRDB) of OS-LMS Adaptive Image Filter

(a) For Random-Valued Impulse Noise

RVIN density, d	**MSE_{in}**	**MSE_{out}**	**NRDB**
0.05	0.0113	0.0075	1.8230
0.1	0.0224	0.0078	4.5839
0.15	0.0332	0.0034	5.9520
0.2	0.0448	0.0094	6.7649

(b) For Additive White Gaussian Noise

AWGN variance σ^2	**MSE_{in}**	**MSE_{out}**	**NRDB**
0.03	0.0087	0.0054	2.1039
0.07	0.0122	0.0060	3.1231
0.10	0.0164	0.0080	3.1380
0.15	0.0264	0.0139	2.7714
0.2	0.0399	0.0232	2.3555

(c) For Salt and Pepper Noise

SPN density, d	**AWGN variance σ^2**	**MSE_{in}**	**MSE_{out}**	**NRDB**
0.025	0.07	0.0223	0.0073	4.8777
0.05	0.05	0.0284	0.0074	5.8759
0.1	0.03	0.465	0.0083	7.4650

4.2.3 Conclusion

The proposed OS-LMS adaptive image filter shows superior performance as compared to the adaptive LMS L-filter proposed by Kotropoulos and Pitas [26]. The proposed filter very easily adapts to any noise type. The reference image used during training needn't have any correlation with the image to be filtered. Thus, an off-line training is also good enough. Therefore, such a scheme reduces the overall computation time (needed for training and filtering) drastically. Thus, it is highly suitable for a real-time application.

Though its noise reduction capability is not very encouraging, the OS-LMS adaptive image filter will receive high appreciation for its nice noise adaptive behaviour.

4.3 Fundamentals of Fuzzy Logic

Prior to developing some efficient fuzzy filters, the fundamentals of a fuzzy system [49,50] are discussed here.

A fuzzy system is represented by *fuzzy variables* that are members of a *fuzzy set*. A fuzzy set is a generalization of a classical set based on the concept of *partial membership*. Let **F** be a fuzzy set defined on universe of discourse *U*. The fuzzy set is described by the membership $\mu_F(u)$ that maps U to the real interval [0,1] i.e. the membership μ varying from 0 to 1: a membership of value 0 signifying the fact that the element $u \in U$ does not belong to the set **F**; a membership of value 1 signifying that the element $u \in U$ belongs to the set **F** with full certainty; a membership of any other value from 0 to 1 representing the element u to be a partial member of the set **F**. Fuzzy sets are identified by linguistic labels e.g. *low, medium, high, very high, tall, very tall, cool, hot, very hot,* etc. The knowledge of a human expert can very well be implemented, in an engineering system, by using fuzzy rules.

Fuzzy image filters are already proposed by many researchers for suppressing various types of noises [81,83,84]. Simple fuzzy moving average (TMAV) filters [94] are proposed using triangular membership function as shown in Fig. 4.4. The membership equals zero at some minimum and maximum gray values of the pixels in the neighborhood of the center pixel under consideration.

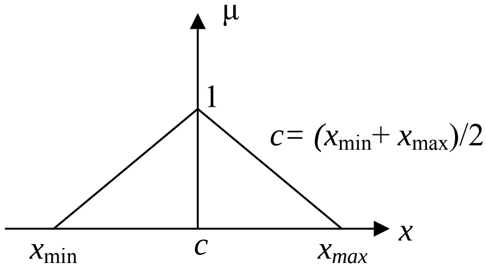

Fig.4.4 Fuzzy Membership for an image filter.

4.4 Designing Fuzzy Weighted ROM (FWROM) Image Filters

The basic structure of the proposed filters is shown in Fig.4.5 (a). The order statistics of the 3×3 neighborhood of the pixel *x(m,n)*, to be filtered, are taken into consideration. Only three/five mid-ordered statistics are the actual inputs for WROM (3,3)/WROM (3,5) filters. The filter weights are computed from fuzzy membership functions. Two fuzzy membership functions: triangular and Gaussian are proposed here. These functions are graphically shown in Fig. 4.5(b) and (c), respectively. First the FWROM filter using triangular fuzzy membership function is discussed.

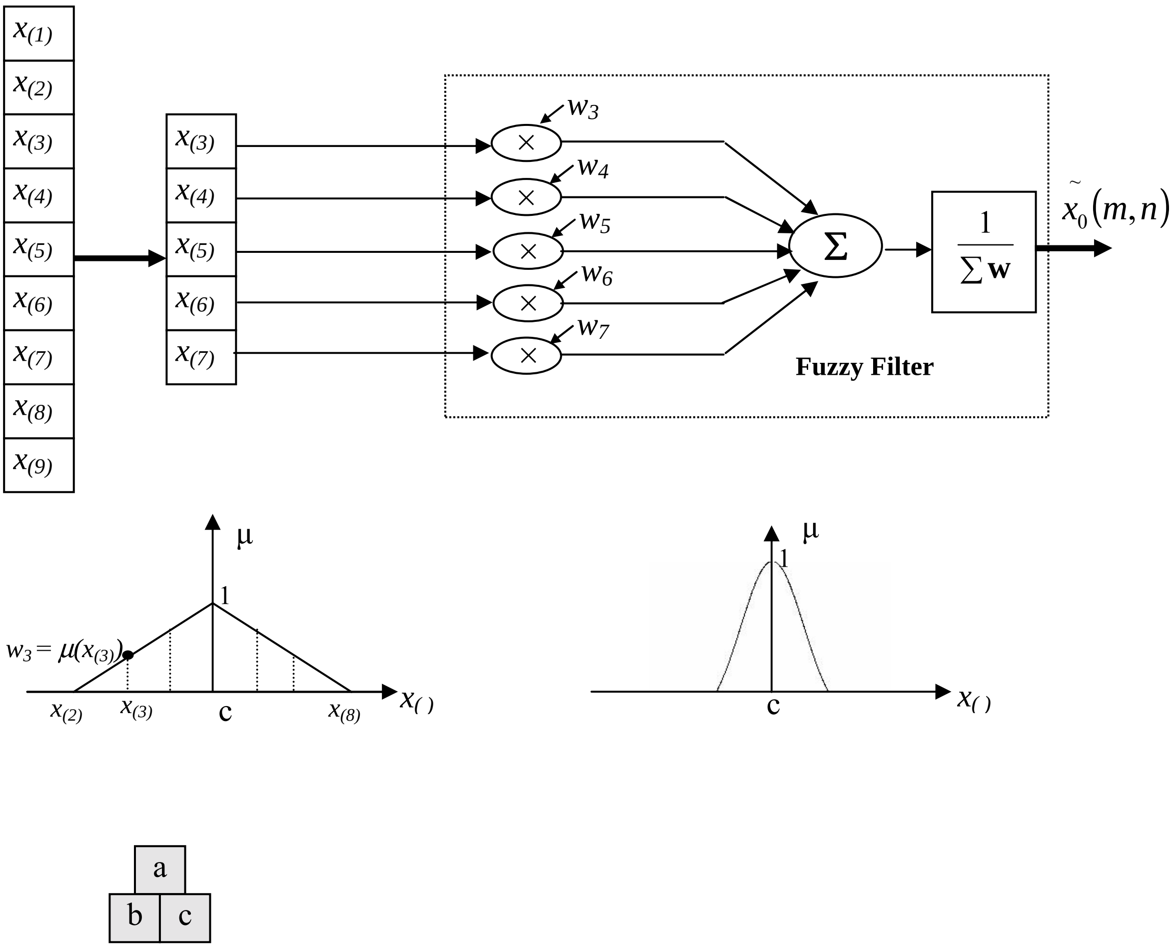

Fig.4.5 (a) Structure of Fuzzy Weighted Rank Ordered Mean Filter
(b) Triangular fuzzy membership associated with the order statistics
(c) Gaussian Fuzzy membership

4.4.1 FWROM-T

The triangular fuzzy membership function $\mu_F(x)$ for WROM (3,5) is given by:

$$\mu_F(x) = \begin{cases} 0, & x \le x_{(2)} \\ \dfrac{1}{c - x_{(2)}}\left(x - x_{(2)}\right), & x_{(2)} \le x \le c \\ \dfrac{1}{x_{(8)} - c}\left(x_{(8)} - x\right), & c \le x \le x_{(8)} \\ 0, & x \ge x_{(8)} \end{cases} \tag{4.5}$$

where $c = \left(x_{(2)} + x_{(8)}\right)/2$.

Similarly, for WROM(3,3), the triangular fuzzy membership function may be defined replacing $x_{(2)}$ with $x_{(3)}$ and, $x_{(8)}$ with $x_{(7)}$ in (4.5). This type of fuzzy membership function is *self-tunable* since the base of the triangle varies depending on the local ordered statistics. So, there is no need of any further fuzzy rule base. The membership $\mu_F(x_{(i)})$ represents how close the ordered statistics $x_{(i)}$ is to the center value c. And, this is the fuzzy weight $w_{(i)}$ that is associated with $x_{(i)}$ to compute the fuzzy weighted rank-ordered mean (FWROM) filter output. The rest part of the filter, aggregation and normalization is self-explanatory. Such fuzzy weighted filters are named as FWROM-T(3,5) and FWROM-T(3,3). Similarly for a 5×5 window, various filters e.g. FWROM-T(5,11), FWROM-T(5,13), etc. may be defined. Next, the development of the FWROM-G filter, using a Gaussian fuzzy membership function, is discussed.

4.4.2 FWROM-G

This filter uses a *Gaussian fuzzy membership* function. In all other respects, it is same as FWROM-T. The Gaussian fuzzy membership function is given by:

$$\mu_F\left(x_{(i)}\right) = e^{-\left(x_{(i)} - c\right)^2 / \sigma^2} \tag{4.6}$$

where σ = the standard deviation of the selected ordered statistics $\mathbf{x}_{(\,)}$, e.g. $x_{(2)}$ to $x_{(8)}$, or $x_{(3)}$ to $x_{(7)}$ for the Gaussian fuzzy weighted ROM filters: FWROM-G(3,7) or

FWROM-G(3,5) respectively. Similarly, filters for a 5×5 window, such as FWROM-G(5,11), FWROM-G(5,13), etc may be defined.

4.4.3 Simulation and Results

Extensive computer simulations are carried out to assess the performance of the proposed filters and to compare the same with the standard MAV, MED and ROM filters, and the fuzzy TMAV filter. 'Lena face' image is taken as the test image. Gaussian noise with variance, varying from 0.03 to 0.09, is added to this image. Fixed valued impulse noise, SPN of density 1% is further applied to this image to simulate a mixed noise condition. **MSE** is taken as the *performance measure*. The performance of the various filters obtained from simulation is listed in Table-4.2.

Table-4.2 Performance Comparison of FWROM-T and FWROM-G with other Standard Filters under Mixed Noise Condition
(1% SPN alongwith AWGN of variance, σ^2)

Filter	MSE			
	σ^2=0.03	σ^2=0.05	σ^2=0.07	σ^2=0.09
ROM(3,3)	0.0034	0.0048	0.0071	0.0100
ROM(3,5)	0.0033	0.0047	0.0070	0.0099
ROM(5,11)	0.0031	0.0046	0.0069	0.0097
ROM(5,13)	0.0035	0.0050	0.0069	0.0098
MAV3×3	0.0034	0.0048	0.0071	0.0100
MAV5×5	0.0035	0.0050	0.0073	0.0103
TMAV	0.0035	0.0050	0.0072	0.0102
FWROM-T (3,5)	0.0026	0.0028	0.0029	0.0032
FWROM-T (5,11)	0.0026	0.0028	0.0032	0.0038
FWROM-T (5,13)	0.0026	0.0029	0.0034	0.0042
FWROM-G (3,5)	0.0029	0.0029	0.0029	0.0030
FWROM-G (5,11)	0.0029	0.0030	0.0031	0.0036
FWROM-G (5,13)	0.0026	0.0027	0.0030	0.0037

Next, the 'Lena face' image is corrupted with Gaussian noise of variance σ^2=0.1 alongwith SPN of density 1%. The output images of some standard filters and the proposed filters are shown in Fig. 4.6. It is observed, by visual inspection, that: (i) the performance of MAV3×3 is very poor; (ii) TMAV performs slightly well; and (iii) the proposed filters FWROM-T(3,5) and FWROM-G(3,5) perform much better than all other filters.

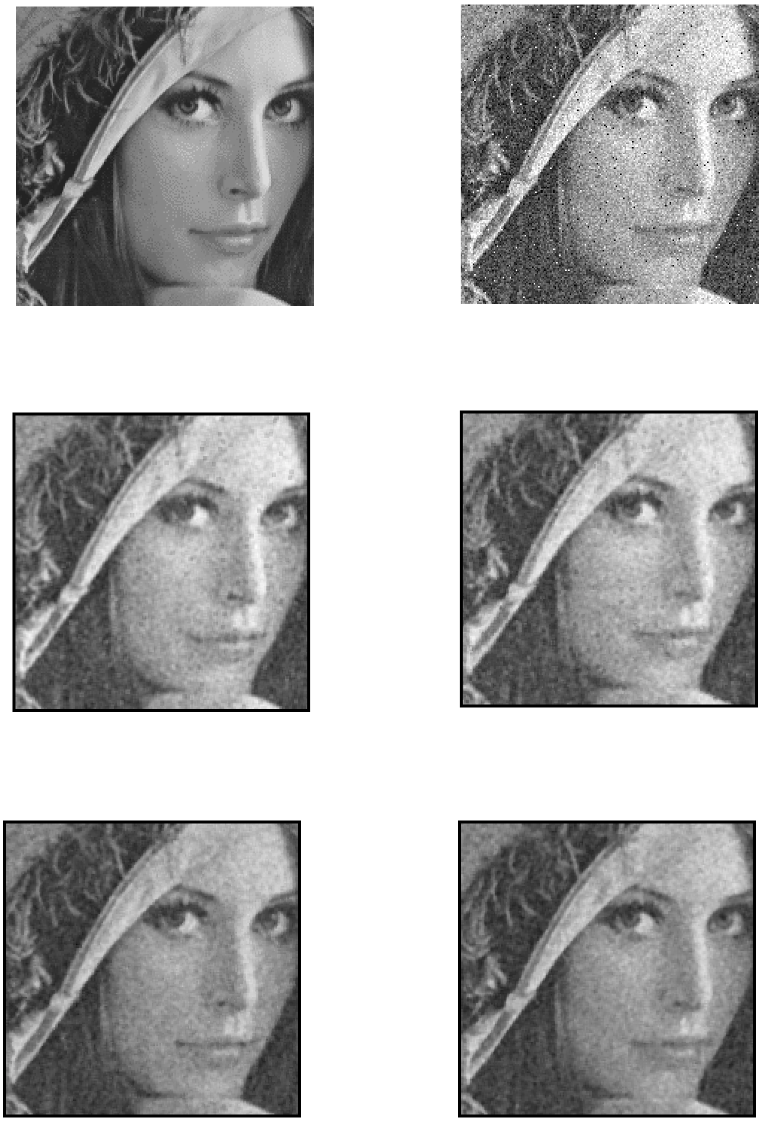

a	b
c	d
e	f

Fig. 4.6 Images for Visual Performance Comparison:
(a) the original Lena face image
(b) noisy Lena face with AWGN(σ^2 =0.1) and SPN(d=1%)
(c) output image of MAV3×3 filter
(d) output image of TMAV filter[94]
(e) output image of FWROM-T(3,5)
(f) output image of FWROM-G(3,5)

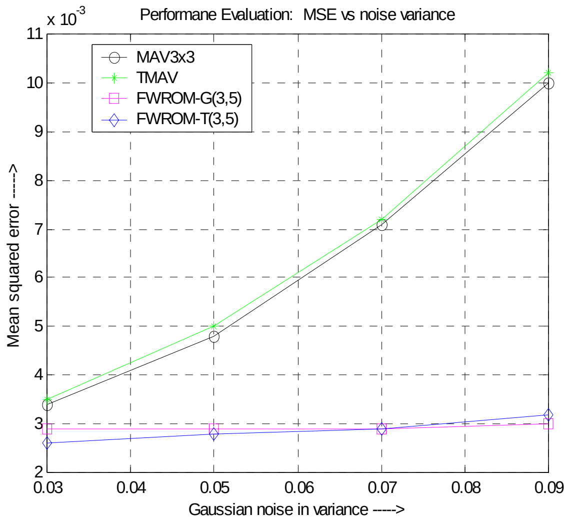

Fig. 4.7 Plot of Mean Squared Error for MAV33, TMAV, FWROM-G(3,5), FWROM-T(3,5) Filters under Additive White Gaussian Noise Condition

The Mean Squared Errors (MSE) for the filters: MAV3×3, TMAV, FWROM-G(3,5) and FWROM-T(3,5) are plotted in Fig. 4.7. It is observed that both the filters: FWROM-G(3,5) and FWROM-T(3,5) show almost the same performance and they are quite superior to the other standard filters. One more interesting point to be noted here is: the MSE increases rapidly with AWGN variance for the MAV and TMAV filters, whereas it remains almost constant in case of the proposed filters FWROM-T(3,5) and FWROM-G(3,5).

4.4.4 VLSI Implementation

FWROM filters are quite computational intensive algorithms. To reduce the computation time, for real-time applications, these filters should be implemented in VLSI in the form of ASICs. Pipelined architecture [72] should be adopted to further reduce the overall time requirement. Such a scheme for FWROM-T(3,5) is shown in Fig. 4.7.

Since sorting nine data takes a lot time (as multi-level comparison processes are involved), the first stage in the pipeline performs only the sorting operations. The weight computation involves center (mean) value, c and slopes, s_1 *and* s_2 given by:

$$\left.\begin{aligned} c &= \frac{x_{(2)} + x_{(8)}}{2} \\ s_1 &= \frac{1}{c - x_{(2)}} \\ s_2 &= \frac{1}{x_{(8)} - c} \end{aligned}\right\} \tag{4.7}$$

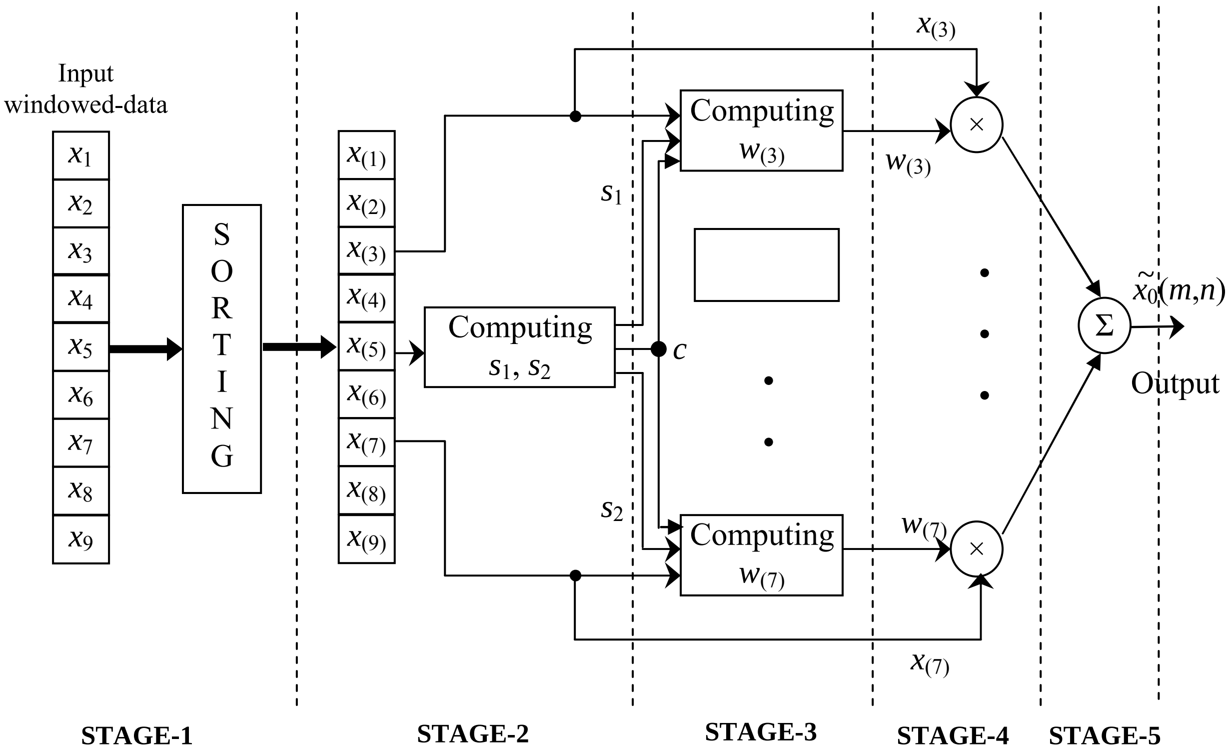

Fig. 4.7 Schematic of a Pipelined VLSI Architecture for FWROM-T(3,5)

The second stage in the pipeline includes the computation units for computing c, s_1 and s_2. It may be noted that computing the slopes requires the value of c. Therefore, this stage is basically a multi-state computing unit. That is why, one stage in the pipeline is dedicated for this purpose, even though the computations are very simple.

The third stage includes the computation units to compute the fuzzy weights $w_{(3)}$, $w_{(4)}$,…… $w_{(7)}$ for FWROM-T(3,5). The forth stage multiplies the chosen order statistics with the fuzzy weights computed in the previous stage. For this purpose five multipliers are used. The last stage, i.e. the addition unit comprises of four adders arranged in a hierarchical tree structure as shown in Fig. 4.8. Each adder computes a partial sum. Such a hierarchical addition unit reduces the overall addition time requirement drastically if the number of addenda is large. In this case, the addition time reduces by 25%.

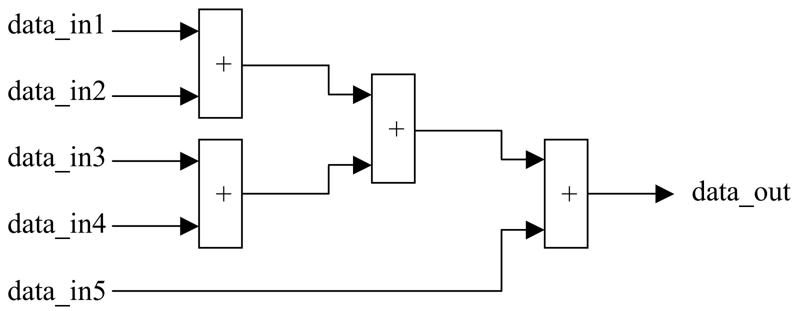

Fig.4.8 A Fast Adder with Hierarchical Tree Structure

Let t_1, t_2, t_3, t_4 and t_5 be the time required for the pipeline stages 1, 2, 3, 4 and 5, respectively. Then the overall time, t, for computing the FWROM-T (3,5) (for a single window operation) is given by :

$$t=\max(\{t_1, t_2, t_3, t_4, t_5\}) \tag{4.10}$$

since all the stages are in pipeline[72]. Otherwise, the time requirement would have been the sum of all these time values. Such a VLSI scheme may highly be appreciated for implementing a FWROM filter in real-time applications.

4.4.5 Conclusion

The filters: FWROM-T(3,5) and FWROM-G(3,5) show much superior performance, for suppressing mixed noise, over the other standard ROM filters, the MAV filters, and the fuzzy filter, TMAV [94] The filter: FWROM-T(3,5) performs better than the filter: FWROM-G(3,5) under low noise variance ($\sigma^2 < 0.07$) and slightly degrades at high noise variance ($\sigma^2 > 0.07$); the performance measure, MSE for both the filters being the same at $\sigma^2 = 0.07$. But the Gaussian membership function is much more computational intensive than the triangular membership function. Therefore, the filter FWROM-T(3,5) is be preferred to FWROM-G(3,5) for real time applications, e.g. in television systems.

The proposed pipelined VLSI architecture for FWROM-T(3,5) is highly suitable for real-time applications since such a structure computes the filter output very fast.

4.5 Conclusion

In this chapter, many novel adaptive filters are developed for efficient suppression of noise in an image. The proposed OS-LMS adaptive image filter trains itself with the type of noise and the noise power level very nicely. Thus, it possesses very good noise adaptive behavior. In real-time applications like television systems, the noise type and the noise power level varies from time to time. Therefore, the proposed scheme is highly useful for such an application.

Another class of adaptive filters based on fuzzy logic is proposed in this chapter. Two types of fuzzy WROM filters using triangular and Gaussian membership functions: FWROM-T and FWROM-G are proposed. They show very good filtering performance for various noise types and noise power levels. Since the FWROM filters get themselves trained for each windowed data set, their filtering performance is very good. But, they are highly computational intensive algorithms. Therefore, they take a long processing time. The FWROM-T(3,5) is less computational intensive as compared to the FWROM-G(3,5) as it is easier to compute the triangular membership than the Gaussian membership.

To enhance the filtering speed, a pipelined VLSI architecture is proposed in Section-4.4.4 for the FWROM-T(3,5) filter. The effective computation time is only the time required to sorting the data vector. Therefore, it becomes as fast as the simple OS filter MED. Thus, the FWROM-T(3,5) implemented in an ASIC is a nice image filter for real-time applications.

CHAPTER-5

Conclusion

Preview

In this thesis, various types of noise in a digital image and their sources, the practical noise levels, and the range of noise power in a practical image are studied. Then, the types of noise and noise levels are studied for communication applications like television and photo-phones. For such real-time applications, efforts have been made to develop efficient nonlinear filters to suppress AWGN, SPN, RVIN and MN. If an image signal is transmitted in analog form, the noise may be a mixed version of AWGN and SPN. On the other hand, if the image signal is transmitted in digital form, then the received signal is corrupted with RVIN. Therefore, many efficient filters are proposed to suppress MN and RVIN quite effectively without blurring the edges and without distorting the fine-details of the image. The proposed filtering schemes are meant for real-time applications.

Various approaches adopted to achieve these goals are:

i) WROM filters to suppress mixed noise quite effectively with very little computational complexity

ii) Three novel impulse detection schemes to detect impulse noise quite effectively

iii) Adaptive OS LMS and Fuzzy WROM filters to adapt themselves to noise type and noise level for better filter performance under varying noise conditions

The following topics are covered in this chapter.

- A Comparative Study
- Conclusion
- Scope for Future Work.

5.1 A Comparative study

Table-5.1 shows the performance of the various proposed filters and some standard filters available in literature. The 'Lena face' is the test image taken for simulation. The NRDB is taken as the performance measure and is listed in the table.

TABLE- 5.1 Performance (NRDB) of Various Filters

Noise Type	**Filter**	**Noise Power (*MSE_{in}*) (at the input of the filter)**	**NRDB (dB)**
AWGN (variance=0.01)	MAV3	0.0097	3.2176
	MED3		3.0396
	ROM(3,3)		3.2385
	WROM(3,7) [P3]		3.3554
	FWROM-T(5,13) [P4]		4.3573
	FWROM-G(5,11)[P4]		**5.1098**
AWGN+SPN (variance=0.01; Impulse density=0.01)	MAV3	0.0127	3.2176
	MED3		3.0396
	ROM(3,3)		3.2385
	WROM(3,7) [P3]		3.3554
	FWROM-T(3,5) [P4]		5.9865
	FWROM-G(3,5) [P4]		6.2668
	DIND + Filter [P2]		**7.8158**
SPN (10%)	MAV3	0.0287	5.3755
	MED3		7.7811
	ROM(3,3)		7.8314
	WROM(3,3) [P3]		8.0336
	PIND + Filter		**24.5788**
	DIND + Filter [P2]		12.1230
	SOD-DDMF [P1]		8.5106
RVIN (10%)	MAV3	0.01301	10.3709
	MED3		6.9115
	DIND + Filter [P2]		**12.3012**
	FWROM-G(3,7) [P4]		4.4491

The results of the Table-5.1 may be summarized as:

(a) The proposed fuzzy filter FWROM-G(5,11) performs better than other standard OS filters in suppressing low variance AWGN.

(b) The proposed DIND plus filtering scheme performs much better than other standard OS filters in suppressing low power MN.

(c) The proposed PIND algorithm followed by median filtering performs much better than other standard filters in suppressing low and medium density SPN.

(d) The proposed DIND plus filtering scheme performs much better than other standard filters in suppressing low and medium density RVIN.

Thus, it is observed that many novel filtering schemes are developed in this thesis to suppress various types of noise in an image.

5.2 Conclusion

The following conclusions may be drawn.

- The WROM filters show very good performance as compared to the standard OS filters. They don’t have much computational complexity since the filter weights are fixed.

- The SOD-DDMF performs well in the presence of SPN and RVIN. Its performance is very good for SPN (upto 40%) and is good for RVIN (upto 20%).

- PIND and DIND algorithms are very good impulse noise detectors. They perform very well under low noise density. The DIND algorithm is a robust impulse noise detector since it can very easily detect impulse noise under mixed noise condition. The DIND algorithm shows very good performance for RVIN as well.

- The performance of the PIND algorithm is excellent in suppressing low density SPN. Its performance is better than many recently reported filters in the literature.

- Two different types of adaptive filters are proposed. The OS LMS adaptive filter is a better candidate than the LMS adaptive L-filter [26] since the former doesn't need a very similar image frame for training. The fuzzy weighted ROM (FWROM) filters show very good performance since the filter weights get updated in each window. No previous training is required for the proposed FWROM filters. As the filter adapts itself during each pixel processing, its computational complexity is very high. But such a filter can very well be implemented in an application specific integrated circuit (ASIC) to provide high throughput so that it may be used in real time applications. A pipelined architecture is proposed for VLSI implementation of FWROM-T(3,5) in Section-4.4.4. Such a hardware implementation of the proposed fuzzy filter enhances the overall throughput and makes it suitable for a real-time application.

- The FWROM filters show very good performance under different types of noise. It is the self-adaptive nature of a fuzzy system that has made the filter effective in all conditions. Though this filter can't reduce the noise level drastically, it retains image-integrity to a high extent. This is very much desired in a real-time application like television system.

Finally, it may be concluded that many efficient nonlinear and adaptive digital image filtering schemes have been developed in this present research work to suppress various types of noise encountered in an image.

5.3 Scope for Future Work

Some new directions of research in the field of image denoising are not yet fully explored. There is sufficient scope to develop very good filters in the directions mentioned below.

(a) Neural Networks (NN) are very good adaptive systems. But, there are only a few neural image filters reported in literature. The performance of a neural image filter can very well be enhanced by associating order statistics (OS) with it. It is expected that many researchers will develop very good filters using OS-NN techniques (presently under investigation).

(b) Fuzzy inference systems (FIS) are very nice adaptive systems. Much more research is expected in the direction of fuzzy image filters in future.

(c) Discrete Wavelet Transform (DWT) is a very good tool for signal processing. Many are expected to carry research in developing very high quality DWT-based image filters in the next 5-10 years.

(d) Since an image is a highly correlated 2-D signal, spatial domain decision-based filters show very high filtering performance. The OS plays an important role in spatial domain filtering. Therefore, many new hybrid filters employing OS and DWT are expected in near future. Such schemes will have the advantages of both the spatial domain and the frequency domain analyses.

(e) Further, many researchers are expected to explore the use of NN and FIS in a hybrid OS-DWT system so that the overall system becomes adaptive to the noise type, noise power level and the spatial image variation.

REFERENCES

[1] A. K. Jain, *Fundamentals of digital Image Processing*, Englewood Cliff, N.J.: Prentice Hall, 1989.

[2] R. C. Gonzalez and R.E. Woods, *Digital Image Processing*, Addison-Wesley Longman Inc., 2000.

[3] W. K. Pratt, *Digital Image Processing,* NY: John Wiley & Sons, 2001.

[4] I. Pitas and A. N. Venetsanopolous, *Nonlinear Digital Filters: Principles and Applications*, Norwell, M. A., Kluwer, USA,1990

[5] T. S. Huang, G. J. Yang, and G. Y. Tang, "A Fast Two Dimensional Median Filtering Algorithm*", IEEE Trans on Acoustics, Speech, Signal Processing*, vol. ASSP-27, no.1, February, 1979.

[6] E. Ataman , V. K. Aatre, and K. W. Wong , "A Fast Method For Real Time Median Filtering*", IEEE Trans. on Acoustics, Speech, Signal Processing*, vol. ASSP –28 , no.4 , August, 1980.

[7] J. S. Lee, "Digital Image Enhancement And Noise Filtering By Use Of Local Statistics", *IEEE Trans. on Pattern Analysis and Machine Intelligence*, vol. PAMI-2, no.2, March, 1980.

[8] J. S. Lee, "Refined Filtering Of Image Noise Using Local Statistics”, *Computer Graphics And Image Processing*, no.15, 1981.

[9] E. Ataman, V. K. Aatre, and K. W. Wong, "Some Statistical Properties Of Median Filters", *IEEE Trans. on Acoustics, Speech Signal Processing*, vol..ASSP-29, no.5,October,1981.

[10] A. Kundu, S. K. Mitra and P. P. Vaidyanathan, "Application of Two Dimensional Generalized Mean Filtering for Removal of Impulse Noises from Images", *IEEE Trans. on Acoustics, Speech, Signal Processing*, vol. ASSP-32, no.3, June, 1984.

[11] I. Pitas, and A. N. Venetsanopoulos, "Nonlinear Mean Filters in Image Processing", *IEEE Trans. on Acoustics, Speech, Signal Processing*, vol..10, no.4, June, 1986.

[12] I. Pitas and A. N. Venetsanopoulos, "Nonlinear Order Statistics Filters For Image Filtering and Edge Detection", *IEEE Signal Processing*, vol.10, no.4, June, 1986.

[13] R. Bernstein, "Adaptive Nonlinear Filter for Simultaneous Removal of Different Kinds of Noise in Images", *IEEE Trans. on Circuits and Systems*, vol.35, no.1, January, 1988.

[14] Y. H. Lee and S. A. Kassam, "Generalized Median Filtering and Related nonlinear Filtering Techniques", *IEEE Trans. on Acoustics, Speech, Signal processing*, vol. ASSP-33, no.3, June,1985.

[15] X. Z. Sun and A. N. Venetsanopoulos, "Adaptive Schemes for Noise Filtering and Edge Detection by Use of Local Statistics", *IEEE trans. on Circuits and Systems*, vol.35, no.1, January, 1988.

[16] Y-Hwan Lee and S. Tantaratana, "Decision –Based Order statistics filters", *IEEE Trans. on Acoustics, Speech, Signal Processing*, vol.38, no.3, March, 1990.

[17] J. H. Lin and E. J. Coyle, "Minimum Mean Absolute Error Estimates over the class of Generalized Stack Filters", *IEEE Trans. on Acoustics, Speech, Signal Processing*, vol.-38,no.4, April, 1990.

[18] J. H. Lin, T. M. Sellke, and E. J. Coyle, "Adaptive Stack Filtering under the Mean Absolute error Criterion", *IEEE Trans. on Acoustics, Speech, Signal Processing*, vol.38, no.6, June, 1990.

[19] Lin Yin, J. Astola, and Y. Neuvo, "A New Class of Nonlinear filters- Neural Filters", *IEEE Trans.on Signal Processing*, vol.41, no.3, March, 1993.

[20] H. Hwang and R. A. Haddad, "Adaptive Median Filters: New Algorithms and Results", *IEEE Trans. on Image Processing*, vol. 4,no.4,April 1995.

[21] F. Russo and G. Ramponi, "A Fuzzy Operator for the Enhancement of Blurred and Noisy Images", *IEEE Trans.on Image Processing*, vol.4, no.8, August, 1995.

[22] M. R. Banham and A. K. Katsaggelos, "Spatially Adaptive Wavelet-Based Multiscale Image Restoration", *IEEE Trans .on Image Processing*, vol.5, no.4, April, 1996.

[23] E. A. Michael Lightstone, S.K. Mitra, and K. Arakawa, "A New Efficient Approach for the Removal of Impulse Noise from Highly Corrupted Images", *IEEE Trans. on Image Processing*, vol.5, no.6, June, 1996.

[24] Y. Li and F. Santosa , "A Computational Algorithm for Minimising Total Variation in Image Restoration", *IEEE Trans. on Image Processing*, vol.5, no.6, June, 1996.

[25] R. Malladi and J. A. Sethian, "A unified approach to Noise Removal, Image Enhancement and Shape Recovery", *IEEE Trans. on Image Processing*, vol.5, no.11, November, 1996.

[26] C. Kotropoulos and I. Pitas, "Adaptive LMS L-Filters for Noise suppression in images, *IEEE Trans. on Image Processing*", vol.5, no.12, December, 1996.

[27] Y. Choi and R. Krishnapuram, "A Robust Approach to Image Enhancement Based Fuzzy Logic", *IEEE Trans. on Image Processing*, vol.6, no.7, July, 1997.

[28] C. S. Regazzoni and A. Teschioni , "A New Approach to Vector Median Filtering Based on Space Filling Curves", *IEEE Trans. on Image Processing*, vol.6, no.7, July, 1997.

[29] Mauro Barni, "A Fast Algorithm for 1-Norm Vector Median filtering", *IEEE Trans. on Image Processing*, vol.6, no.10, October, 1997.

[30] R .P. Kleihorst , R .L.Lagendijk and Jan Biemond , "An Adaptive Order Statistic Noise Filter For Gamma Corrected Image Sequence", *IEEE Trans. on Image Processing*, vol.6, no.10,October, 1997.

[31] W. H. Lau, F.L. Hui, S.H. Leung and A. Luk, “Blind Separation of Impulsive Noise from Corrupted Audio Signal", *Electronics Letter*, vol.32, no.3, pp.166-168, Feb., 1996.

[32] Ralph Sucher, "A New Adaptive nonlinear filtering Algorithm", *Proceedings of IEEE, International Conference on Signal Processing, Circuits & Systems*, pp. 1-4, Singapore, July 1995.

[33] S. E. Umbaugh, *Computer Vision and Image Processing: A Practical Approach*, Eagle wood Cliffs, NJ, prentice Hall, 1998, pp. 151-193.

[34] A. Neirman, P.Heinonen and Y. Neuvo, "A New Class of Detail Preserving Filters for Image Processing", *IEEE Trans. on Pattern Analysis*, Machine Intelligence, vol. PAMI-9, pp. 74-90, January,1987.

[35] S. J. Ko, Y.H. Lee, "Centre weighted Median Filters and their Applications to Image Enhancement", *IEEE Trans. on Circuits and Systems*, vol. 38, pp. 984-983, September 1991.

[36] E. J. Coyle, J. H. Cin and M. Gabbouj, "Optimal stack filtering and the estimation of structural approaches to Image Processing", *IEEE Trans. on Signal Processing*, vol. 37, pp. 2037-2066, December,1989

[37] T. Chen, H. R. Wu, "Space variant Median Filters for restoration of Impulse Noise Corrupted images", *IEEE Trans. on Circuits and Systems – II, Analog and Digital Signal Processing*, August, 2001, vol. 48, no. 8, pp. 784-789.

[38] T. Chen, K. K. Ma and L. H. Chen, "Tri-state Median filter for Image Denoising", *IEEE Trans. on Image Processing*, vol. 8, pp.1834-1838, December, 1999.

[39] P. S. Windyga, "Fast Impulsive Noise Removal", *IEEE Trans. on image Processing*, vol.10, no. 1, pp.173-179, January, 2001.

[40] S. R. Kim and A. Effron, "Adaptive robust impulse noise Filtering", *IEEE Trans. on Signal Processing*, vol.43, no.8, pp.1855-1866, August, 1995.

[41] R. Sucher, "Removal of impulse noise by selective filtering", *Proceedings of IEEE International Conference on Image Processing*, vol.2, pp.502-506, Austin, November,1994.

[42] T. Chen and H. R. Wu, "Adaptive Impulse Detection Using Centre-Weighted Median Filters", *IEEE Signal processing Letter*, vol.8, no.1, January, 2001.

[43] E. Abreu, M. Lightstone, S. K. Mitra, K. Arakawa, "A new Efficient approach for Removal of impulse noise from highly corrupted images", *IEEE Trans. on Image processing*, vol.5, no.6, pp. 1012-1025, June,1996.

[44] A. B. Hazma and H. Krim, "Image Denoising: A nonlinear robust statistical approach", *IEEE Trans. on Image processing*, vol.49, no.12, pp. 3045-3054, Dec,2001.

[45] N. Weyrich and G. T. Warhula, "Wavelet Shrinkage and Generalized Cross Validation for Image Denoising", *IEEE Transaction, Image Processing*, vol. 7, no. 1, pp. 82-90, Jan. 1998.

[46] M. L. Hilton and R. T. Ogten, “Data Analytic Wavelet Threshold Selection in 2-D Signal Denoising”, *IEEE Transaction, Signal Processing*, vol. 45, no. 2, pp. 496-500, Feb. 1997.

[47] S. G. Chang, B. Yu, and M. Vetterli, “Adaptive Wavelet Thresholding for Image denoising and Compression”, *IEEE Transaction, Image Processing*, vol. 9, no. 9, pp. 1532-1546, Sept. 2000.

[48] X. P. Zhang, “Thresholding Neural Network for Adaptive Noise Reduction”, *IEEE Trans. Neural Network*, vol. 12, no. 3, pp. 567-584, May. 2001.

[49] L. A. Zadeh, “Fuzzy Sets”, *Information and control*, vol.8, pp. 338-353, 1965.

[50] L. A. Zadeh,”Fuzzy Logic”, *IEEE Computer Megazine*, pp. 83-93,April, 1988.

[51] J. C. Patra, G. Panda, R. N. Pal, and B. N. Chatterjee, “Neural Networks for signal Processing Applications”, *Journal of Computer Science and Informatics*, India, vol.27, no.3, pp.24-34, September, 1997.

[52] Simon Haykin, *Neural Networks, A Comprehensive Foundation*, Prentice Hall International Inc., 1999.

[53] G. Panda, B. Majhi, P. K. Dash, “Development of Efficient Filtering Techniques for Image Data Corrupted by Impulse Noise”, *The Journal of the Computer Society of India*, vol. 30 no.1, March 2000, pp.25-33.

[54] G. Panda, B. Majhi, and P.K. Dash, "Selective Median Filtering using Fuzzy Detector for Impulse Noise Removal", *Proceedings, National Conference on Communications*, IIT, Kanpur, pp. 105-109, Jan 27-28, 2001.

[55] G. Panda, B. Majhi, and P. K. Dash, "A Novel Impulse Filtering Scheme for Corrupted Image using ANN Detector", *Proceedings, Int. Conf. on Communications, Computers, & Devices (ICCCD-2000)*, IIT, Kharagpur, pp. 603-606, December, 14-16,2000.

[56] S. Mallat, “A Theory for Multiresolutional Signal Decomposition: The Wavelet Representation”, *IEEE Trans. Pattern Recognition and Machine Intelligence*, vol. 11, no.7, pp. 674-693, July 1989.

[57] D. L. Donoho and I. M. Johnstone, “Ideal Spatial Adaptation by Wavelet Shrinkage”, *Biometrika*, vol. 81, pp. 425-455, 1995.

[58] Daubechies, “The Wavelet Transform, Time-Frequency Localization and Signal Analysis”, *IEEE Trans. on Information Theory*, vol. 36, pp.961-1005, 1990.

[59] D. L. Donoho, "Denoising by soft-thresholding", *IEEE Trans. on Information Theory*, vol.41, pp. 613-627, May,1995.

[60] S. G. Chang, B. Yu, and M. Vetterli, "Spatially Adaptive Wavelet Thresholding with Context Modeling for Image Denoising", *IEEE Transaction, Image Processing*, vol. 9, no. 9, pp. 1522-1531, Sept. 2000.

[61] Simon Haykin, *Adaptive Filter Theory*, Prentice-Hall Inc. 3rd edn,1996. U.S. River, New Jersey.

[62] B. Widrow, *Adaptive Filter I: Fundamentals,* Rep. SEL-66-126(TR 6746-6), Stanford Electronics Laboratory, Stanford, Calif.

[63] B. Widrow , "Adaptive Filters" in *Aspects of Neural Network and System Theory*, ed. R.E. Kalman and N.Declaris, Holt, Rinehart and Winston, New York.

[64] B. Widrow and M.E. Hoff, " Adaptive Switching Circuits", *IRE WESCON Conv. Rec.* pt.4, pp. 96-104, 1960.

[65] B. Widrow, S. D. Stearns, *Adaptive Signal Processing,* Prentice-Hall, Englewood Cliffs, N. J. 1985.

[66] B. Widrow and M. Lehr, "30 years of adaptive neural networks: Perception, madaline, and back-propagation ", *Proc. IEEE, Special Issue on Neural Networks 1*, vol. 78, September 1990.

[67] M. Janshidi, N. Vedice, T. Ross, *Fuzzy Logic & Control: software and hardware Applications*, Prentice Hall Inc., 1993

[68] J. Klir, B. Yuan, *Fuzzy Sets and Fuzzy Log c: Theory and Applications,* Prentice Hall Inc., 1995.

[69] J. Yen, R. Langari, *Fuzzy Logic: Intelligence, Control and Information,* Prentice Hall Inc., 1999.

[70] J. Mendel, *Uncertain Rule-Based Fuzzy Logic Systems: Introduction and New Directions,* Prentice Hall Inc., 2001.

[71] W-Y. Han and J-C. Lin, "Minimum-maximum exclusive mean (MMEM) filter to remover impulse noise from highly corrupted images", *IEE, Electronics Letters*, vol. 33, No. 2, pp 124-125, Jan 1997.

[72] Keshab K. Parhi, *VLSI Digital Signal Processing Systems: Design and Implementation*, John Wiley & Sons, Inc. New York, 1999.

[73] H. G. Longotham and A.C. Bovik, "Theory of Order Statistics Filters and Their Relationship to Linear FIR Filters", *IEEE Trans. on Acoust. Speech, Signal Processing*, vol. ASSP-37, no.2, pp. 275-287, February 1989.

[74] J. W. Tukey, "*Experimental Data Analysis*", Reading, M. A: Addison-Wesley; 1971.

[75] N. C. Gallagher and G. L. Wise, "A Theoretical analysis of the properties of median filters", *IEEE Trans. Accoust. , Speech, Signal Processing*, vol. ASSP-29, pp. 1136-1141, Dec 1981.

[76] S. G. Tyan, "Median filtering: Deterministic properties", in *Two-Dimensional Signal Processing : Transforms and Median Filters,* T. S. Huang, Ed. New York: Springer-Verlag, 1981.

[77] T. A. Nodes and N. C. Gallagher, Jr., "Median Filters: Some modifications and their properties", *IEEE Trans. Accoust. , Speech, Signal Processing*, vol. ASSP-30, pp. 739-746, Oct. 1982.

[78] A. C. Bovik, T. S. Huang and D. C. Munson, Jr., "A generalization of median filtering using linear combination of order statistics", *IEEE Trans. Accoust. , Speech, Signal Processing*, vol. ASSP-31, pp. 1342-1350, Dec 1983.

[79] H. A. David, *Order Statistics*. New York: Wiley, 1982.

[80] L. Naaman and A. C. Bovik, "Optimal order statistics filters with coefficient censoring" in Proc. *IEEE Int. Conf. Accoust. , Speech, Signal Processing*, New York, Apr. 11-14, 1988.

[81] F. Russo, "Evolutionary Neural Fuzzy System for Noise Cancellation in Image Processing", *IEEE Trans. Inst & Meas*., vol. 48, no. 5, pp. 915-920, Oct. 1999.

[82] K-E Barner, A-M Sarhan and Russell C. Hardie, "Partion Based Weighted Sum Filters for Image Restoration", *IEEE Trans. on Image Processing*, vol. 8, no. 5, pp. 740-745, May 1999.

[83] F. Farbiz, M. B. Menhaj, S.A. Motamedi and M.T. Hagan," A new Fuzzy logic Filter for Image Enhancement", *IEEE Trans. on Syst. Meas. Cybernetics* – Part B: Cybernetro, vol.30, no.1, pp. 110-119, Feb 2000.

[84] F. Russo, "Noise Removal from Image data using recursive Neuro-fuzzy filters", *IEEE trans on Inst & Meas*, vol. 49, no.2, pp.307-314 April 2000.

[85] M. Okano, A. Tagnchi and M. Sone, “ Restoration Method of Image Corrupted by High Probability Impulse Noise by Using Fuzzy Techniques”, *Proceedings of IEEE Int. Conf. ICSP 2000*, pp 244-246.

[86] T. Chen and H.R. Wu, “Application of Partion- Based Median Type filters for Suppressing Noise in Images”, *IEEE Trans on Image Processing*, vol. 10, no.6, June 2001.

[87] T. Chen and H.R. Wu, “Recursive LMS L-Filter for Noise Removal in Images”, *IEEE Signal Processing Letters*, vol. 8, no.2, pp.36-38, Feb 2001.

[88] H-L Eng and K-K Ma, “ Noise Adaptive Soft switching Median Filter”, *IEEE Trans. on Image Processing*, vol.10, no.2, pp. 242-251, Feb 2001.

[89] T. Chen and H.R. Wu, “Adaptive Impulse Detection Using center-weighted Median Filters”, *IEEE Signal Processing Letters*, vol. 8, no. 1, pp.1-3, Jan 2001.

[90] T. Chen and H. R. Wu, “Space Variant Median Filters for Restoration of Impulse Noise Corrupted Images”, *IEEE Trans. on CAS-II, A & D SP*, vol.48, no.8, pp.784-789, Aug 2001.

[91] K. Kando, M. Haseyama and H. Kitajima, “An Accurate Noise Detector for Image Restoration”, *Proceedings of IEEE conf. ICIP 2002*, ppI-321-I-324.

[92] S. Zhang and M. A. Karim, “A new Impulse Detector for Switching Median Filters”, *IEEE Signal Processing Letters*, vol. 9, no.11, pp.360-363, Nov 2002.

[93] F. Russo, “An Image Enhancement Technique Combining Sharpening and Noise Reduction”, *IEEE Trans on Int & Meas*, vol. 51, no.4, pp.824-828, Aug 2002.

[94] H. K. Kwan and Y. Cai, “Fuzzy Filters for Image Filtering”, *Proc. of Circuits and Systems, MWSCAS-2002, The 2002 45th Midwest Symposium*, vol.3, pp. III-672-675, August 2002.

[95] M. Ma, X. Jiao and X. Tan, “Fuzzy Hybrid filter for Removal of Impulsive Noise from Highly Corrupted Images”, *Proceeding of IEEE Conf. TENCON*”02 pp.885-888.

[96] Y. Hawwar and Ali Reza.” Spatially Adaptive Multiplicative Noise Image Denoising Technique”, *IEEE Trans. on Image Processing*, vol. 11, no.12, pp. 1397-1404, Dec 2002.

[97] D.V.D. Ville, M. Nachetegael, D.V. Wekan, E.E. Kere, W. Philips, I. Lemahievm, "Noise Reduction by Fuzzy Image Processing", *IEEE Trans. on Fuzzy systems,* vol.11, no.4, pp. 429-436, Aug 2003.

[98] F. Russo and A. Lazzari, "A robust approach based on hybrid Fuzzy Networks for Removing Impulse noise from Images", *Proceedings of IEEE Conf. on Inst & Meas Technology IMTC-2003*, Vail, CO, USA, pp. 545-550., 20-22 May 2003.

[99] F. Russo, " A Method for Estimation of Filtering of Gaussian Noise in Images", *IEEE Trans. on Inst & Meas*, vol 52, no.4, pp. 1148-1154, Aug 2003.

[100] I. Aizenberg and C. Butakoff, "Effective Impulse Based on Rank Order Criteria", *IEEE Signal Processing Letters*, vol.11, no.3, pp.363-366, Mar 2004.

[101] M. Kazubek, "Wavelet Domain Image Denoising by Thresholding and Wiener Filtering", *IEEE Signal Proc. Lett.*, vol.-10, No.-11, pp. 324-326, November-2003.

[102] X. Xu, E. L. Miller, D. Chen and M. Sarhadi, "Adaptive Two-Pass Rank Order Filter to Remove Impulse noise in Highly Corrupted Images", *IEEE Trans on Image Processing,* vol.13, no.2, pp.238-247, Feb 2004.

[103] Russo F., and Ramponi G., "A Fuzzy Filter for Images corrupted by Impulse Noise", *IEEE Signal Processing Letters,* vol-3, no. 6, pp. 168-170, June 1996.

[104] M. Mestari, "An Analog Neural Implementation in fixed time of Adjustable-Order Statistics Filters and Application", *IEEE Trans. on Neural Network*, vol.15, no.3, pp. 766-785, May 2004.

[105] N. Ebrahimi, E. S. Sofi and H. Zahedi, "Information Processing via Order Statistics and Spacing" *IEEE Trans. on Image Processing*, vol. 50.no.1, pp.177-183, Jan 2004.

[106] V. Crnojevic, V. Senk and Z. Trpovski, "Advanced Impulse Detection Based on Pixel-Wise MAD", *IEEE Signal Proc. Lett.*, vol.-11, No.-7, pp. 589-592, July 2004.

CONTRIBUTION BY THE CANDIDATE

[P1] B. Majhi, G. Panda, **S. Meher**, "Decision-Directed Median Filter (DDMF) for Impulse Noise Removal from Images", revised and submitted to *IEEE Trans. on Image Processing*.

[P2] **S. Meher**, G. Panda, B. Majhi, "Deviation based Impulse Noise Detection (DIND) Algorithm Directed Digital Image Filter for Efficient Suppression of Impulse Noise", communicated to *IEE, Electronics Letters*.

[P3] **S. Meher**, G. Panda, B. Majhi, M. R. Meher, "Weighted Order Statistics Filters", *Proceedings of National Conference*, *APSC-2004*, pp 167-173, November 2004.

[P4] **S.Meher**, G.Panda, B.Majhi, M.R.Meher, " Fuzzy Weighted Rank-Ordered Mean (FWROM) Filters for Efficient Noise Suppression", *Proceedings of National Conference on Communications* , NCC-2005, Indian Institute of Technology, Kharagpur (Accepted for presentation in January 2005).